High-Throughput Characterization of Mar-Sox-Rob Network Regulation Across Chemical Environments and its Impact on Drug Transport in *Escherichia coli*

Dissertation

der Mathematisch-Naturwissenschaftlichen Fakultät

der Eberhard Karls Universität Tübingen

zur Erlangung des Grades eines

Doktors der Naturwissenschaften

(Dr. rer. nat.)

vorgelegt von

Christoph Binsfeld

aus Frankfurt am Main

Tübingen

2025

Gedruckt mit Genehmigung der Mathematisch-Naturwissenschaftlichen Fakultät der Eberhard Karls Universität Tübingen.

Tag der mündlichen Qualifikation:	02.12.2025
Dekan:	Prof. Dr. Thilo Stehle
1. Berichterstatter/-in:	Jun.-Prof. Dr. Ana Rita Brochado
2. Berichterstatter/-in:	Prof. Dr. Lisa Maier

Table of Contents

Table of Figures

Abbreviations

5’-UTR – 5’ untranslated region

AMR – Antimicrobial resistance

AUC – Area under the curve

DNA – Desoxyribonucleic acid

EVC – Empty vector control

GOF – Gain of function

IM – Inner membrane

ITC – Isothermal Calorimetry

LOF – Loss of function

LPS – Lipopolysaccharide

MIC – Minimum inhibitory concentration

MOA – Mode of action

mRNA – Messenger RNA

NGS – Next generation sequencing

OD – Optical density

OM – Outer membrane

OMP – Outer membrane porin

PG – Peptidoglycan

PMS – Phenazine methosulfate

RBS – Ribosome binding site

RNA – Ribonucleic acid

ROS – Reactive oxygen species

SMM – Sulfamonomethoxine

SMX – Sulfamethoxazole

TPP – Thermal Proteome Profiling

Zusammenfassung

Die Inhalte dieser Zusammenfassung wurden im Manuskript „Systematic Characterization of Transport Regulation in *Escherichia coli* across defined environmental cues“ verwendet und als Preprintartikel auf “biorxiv.org” (doi: https://doi.org/10.1101/2024.08.26.609649) veröffentlicht. Das Manuskript wurde anschließend in PLOS Biology publiziert: „Binsfeld C, et al. (2025) Systematic screen uncovers regulator contributions to chemical cues in *Escherichia coli*. Doi: https://doi.org/10.1371/journal.pbio.3003260, PLoS Biol 23(7): e3003260“. Diese Zusammenfassung habe ich selbst geschrieben, betreut von Prof. Dr. Ana Rita Brochado.

In gramnegativen Bakterien erfolgen Import und Export vielfältiger Moleküle, inklusive Antibiotika, über Porine und Effluxpumpen. Aufgrund ihrer Bedeutung für die Regulation der Permeabilität von äußerer und innerer Membran sind diese Transportmaschinerien auf transkriptioneller und post-transkriptioneller Ebene stark reguliert. Allerdings ist über den Einfluss externer chemischer Stimuli auf die Regulation des Transports bisher nur wenig bekannt. In diesem Projekt haben wir daher den Einfluss von 94 definierten chemischen Reizen auf die transkriptionelle Regulation dreier bekannter Transportergene in *Escherichia coli* untersucht und gleichzeitig die Beiträge der Transkriptionsfaktoren MarA, SoxS und Rob zur Promotoraktivität quantifiziert. Dabei löste ein Drittel aller getesteten Chemikalien transkriptionelle Veränderungen aus, wobei die meisten dieser Interaktionen bisher unbekannt waren. Auf diese Weise konnten wir herausfinden, dass bakteriostatische, aber nicht bakteriozide Antibiotika die Expression von Effluxpumpen auslösen. Zudem trägt der Transkriptionsfaktor Rob zu etwa einem Drittel aller gemessenen transkriptionellen Veränderungen bei und erweist sich somit als deutlich wichtigerer Regulator des Transports als bisher angenommen. Das Potential unseres Datensatzes wird dadurch verdeutlicht, dass wir den molekularen Mechanismus von Antibiotika-Antagonismen mit dem weit verbreiteten Molekül Koffein in *E. coli* aufklären konnten. Zusammenfassend bietet unsere Arbeit einen quantitativen Überblick darüber, wie verschiedene Transkriptionsfaktoren die transkriptionelle Reaktion wichtiger Transportmaschinerien auf chemische Umweltreize umsetzen.

Summary

The contents of this summary have been used in the manuscript “Systematic Characterization of Transport Regulation in *Escherichia coli* across defined environmental cues” and shared as a preprint version on “biorxiv.org” (doi: https://doi.org/10.1101/2024.08.26.609649).
The manuscript was subsequently published at PLOS Biology: “Binsfeld C, et al. (2025) Systematic screen uncovers regulator contributions to chemical cues in *Escherichia coli*. Doi: https://doi.org/10.1371/journal.pbio.3003260, PLoS Biol 23(7): e3003260“. This abstract was written by me under supervision from Prof. Dr. Ana Rita Brochado.

In Gram-negative bacteria, the uptake and export of a wide range of molecules, including antibiotics, is facilitated by porins and efflux pumps. Because of their role in regulating the permeability of the outer and inner membrane to small molecules, these transport machineries are tightly regulated at the transcriptional and post-transcriptional levels. However, regulation of transport by external chemical cues remains poorly understood. Here we investigated transcriptional regulation of three prominent transporter genes in *Escherichia coli* across 94 defined chemical cues, and simultaneously mapped the contributions of the key regulators MarA, SoxS and Rob to promoter activity. One third of all tested compounds triggered transcriptional changes, the majority of which were previously unknown. Importantly, we exposed main drivers of transport control in *E. coli*, e.g. bacteriostatic but not bactericidal antibiotics trigger the expression of efflux pumps, and Rob contributes to ~1/3 of all measured transcriptional changes, thereby emerging as a more prominent regulator of transport than previously thought. We showcase the potential of our resource by elucidating the molecular mechanism of antibiotic antagonisms with widely consumed caffeine in *E. coli*. Altogether, our analysis provides a quantitative overview of how different regulators orchestrate the transcriptional response of major transport determinants to environmental chemical cues.

Introduction

Antimicrobial Resistance, Tolerance and Related Survival Mechanisms

The discovery of synthetic and natural antibiotics a century ago has revolutionized treatment and management of bacterial infections and allowed to rescue countless lives. However, this breakthrough was rapidly followed by the discovery and spread of antimicrobial resistance (AMR) (Hutchings et al., 2019). In the following decades this led to an arms race between development of novel antibacterial compounds and emergence and spread of respective resistance mechanisms (Hutchings et al., 2019). Development of new antibiotics slowed down towards the beginning of the 21st century as profitability for pharmaceutical companies became uncertain due to the short windows of usability caused by antimicrobial resistance (Piddock et al., 2024). Ultimately, this led to the current situation where widespread resistance against almost all clinically used antibiotics culminates in close to untreatable infections by pan-resistant bacteria (Karakonstantis et al., 2019). Taken together, spread of antimicrobial resistance and lack of novel antimicrobial compounds continue to pose a major threat to public health, with millions of deaths per year being directly or indirectly attributable to AMR and predictions forecasting up to 10 million deaths annually by 2050 (Murray et al., 2022; Naghavi et al., 2024). Amongst the most troublesome species in terms of AMR are many Gram-negative species, such as *Pseudomonas aeruginosa*, *Klebsiella pneumoniae,* and *Acinetobacter baumanii*, but also *Escherichia coli*, perhaps one of the best studied model organisms in the world (Murray et al., 2022; Naghavi et al., 2024).

Antimicrobial resistance mechanisms vary in the degree of protection they offer against a given drug and can be broadly classified into two categories – intrinsic and acquired resistance mechanisms (Darby et al., 2023). The latter are usually acquired by uptake of mobile genetic elements, like plasmids, bacteriophages or transposons harbouring the respective antimicrobial resistance gene, allowing transfer of resistance determinants and spread of AMR even between unrelated bacterial

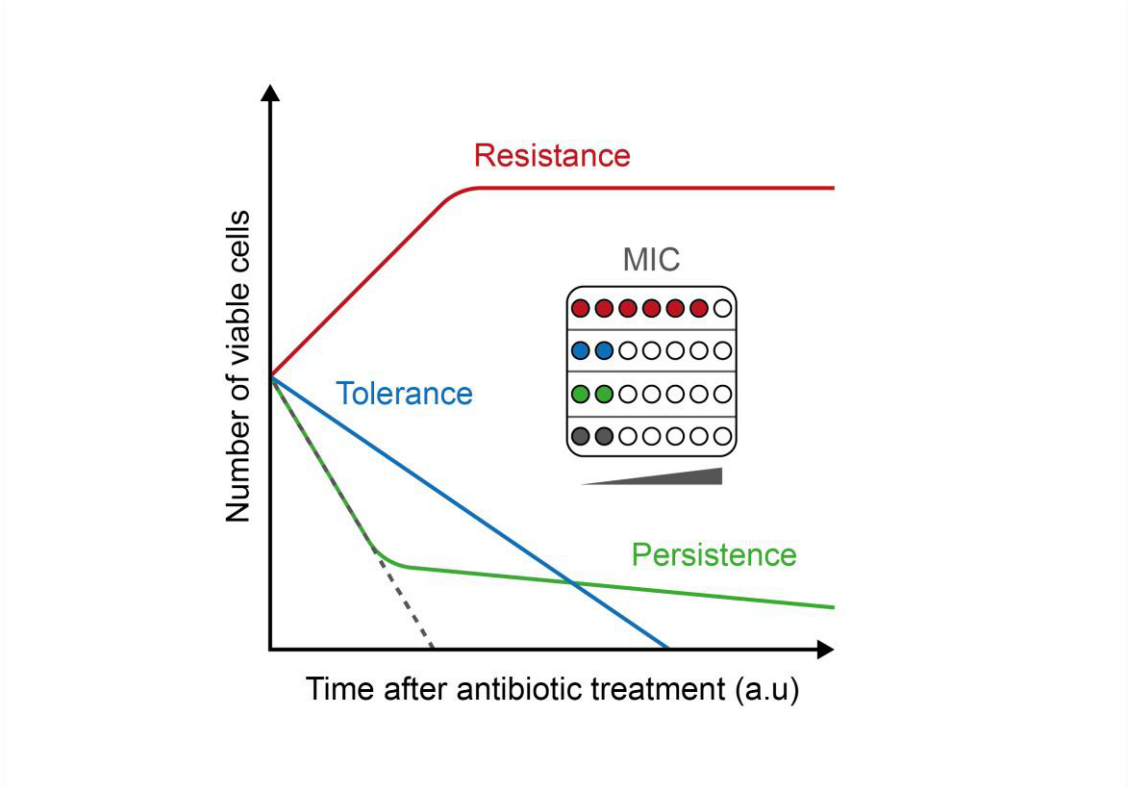

Figure 1: Schematic of cell viability dynamics during antibiotic treatment of resistant, tolerant and persister cells. Resistant cells (red) are able to continue growth during antibiotic treatment, while susceptible cells (dashed, grey) are decimated. Tolerant cells (blue) ultimately are decimated too, but at a slower pace than susceptible cells. Persister cells (green) make up a small fraction within a susceptible population that can emerge as highly tolerant. Only resistant bacteria feature increased minimum inhibitory concentration (MIC).

species (Von Wintersdorff et al., 2016). Common types of resistance mechanisms found on such mobile elements include genes encoding alternative, non-susceptible targets or enzymes that modify and inactivate the respective antibiotic, such as beta-lactamases or acetyltransferases (Darby et al., 2023). Alternatively, *de novo* mutations in genes of antibiotic targets or metabolic pathways may cause resistance due to reduced binding affinity towards the antibiotic. For example, ribosomal genes or topoisomerase enzymes, which are targeted by protein synthesis inhibitors and quinolones respectively, can acquire mutations that retain enzymatic activity but prevent antibiotic action, hence causing resistance to these drugs (Darby et al., 2023). In contrast, intrinsic resistance is genetically encoded in the bacterial genome, without the need to mutate *de novo*. These mechanisms often aim to decrease intracellular drug concentrations, for example, by induction of efflux pumps, or hampering antibiotic efficacy by altering central metabolic pathways.

Alongside antimicrobial resistance, there is the phenomenon of antimicrobial tolerance, which is characterized by alterations in the dynamics of killing rather than changes in minimal inhibitory concentration (MIC). Therefore, tolerant bacteria are able to withstand antibiotic treatment for extended time periods before being eradicated (Brauner et al., 2016; Helaine et al., 2024). This is often caused by alterations in growth rate and metabolism, reducing the efficacy of antibiotics and buying time for the bacteria to survive exposure. Persistence is a special type of tolerance where a small fraction of a susceptible isogenic bacterial population is metabolically dormant and hence highly tolerant to most antibiotics, which only act on growing bacteria (Figure 1: Schematic of cell viability dynamics during antibiotic treatment of resistant, tolerant and persister cells.. Once the antibiotic stress ceases, these bacteria can resume growth and form cultures that are again susceptible to antibiotics (Brauner et al., 2016; Fisher et al., 2017; Helaine et al., 2024). Finally, the phenomenon of bacterial heteroresistance resembles persistence in that it only affects a subpopulation of an otherwise susceptible culture. Here, some cells in a culture emerge as resistant with increased MICs, however, similarly to persistent cells, this phenotype is reversible within a few generations after antibiotic pressure ceases. The mechanisms that lead to this phenotype are lesser understood but one explanation is transient availability of multiple copies of genes through tandem amplification that are then able to cause resistance (Andersson et al., 2019).

Gram-negative Bacteria and Their Cell Envelope

While AMR is common among Gram-negative and Gram-positive species, in general, Gram-negative species are intrinsically more resistant to antibiotics due to unique properties of their cell wall (Figure 2: Schematic representation of the Gram-negative cell envelope.). While Gram-positive bacteria possess a single plasma membrane topped with a thick layer of peptidoglycan (PG), Gram-negative bacteria feature a thinner layer of PG and an additional outer membrane (OM). This outer membrane of the Gram-negative cell envelope acts as a further permeability barrier and greatly restricts access of antibiotics into the cell (Cox and Wright, 2013; Darby et al., 2023). Therefore, many antibiotics

that are available to be used against Gram-positive pathogens do not work against Gram-negative bacteria, despite conserved intracellular targets (Cox and Wright, 2013). The space between inner membrane (IM) and outer membrane is termed periplasm and contains a great number of enzymes and proteins central to the organization of the cell envelope, some of which may prove as potential targets for future drugs.

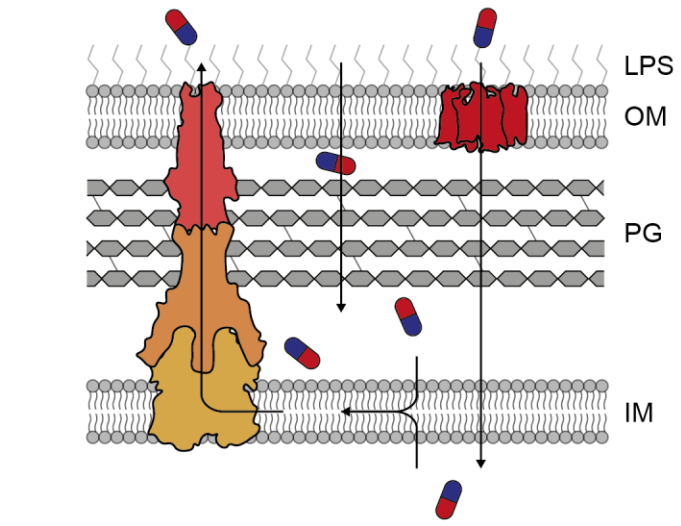

Figure 2: Schematic representation of the Gram-negative cell envelope. Extracellular compounds and nutrients can cross the outer membrane (OM) directly or via porins, depending on whether they are lipophilic or hydrophilic and on their polarity. Peptidoglycan (PG) and inner membrane (IM) can be crossed comparatively freely. Efflux pumps situated in the inner membrane can pick up compounds from periplasm and cytosol in order to pump them out of the cell. Tripartite efflux machineries span the whole cell envelope and consist out of an inner membrane efflux pump, a periplasmatic adaptor protein and an outer membrane porin.

As bacteria need to be able to consume nutrients from the environment there is a need for uptake routes provided by outer membrane proteins. The most prominent group of outer membrane proteins are porins, which form channels in the outer membrane allowing small compounds, solutes and nutrients to diffuse into the periplasm. In the Gram-negative model organism *Escherichia coli* the most important, non-specific outer membrane porins (OMPs) are OmpF and OmpC, which differ in terms of penetration rates, as well as preferred charge and polarity of transported solutes (Masi et al., 2017). Interestingly, OmpF serves as the preferred entry point for many classes of structurally unrelated antibiotics like β-lactams, fluoroquinolones and tetracyclines, due to its slightly wider channel compared to OmpC (Nikaido, 2003).

Since these non-specific porins allow entry of harmful substances into the periplasm, bacteria developed efflux machineries as a means to rid themselves of harmful external substances and toxic intracellular metabolites (Li et al., 2015a). In the case of *E. coli*, at least 35 such efflux pumps across six families have been identified with widely varying substrate specificities and functions (Li et al., 2015a; Teelucksingh et al., 2022a). Most of these machineries are situated in the inner membrane and transport substrates from the cytoplasm into the periplasm. However, there are also a few tripartite efflux pumps consisting of three functional units that span the entire cell envelope (Du et al., 2018a). The most important and best characterized efflux machinery in *E. coli* in terms of intrinsic antimicrobial resistance is such a tripartite assembly named AcrAB-TolC. Here, AcrB acts as an efflux pump anchored to the inner membrane, where it is connected to the outer membrane channel TolC via the periplasmatic adaptor protein AcrA (Du et al., 2018a). In this case, substrates enter the pump from the periplasm or the interface between periplasm and inner membrane (Elkins and Nikaido, 2002; Husain and Nikaido, 2010). The export is then driven by proton-motif force, as is the case for many other efflux pumps (Du et al., 2018a). Due to their non-specific nature, efflux pumps contribute substantially to antibiotic sensitivity of bacteria, with notable examples like *Pseudomonas aeruginosa* being able to efficiently export the most commonly used antibiotics, limiting treatment options in such species with capable efflux machineries (Li et al., 2015a).

On top of porins and efflux machineries, the lipopolysaccharide (LPS) composition on the exterior of the outer membrane plays a crucial role in regulating membrane permeability. These sugar moieties, which are anchored to the outer membrane, affect the charge of the membrane towards the exterior. Differences in outer membrane charge broadly affect penetration rates of charged antibiotics. Therefore, mutations in genes associated to LPS production, maintenance and reorganization are frequently found in clinical isolates (Delcour, 2009; Maher and Hassan, 2023).

Regulation of Transport and its Role in Antimicrobial Resistance

Clinical isolates of resistant pathogenic bacteria often feature mutations in genes associated to membrane permeability, usually leading to a relatively modest increase in MICs. However, many of these mutations can accumulate and together cause high-level resistance (Fernández and Hancock, 2012). As many of these mutations affect expression of non-specific uptake or exit routes (e.g. OmpF or AcrAB-TolC, respectively), this consequently causes a broad resistance phenotype to any drug using the same path. In pathogenic isolates of *E. coli,* the previously mentioned porin OmpF is frequently found to be deleted or mutated in a way that alters its substrate specificity, which greatly restricts entry of substrate antibiotics (Nikaido, 2003; Delcour, 2009; Maher and Hassan, 2023). Likewise, efflux machineries like AcrAB-TolC are frequently found to be overexpressed in clinical isolates, resulting in increased efflux of wide ranges of antibiotics. The deregulation of efflux pumps is often achieved by deletion of repressors (e.g. AcrR) and overexpression or activation of transcription factors able to increase expression (Li et al., 2015a; Maher and Hassan, 2023).

Indeed, the expression of porins and efflux pumps is subject to complex regulation to enable adaptation to a multitude of environmental stresses. Expression of the two major porins OmpF and OmpC is controlled to a large extent by the EnvZ/OmpR two-component system (Mizuno and Mizushima, 1990). Usually such two-component systems consist of a sensor and a transcriptional regulator, whose activity is affected by the sensor protein. EnvZ serves as sensor at the inner membrane where it interacts with the environment. Here, it is able to sense external cues like alterations in pH, osmolarity and nutrient limitation, which then affect transcription of *ompF* and *ompC* in an EnvZ/OmpR-dependent manner (Vergalli et al., 2020). As a sensor histidine kinase, EnvZ is able to phosphorylate and activate OmpR (OmpR~P), which leads to repression of *ompF* and induction of *ompC* expression (Mizuno and Mizushima, 1990). In nutrient limiting environments (low osmolarity) such as laboratory experiments in standard media, OmpF is therefore the most common porin, while OmpC is the predominant porin in nutrient rich environments such as the gut of humans and animals (Yoshida et al., 2006). On top of that, the prominent two component system CpxAR is involved in the

transcriptional regulation of both *ompF* and *ompC*, further increasing the capacity to integrate environmental cues (Batchelor et al., 2005). The CpxAR system broadly controls and regulates membrane integrity, with porin composition of the membrane being a key determinant. Similar to EnvZ, CpxA can sense changes in medium pH and osmolarity, but also damaged LPS and misfolded proteins (Mitchell and Silhavy, 2019). The interplay between both two-component systems is further strengthened by the inner membrane protein MzrA, which interacts with EnvZ to stabilize OmpR~P upon CpxAR activation (Gerken et al., 2009).

On a posttranscriptional level, translation of *ompF* and *ompC* is regulated by small RNAs such as MicF and MicC (Mizuno et al., 1984; Chen et al., 2004). These small RNAs bind to the 5' untranslated region (5'-UTR) of the *ompF* and *ompC* mRNA, respectively, and prevent their translation by masking the ribosome binding site (RBS). Additionally, stability of porin mRNAs is reduced upon *micF* or *micC* binding, further limiting translation (Andersen et al., 1989; Andersen and Delihas, 1990; Chen et al., 2004). Expression of *micF* is positively controlled by OmpR, amongst others, further strengthening the importance of the EnvZ-OmpR system for regulation of *ompF* (Coyer et al., 1990). Furthermore, both porins are target of inhibition by the small RNA RybB, which is expressed during stationary phase, causing porin levels to drop in response to nutrient starvation (Gogol et al., 2011).

Transcriptional regulation of the well characterized efflux pump AcrAB-TolC shows similar levels of complexity. The *acrAB* operon is controlled by the divergently transcribed repressor AcrR, which binds to the *acrAB* promoter region and negatively regulates transcription (Ma et al., 1996). Binding of compounds such as the dyes rhodamine 6G, proflavine or ethidium bromide cause conformational changes in AcrR leading to dissociation and consequently derepression of the *acrAB* promoter (Su et al., 2007). As is the case with porins, two-component systems are also involved in the transcriptional regulation of *acrAB*. Expression of *acrAB*, *tolC* and several other efflux pumps is increased by the EvgAS system in response to mild acidic stress and high concentrations of alkali metals (Eguchi et al., 2003; Eguchi and Utsumi, 2014). In this case,

induction of *tolC* by the EvgAS system is indirect, as EvgS induces a small protein called SafA, which in turn activates the PhoPQ system, leading to increased *tolC* expression (Eguchi et al., 2004, 2007, 2011). The PhoQP system is otherwise activated by low extracellular pH conditions, as well as low Mg^{2+} concentrations in the medium, and increases expression of *tolC* (Eguchi et al., 2003). Similarly to the OmpC porin discussed above, a small RNA – SdsR – is involved in posttranscriptional repression of *tolC* during stationary phase (Parker and Gottesman, 2016), and the EnvZ-OmpR system induces expression of *tolC* in response to high osmolarity (Shimada et al., 2015).

Finally, expression of both the *acrAB* operon and *tolC* is controlled by a set of three paralogous transcriptional regulators – MarA, SoxS and Rob (Martin et al., 1999; Rosenberg et al., 2003; Zhang et al., 2008; Seo et al., 2015). These three regulators are capable of reacting to a wide range of environmental signals, upon which they induce a global stress response causing multiple antibiotic resistance (Figure 3) (Chubiz, 2023). Part of the common regulon of all three regulators are more than 30 genes, amongst others *acrAB*, *tolC* and *micF*, underscoring the importance of the so-called Mar-Sox-Rob network for regulation of transport (Nunoshiba et al., 1992a; Barbosa and Levy, 2000; Bennik et al., 2000; Martin and Rosner, 2002).

The Mar-Sox-Rob Network and its Role in Regulation of Transport

MarA, SoxS and Rob bind to a degenerate binding sequence termed the *mar-sox-rob* box, which is 19 base pairs (bp) long and can be found in various orientations and distances in the promoter region of regulated genes (Martin et al., 1999). This degenerate sequence allows all three regulators to control the expression of a common set of more than 30 genes, the Mar-Sox-Rob regulon, with important functions in drug efflux, membrane permeability, detoxification and alternative metabolic pathways, allowing bacteria to adapt to a wide array of external and internal stresses (Martin and Rosner, 2002). The Mar-Sox-Rob network is distributed widely across the *Enterobacteriaceae* including related pathogenic species such as *Salmonella enterica* or *Klebsiella pneumoniae*. In this instance, *E. coli* is special in that it lacks a fourth regulator – the MarA

homolog RamA – which expands the Mar-Sox-Rob network in the most related enterobacterial species (Chubiz, 2023). RamA is able to integrate environmental signals such as indole or bile acids and dominantly regulates expression of *acrAB* in *S. enterica* (Nikaido et al., 2008).

Amongst the three regulators, MarA is the best characterized one to date. It was discovered during screenings for determinants of intrinsic antimicrobial resistance and was found to cause multiple antibiotic resistance, hence the name of the *mar* operon (Hächler et al., 1991; Cohen et al., 1993a). The *marRAB* operon encodes its own repressor MarR, the transcriptional regulator MarA and the presumably periplasmatic small protein MarB, whose function is yet unclear. Expression of the *marRAB* operon is controlled primarily by its repressor MarR and autoinduction by MarA via the *mar-sox-rob* box upstream of the two MarR binding sites within the promoter region (Martin et al., 1996; Martin and Rosner, 1995; Vinué et al., 2013). Furthermore, many other global regulators connected to central metabolism and envelope stress, such as Fis, Crp, CpxR and AcrR are able to fine tune expression of the *marRAB* operon in response to diverse growth conditions and stresses (Martin and Rosner, 1997; Ruiz and Levy, 2010; Lee et al., 2014). Repression of the operon by MarR is alleviated by small phenolic compounds such as its canonical inducer salicylate, which causes the MarR dimer to undergo conformational changes and ultimately dissociate from its binding site (Martin and Rosner, 1995). Curiously, some protein biosynthesis inhibitors like chloramphenicol and tetracycline appear to induce the *marRAB* operon without binding to MarR. However, the mechanism behind this induction is yet unknown (Martin and Rosner, 1995). Additionally, MarR may act as a sensor for copper ions (Cu^{2+}), which cause the formation of cysteine-cysteine disulfide bonds leading to conformational changes. Interestingly, salicylate appears to be able to release copper from metabolic enzymes, which could further explain its ability to derepress the *marRAB* operon (Hao et al., 2014). As mentioned before, overexpression of *marA* leads to a multiple antibiotic resistance phenotype, whereas deletion of *marA* causes cells to become more sensitive to a range of antibiotics (Hächler et al., 1991; Cohen et al., 1993a). These phenotypes can be mostly attributed to the regulation of the AcrAB-TolC efflux pump and MicF small RNA, which in turn

regulates translation of OmpF porin (Cohen et al., 1988; Rosner et al., 1991; Cohen et al., 1993b; Okusu et al., 1996; Chubiz and Rao, 2011).

Even though SoxS and MarA share an identity of almost 50%, they differ greatly in the genes they regulate, despite the shared regulon. The preference of either of the three regulators towards specific genes within the regulon may be explained by the degeneracy of the *mar-sox-rob* box (Martin et al., 2000). SoxS was identified as a determinant for survival during oxidative stress conditions caused by reactive oxygen and nitrogen species or redox-cycling compounds (Greenberg et al., 1990; Tsaneva and Weiss, 1990; Amábile-Cuevas and Demple, 1991; Wu and Weiss, 1991; Nunoshiba et al., 1992a). Regulation of *soxS* is in some ways opposite to the *marRAB* operon, even though it is also based on a specific regulator named SoxR. In this case, *soxR* and *soxS* are transcribed divergently and SoxR acts as a transcriptional activator instead as a repressor (Nunoshiba et al., 1992a). Furthermore, the SoxR dimer needs to be activated to function as a transcriptional activator. This is achieved by oxidation of an iron-sulfur cluster [2Fe-2S] within each SoxR monomer, leading to a conformational change, allowing SoxR to induce transcription of *soxS* (Hidalgo and Demple, 1994). Canonical inducers of *soxS* expression are the redox-cycling compound paraquat (methyl viologen) or phenazine, which ultimately cause oxidative stress due to formation of reactive oxygen species (ROS) (Nunoshiba et al., 1992a; Gu and Imlay, 2011). Contrary to MarA, SoxS is an autorepressor, instead of an autoinducer, ultimately limiting its own expression (Nunoshiba et al., 1993). Consistent with the role of SoxR in sensing oxidative conditions, SoxS rather specifically induces expression of several genes involved in detoxification of reactive oxygen species, such as *sodA* and *fumC*. (Greenberg et al., 1990; Liochev and Fridovich, 1992).

The least well characterized regulator out of the three is Rob, which was initially identified as a DNA binding protein at the origin of replication (**r**ight **o**rigin **b**inding), hence its name (Skarstad et al., 1993). Later on, Rob was grouped together with MarA and SoxS based on its sequence similarity and its capability to induce genes related to antimicrobial resistance and oxidative stress (Ariza et al., 1995; Jair et al., 1996). In contrast to MarA and SoxS, regulation of Rob

appears to happen mostly at the posttranscriptional level. Rob is transcribed constitutively at about 5000-10000 copies per cell, albeit in an inactive form due to its unique C-terminal domain (Skarstad et al., 1993). This domain causes Rob to form intracellular aggregates or foci, preventing DNA binding and therefore its function as transcription factor (Azam et al., 2000). Chemically unrelated compounds such as bile acids, decanoate or 2,2-bipyridyl are able to activate Rob by causing dispersion of the intracellular aggregates (Griffith et al., 2009). Currently, it is not clear how exactly this "sequestration-dispersal" mechanism works, since purified Rob does not aggregate and is fully active, opening up possibilities for yet undescribed factors involved in the regulation of Rob *in vivo* (Rosner et al., 2002; Griffith et al., 2009). Contrary to its constitutive expression, Rob acts as an autorepressor at its own promoter, which might serve to limit extensive induction but allows limited expression throughout growth (Chubiz et al., 2012).

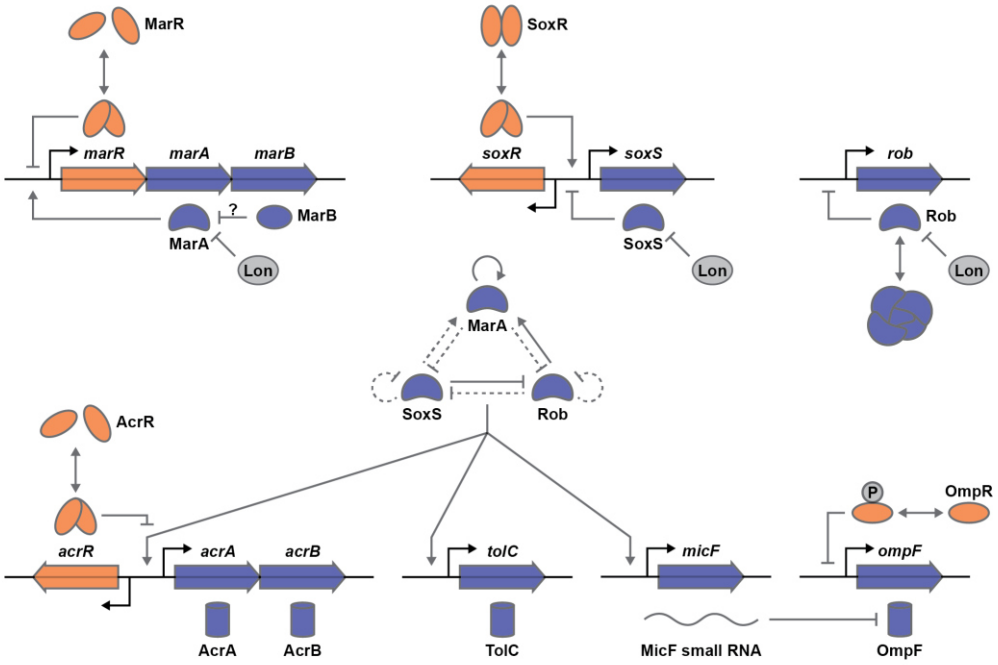

Figure 3: Cross-regulation within the Mar-Sox-Rob network and transport related regulon genes. MarA induces expression of its own operon *marRAB*, whereas SoxS and Rob repress their own genes expression, respectively. MarA is able to repress expression of SoxS and Rob, while both these regulators can induce expression of the *marRAB* operon. SoxS and Rob are able to inhibit expression of each other, respectively. Some of these regulatory interactions can be observed at physiological conditions, while others are only relevant during over-expression of a given regulator. Figure adapted (Chubiz et al., 2012; Du et al., 2018a).

In addition to the regulatory mechanisms of *marRAB, soxRS* and *rob* mentioned above, all three regulators also feature a *mar-sox-rob* box in their respective promoter regions, implicating cross regulation by each other (Chubiz et al., 2012). This aspect of how the Mar-Sox-Rob network operates has only been studied to a limited extent using a few selected canonical inducers and gene deletions to infer how much the regulators affect each other. The *marRAB* operon can be induced by both SoxS and Rob, with Rob being accountable for up to half the basal expression of *marA* under physiological conditions (Chubiz et al., 2012). On the contrary, *rob* and *soxS* can be repressed by both of the other regulators, on top of their negative autoregulation. However, this repression appears to be relevant only at elevated levels of all three regulators and less so under physiological conditions (Chubiz et al., 2012). Finally, all three regulators are degraded by the Lon protease, although Rob in its sequestered form is shielded from Lon by its unique C-terminal domain (Griffith et al., 2004, 2009). This posttranslational layer of regulation may serve to limit activation of the stress responses in a temporal manner.

Systematic Approaches to Study Gene Function and Regulation

Gene regulation and impact on corresponding protein levels have been studied for decades in a way that only encompassed few genes or proteins per study due to the lack of high-throughput methodologies. In terms of nucleic acids, this changed with the development and increased availability of sequencing techniques, such as next generation sequencing (NGS), microarrays and RNA sequencing, allowing to monitor the whole RNA pool (transcriptome) in a given sample using transcriptomics. Likewise, improved mass spectrometry techniques allowed surveying the entirety of proteins (proteome) or metabolites (metabolome). Taken together, all these methodologies allow tracking thousands of biomolecules simultaneously, hence enabling global comparative studies between samples. Usually, the bottleneck with these techniques lies in the amount of samples that can be processed, limiting the number of perturbations that can be compared, due to the complex machinery and associated cost required. Another major limitation is the lack of functional

annotation of the many putative genes identified by sequencing, making more systematic approaches necessary.

Development of bacterial loss-of-function (LOF) and gain-of-function (GOF) genetic libraries made it possible to determine conditionally essential genes and assign function to uncharacterized genes. Such libraries consist of thousands of individual strains in which single genes are either deleted or overexpressed, enabling characterization of the whole genome of organisms at once (Baba et al., 2006; Kitagawa et al., 2005). LOF libraries can be produced using gene editing methods based on transposon mutagenesis, Lambda RED recombineering or CRISPR Cas9. GOF libraries, on the other hand, are usually plasmid-based and utilize either strong constitutive promoters or ones that are inducible by e.g. IPTG or L-arabinose. Generally, genetic libraries can be used either pooled, with thousands of individual mutant strains in the same liquid culture, or they can be used arrayed, requiring robotics to handle the strains on agar plates or microtiter plates (Figure 4).

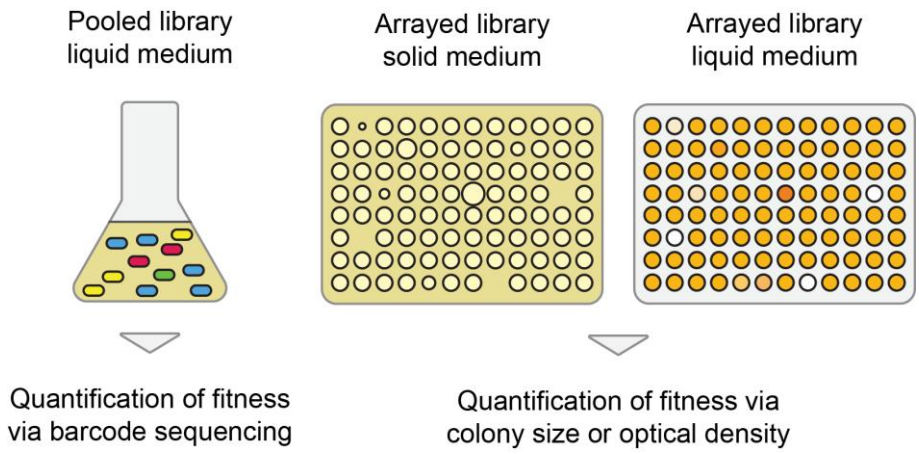

Figure 4: Schematics of high-throughput genetic phenotyping approaches. a) Differences between pooled and arrayed screening methods. Quantifcation of mutant quantities in pooled screening approaches is done with barcodes, which can be detected either by sequencing or using microarrays. Arrayed screenings are performed either in liquid with optical density as measure of growth or on agar plates using colony size and density to measure fitness.

Both approaches have their strengths and weaknesses in terms of ease of use and experimental suitability. Use of pooled libraries does not need robotics equipment but relies on quantification via sequencing, which is overall more

accessible and can be scaled up well. On the other hand, pooled libraries are biased in a way that all strains compete with each other, causing slow growing mutants to be potentially under-represented. Conversely, some mutations that would normally lead to growth deficits can be alleviated by secreted metabolites within the whole population. Use of arrayed libraries comes with the immediate downside of requiring robotics and high expenses in consumables, severely limiting accessibility. On the positive side, arrayed libraries allow tracking growth of every mutant strain individually, independent of all other mutant strains, and are more suitable for genetic interaction screens or alternative readouts, e.g. fluorescence or luminescence based reporters.

Arrayed LOF libraries made it possible to systematically generate double mutants across the whole genome, by transferring a deletion with a second resistance cassete to the arrayed library (Butland et al., 2008; Typas et al., 2008). Comparison of fitness between the single deletions and the double mutant provides information that can be used to identify genes or proteins that belong to the same pathways or fulfill similar functions. This facilitates discovery of new cellular machineries or missing links in known pathways and between cellular processes and therefore allows assigning function to undescribed genes. Furthermore, gene-gene interactions can be used to find conditionally essential genes, again providing context about gene function and genetic networks (Babu et al., 2011).

Similarly, genetic libraries allow studying gene-drug interactions using chemical genomics approaches, treating whole libraries with drugs and comparing each mutant's fitness to a non-treated control. This approach can again be used to infer information about a gene's function or to place it into specific pathways, but also to identify the mode of action (MOA) of the drugs used to treat the bacteria. The latter can be achieved by using inducible promoters or plasmids increasing the copy number of a gene to consequently increase protein levels. As increased target protein levels usually require increased concentrations of the drug, this approach usually leads to drug resistance and allows identification of the main drug target.

Finally, liquid handling robotics made it possible to study drug-drug interactions at a larger scale than ever before. Especially synergistic combinations of antibiotics have the potential to overcome resistance against individual drugs. Instead of a clinical application, drug combinations can also be used to perturb multiple cellular processes at once and to study, e.g., the evolution of resistance to the combinations compared to the single drugs (Yeh et al., 2009). On the other hand, some antagonistic antibiotic combinations were shown to suppress evolution of antimicrobial resistance and therefore need to be understood better (Chait et al., 2007). Chemical genomics approaches, as mentioned before, can provide information about the mode of action of individual drugs, but can also be used to elucidate the mechanisms behind drug interactions (Nichols et al., 2011). Beyond traditional antibiotics, also non-antibiotics have the potential to modulate antimicrobial action and therefore need to be systematically explored (Ejim et al., 2011). Finally, high throughput characterization of drug-interactions across three gram-negative species revealed drug interactions to be highly species dependent, adding yet another layer of complexity (Brochado et al., 2018). Understanding the mechanisms behind drug interactions may enable rationally design of drug combination treatments in the future that are optimized for maximum efficacy and low potential to promote evolution of antimicrobial resistance.

Aims of this thesis

Inhibition of drug transport across the bacterial membrane has been identified as one potential mechanism behind antagonistic drug interactions (Brochado et al., 2018). Therefore, the overarching goal of this thesis is to gain novel insights into how a multitude of structurally diverse chemicals – including antibiotics – affect core determinants of drug transport, e.g. AcrAB-TolC and OmpF. As the Mar-Sox-Rob network is highly important for the regulation of these transport machineries, as well as antimicrobial resistance and stress responses generally, this thesis also aims to understand how expression of all of these genes is affected by chemical stress. As mentioned above, the dynamics within the Mar-Sox-Rob network have been tested only using artificial overexpression systems and using a limited range of canonical inducers. To this end, the goal of this thesis is to learn more about how the whole Mar-Sox-Rob network behaves under more diverse chemical stress, how cross-regulation is affected and how much each regulator contributes to the expression of the respective regulon genes. Understanding of how chemical cues alter bacterial transport may facilitate the design of novel drugs or drug combination therapies, avoiding potential drug antagonisms caused by alterations in transport.

Chapter 1) Probing the Mar-Sox-Rob network with chemical screening

The contents of this chapter have been used in the manuscript “Systematic Characterization of Transport Regulation in *Escherichia coli* across defined environmental cues” and shared as a preprint version on “biorxiv.org” (doi: https://doi.org/10.1101/2024.08.26.609649).
The manuscript was subsequently published at PLOS Biology: “Binsfeld C, et al. (2025) Systematic screen uncovers regulator contributions to chemical cues in *Escherichia coli*. Doi: https://doi.org/10.1371/journal.pbio.3003260, PLoS Biol 23(7): e3003260“. The pTU175-lux empty vector that was used by me to construct all reporter plasmids was constructed and shared Morgane Wartel. Cloning of reporter plasmids and corresponding strains was done by me with help from Regina Tschertok. I performed all screening and follow up experiments in this chapter and conceptualization and data analysis were done under supervision from Prof. Dr. Ana Rita Brochado. All figures and text in this chapter were produced by me under supervision from Prof. Dr. Ana Rita Brochado.

Unravelling transcriptional regulation of transport-related genes in *E. coli* under chemical stress

We set out to systematically investigate the transcriptional response of a set of prominent genes controlling transport in *E. coli* across 94 defined chemical stresses in a concentration resolved manner. To meet our aim of uncovering the cross-talk between transport-related genes, rather than genome-wide transcriptional analysis, we prioritized an experimental design that enables close quantitative monitoring of transcriptional changes (even if small) in a set of promoters over a range of compound concentrations. Therefore, we constructed plasmid-based luminescence reporters for 7 genes, 6 of which contain the degenerate Mar-Sox-Rob box in their promoter region: the key transcription factors *marA*, *soxS* and *rob*, *acrAB* and *tolC*, which are both components of the major efflux pump AcrAB-TolC, and the small-RNA MicF, a

post-transcriptional regulator of *ompF* (Ramani et al., 1994). In addition, we included a reporter of *ompF* transcription, to monitor the transcriptional response of transport-related genes that are not under direct control of MarA, SoxS or Rob (Methods, Tables 1 and 2). Our promoter selection was prioritized based on impact of each gene product on intrinsic antibiotic resistance. Even though *E. coli* has more than 30 efflux pumps, AcrAB-TolC is widely described as the most impactful for intrinsic antibiotic resistance, and, in addition, it is under tight transcriptional control (Nishino and Yamaguchi, 2001; Sulavik et al., 2001; Teelucksingh et al., 2022b). Similarly, OmpF is the dominant porin for intrinsic resistance under our working conditions (Choi and Lee, 2019; Nichols et al., 2011), and mutations in *acrB* and *ompF* are frequently selected in laboratory evolution experiments under antibiotic pressure, highlighting their determinant role in intrinsic resistance (Suzuki et al., 2014). MicF was included because of its prominent OmpF posttranscriptional control while being itself under tight transcriptional regulation (Ramani et al., 1994), and MarA, SoxS and Rob were included because they orchestrate large transcriptional responses to different environmental and chemical stresses, and their regulons include several of the transport genes mentioned above.

In total, we probed 658 compound-promoter pairs. As many compounds, and specifically antibiotics, are known to cause vast transcriptional effects (Andersson and Hughes, 2014; Goh et al., 2002), we included a reporter strain containing a promoterless/leaky luminescence reporter (empty vector control, EVC) to better control for possible non-specific transcriptional effects of each compound. We assembled a collection containing 94 compounds including all major antibiotic classes, human-targeted drugs (e.g. aspirin), gut metabolites (e.g. bile acids) and small-molecules found in common foods (e.g. vanillin, Figure 5, Table 4). We ensured high overlap of the compound library with our previous work on systematic assessment of drug combinations in Gram-negative bacteria (61 out of 79 compounds) (Brochado et al., 2018) , to enable downstream integration of the datasets for interpretation purposes. All compound-promoter pairs were probed in duplicates across four compound concentrations (2-fold dilutions, Figure 31). Maximum concentrations were adjusted to be close to minimum inhibitory concentration (MIC) for

antimicrobials, 500 µM for most non-antimicrobials, and up to 1 mM for small compounds with similarity to canonical inducers (positive controls, e.g. salicylate, Table 4, Methods).

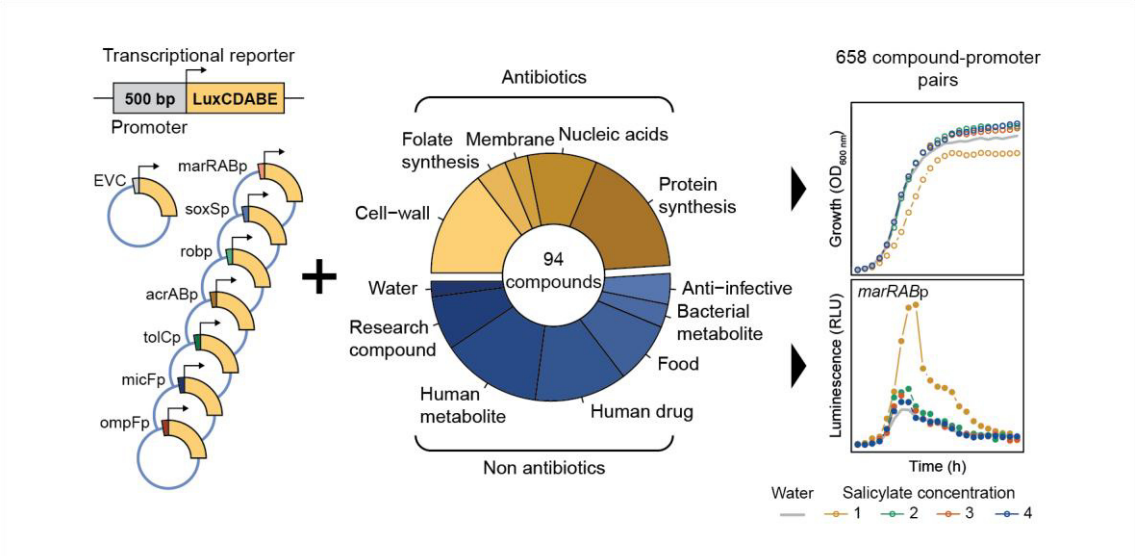

Figure 5: Schematic overview of screening approach. Lux-based transcriptional reporters of 7 key transport-related genes and the compound library used in this study to probe 658 compound-promoter interactions. Growth and luminescence were periodically measured over 12 h. Figure adapted from manuscript (Binsfeld et al., 2025).

Briefly, growth (optical density, $OD_{600\ nm}$) and luminescence for each reporter strain were periodically monitored over 12 hours in the presence of each individual compound at all concentrations (Methods). Area under the curve for a period of 8h (AUC) was used as a proxy for growth (OD_{AUC}) and luminescence (Lux_{AUC}) profiles (onset of stationary phase, Figure 31). As expected, growth was reasonably constant across all reporter strains, while luminescence showed a large dynamic range depending on the promoter, with tolCp showing the lowest and ompFp the highest signal (Figure 6a and 6b). High data quality is reflected by Pearson correlation between replicates above 0.8 across all promoters, except for tolCp, likely due to its weak promoter strength (Figure 6c). We excluded the possibility that some compounds, namely protein synthesis inhibitors, could increase plasmid copy number (as previously reported for different origin of replication (Sambrook et al., 1989)) by quantitative PCR (Figure 6d). Nonetheless, since the effect of compounds expected to trigger its expression via oxidative stress – e.g. phenazine methosulfate – could be captured here, we decided to keep tolCp in our dataset.

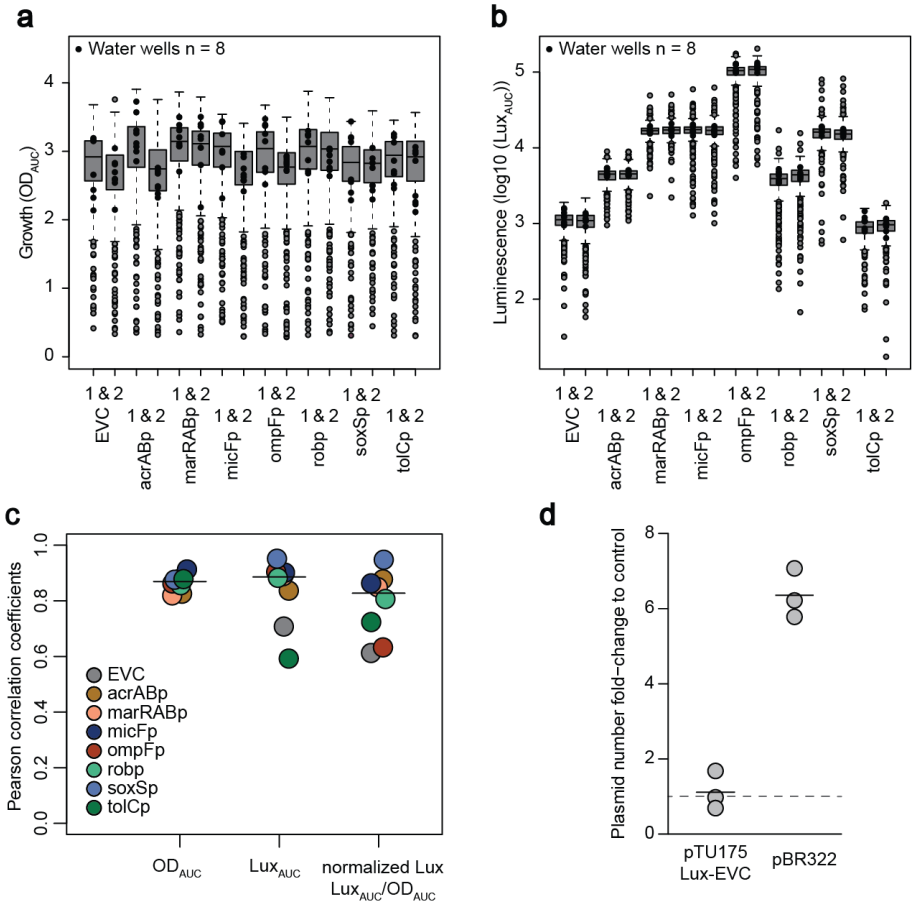

Figure 6: Quality controls of growth and luminescence screening data. a) Boxplots of growth (OD_{AUC}) across all reporters and replicates. Each boxplot represents a 384 well-plate (n = 384). Negative controls (water treatment) are displayed in black (n = 8 per strain). 1 & 2 refer to biological replicates. Center, upper and bottom lines represent 50, 75 and 25% percentiles, whiskers extend to 1.5x inter-quartile range (IQR) and points beyond whiskers are represented individually. **b)** Boxplots of luminescence (AUC_{LUX}) data across all reporters and replicates. Each boxplot represents a 384 well-plate (n = 384). Negative controls (water treatment) are displayed in black (n = 8 per strain). 1 & 2 refer to biological replicates. Center, upper and bottom lines represent 50, 75 and 25% percentiles, whiskers extend to 1.5x IQR and points beyond whiskers are represented individually. **c)** Pearson replicate correlation of growth (OD_{AUC}), luminescence (LUX_{AUC}) and normalized luminescence (LUX_{AUC}/OD_{AUC}) between the duplicates of each strain. **d)** Treatment with protein biosynthesis inhibitors does not affect copy number of pTU175 plasmids. Relative fold-change of pTU175-Lux-EVC and pBR322 after treatment with 2 µg/ml chloramphenicol compared to a negative control using qPCR. Three biological replicates are shown. Figure adapted from manuscript (Binsfeld et al., 2025).

Next, we systematically assessed *Compound-Promoter Interactions* (CPIs), which we define as increased or decreased *promoter* activity as measured by our luminescence reporter in the presence of the *compound* (Methods, Figure 31). Briefly, we computed an *interaction score* for any given *compound-promoter* pair based on its deviation of normalized luminescence (Lux_{AUC}/OD_{AUC}) to the c*ompound-EVC*. We subsequently Z-transformed the

interaction scores (Z-scores) to allow comparability of promoters of varying signal intensity. Finally, significant CPIs were called based on a double cutoff on mean Z-scores and rank-sum test p-value comparing the Z-score distributions of each compound-promoter with that of water-promoter (Figure 7a, Methods).

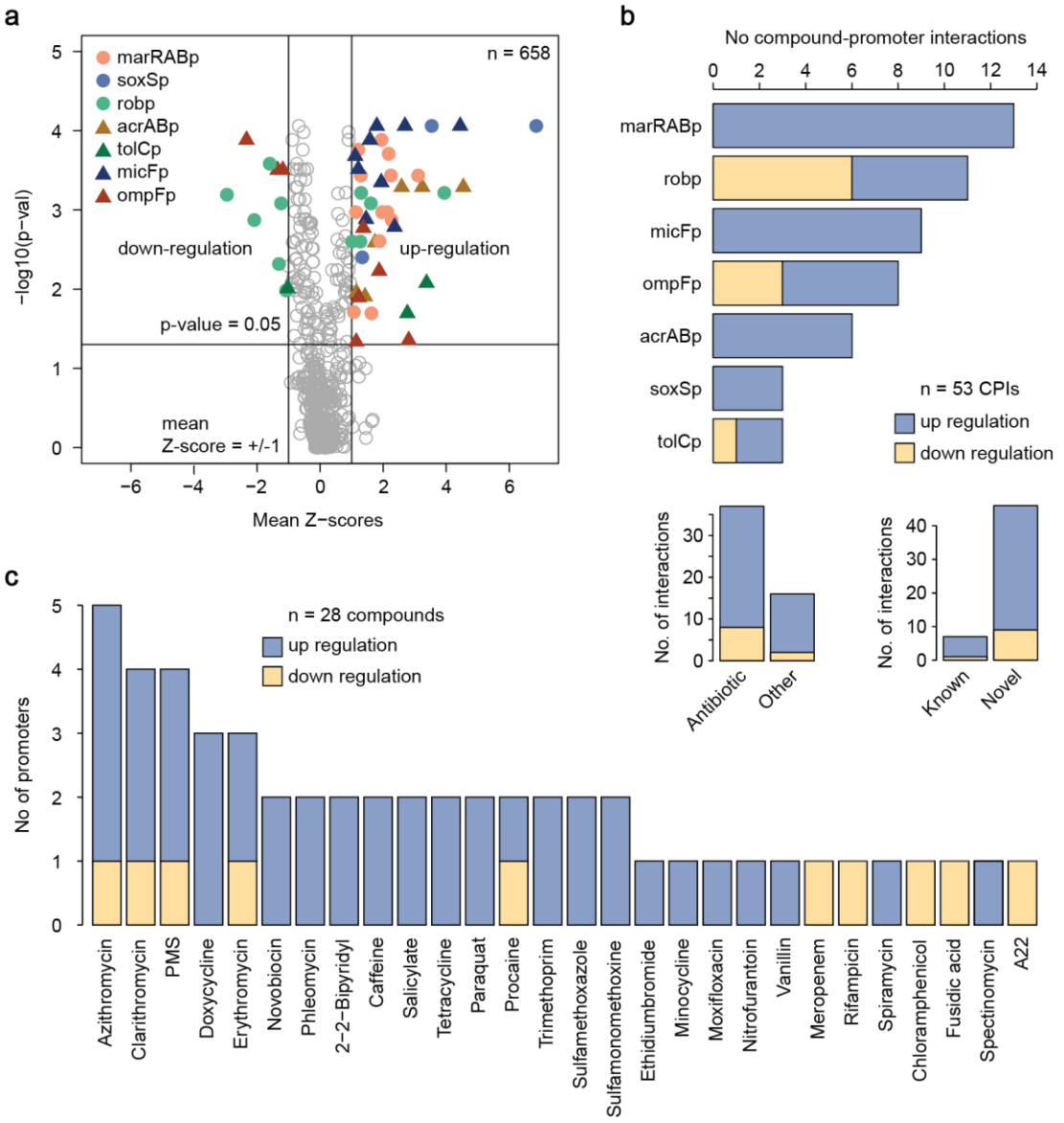

Figure 7: Summary of screening results. a) Compound-promoter interactions in *E. coli*. Volcano plot summarizing the screen results shows 53 significant CPIs (colored by promoter) amongst 658 tested (+water, n=672 in total). X-axis: mean Z-scores (n=4 concentrations x 2 biological replicates = 8). Y-axis: Benjamini Hochberg adjusted p-value of double-sided rank-sum statistical tests between Z-scores of compound-promoter pairs (n=8) and water (n=16). **b)** General features of compound-promoter interactions (CPIs). Number (No) of interactions per promoter (left), their classification according to novelty (upper right corner) and whether they involve an antibiotic (lower right corner) are shown. **c)** General features of CPIs: number of CPIs per compound classified as up and down-regulation. Figure adapted from manuscript (Binsfeld et al., 2025).

While the majority of the 28 compounds are antibiotics, ~1/3 of all identified CPIs involve non-antibiotic compounds, showing that non-antibiotics also modulate transport across the cell envelope (Brochado et al., 2018; Ricaurte et al., 2024) (Figure 7c). The number of interactions per promoter varies between three for soxSp and tolCp and 13 for marRABp, confirming differences in promoter specificity towards chemical cues.

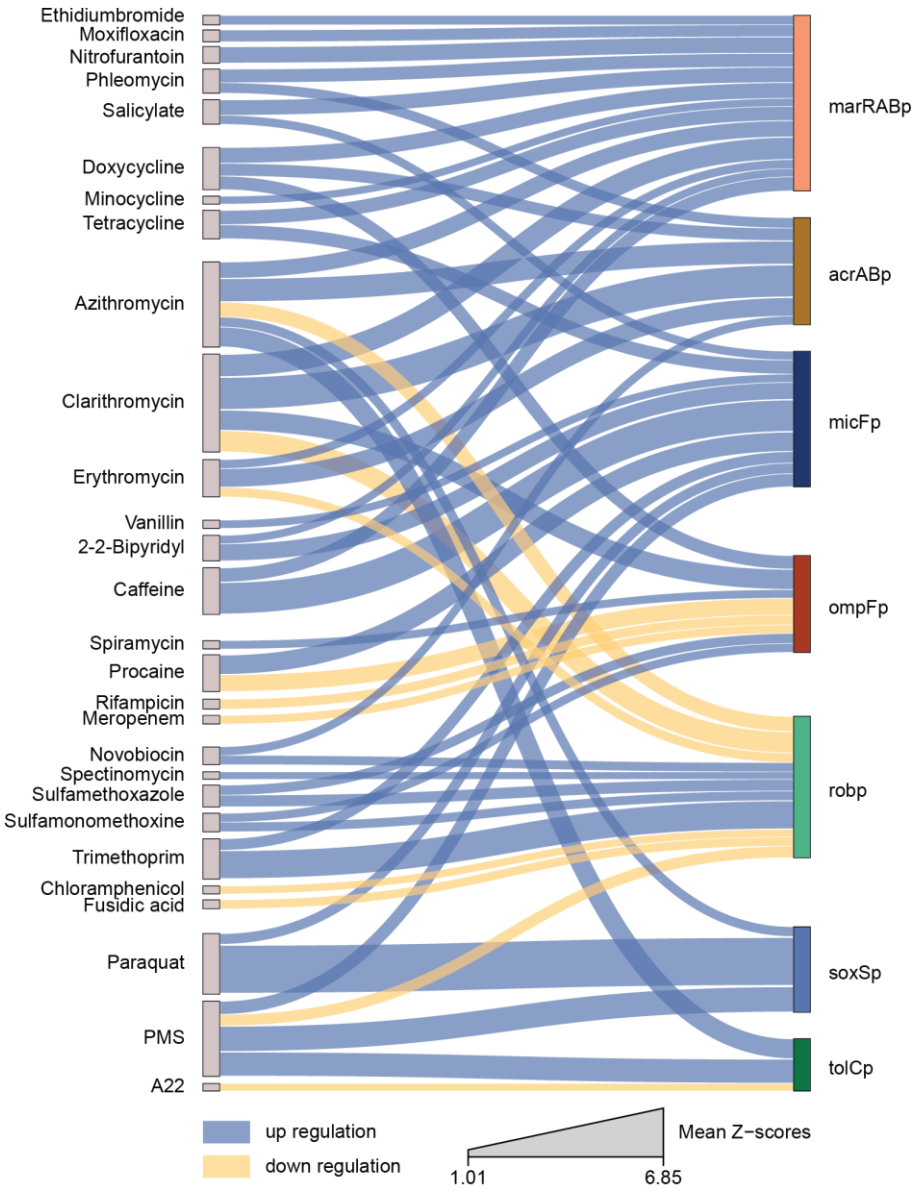

Figure 8: Network of identified compound-promoter interactions. 53 significant compound-promoter interactions are shown as edges in a Sankey diagram connecting the compounds (left, source nodes) to the promoters (right, target nodes). Edge thickness represents mean Z-scores (n = 8), while node size represents the total number of interactions. Figure adapted from manuscript (Binsfeld et al., 2025).

In addition, more than half of the 28 compounds triggered at least two promoters, confirming vast regulatory cross-talk between the major players of transport in *E. coli* (Figure 7b). Protein synthesis inhibitors emerge as the most promiscuous compounds, as tetracyclines and macrolides triggered simultaneous transcriptional responses in up to 5 out of 7 promoters (Figure 8c). Looking at individual CPIs, we were able to recapitulate several canonical compound-promoter pairs, including salicylate-marRABp (Alekshun and Levy, 1999; Cohen et al., 1993b), paraquat-soxSp (Nunoshiba et al., 1992b), procaine-micFp (Ramani et al., 1994), procaine-ompFp (Rampersaud and Inouye, 1991), and 2,2-bipyridyl-micFp (Rosner et al., 2002), confirming that our screen correctly captures existing knowledge (Figure 8 and examples at Figure 9a and 9b).

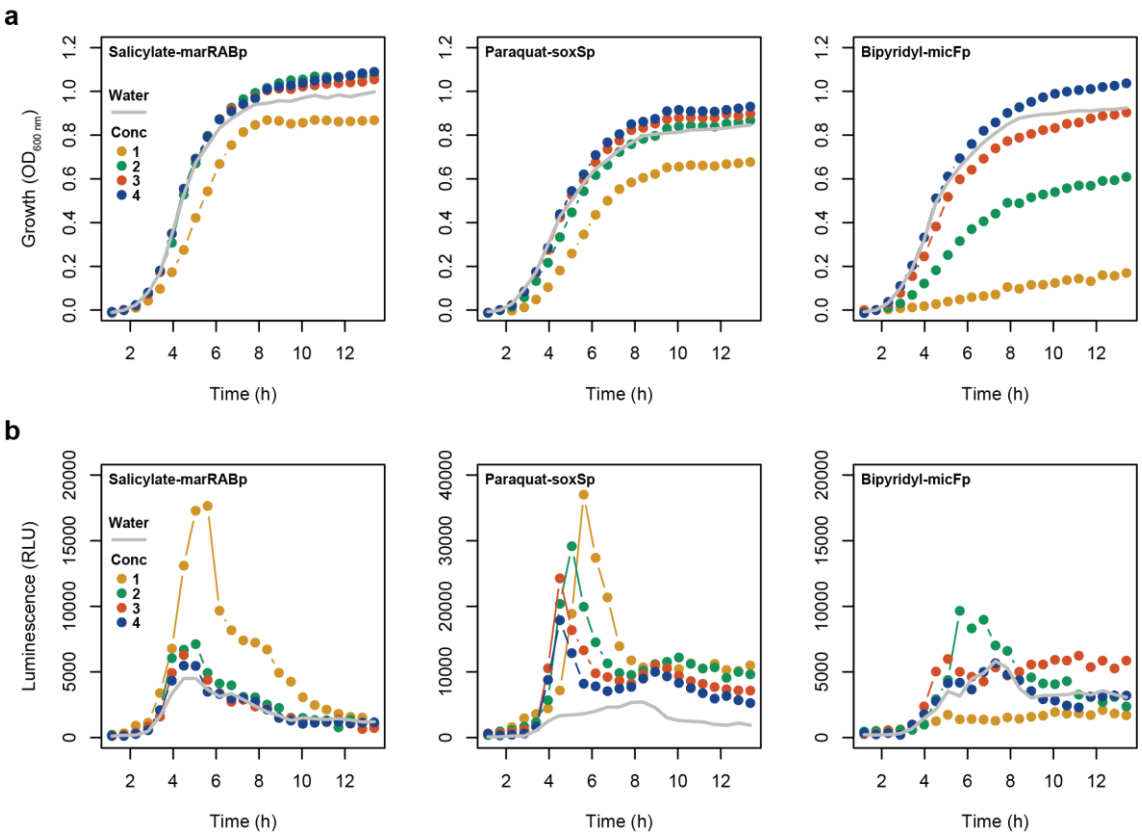

Figure 9: Screening identifies canonical *marA*/*soxS*/*micF* promoter interactions. Previously known CPIs salicylate-marRABp, paraquat-soxSp and 2,2-bipyridyl-micFp are captured by our screening approach. **a)** Growth ($OD_{600\ nm}$) and **b)** luminescence (RLU) profiles over time for marRABp (left), soxSp (middle) and micFp (right) basal activity (grey) and with increasing concentrations of salicylate, paraquat or 2,2-bipyridyl, respectively (conc., Table 4) are shown. One out of two biological replicates is shown. Figure adapted from manuscript (Binsfeld et al., 2025).

Compound-dependent repression occurred mostly for the *rob* promoter, consistent with previous reports that *rob* is subject to repression by e.g. MarA and SoxS (Chubiz et al., 2012; Michán et al., 2002; Schneiders and Levy, 2006) (Figure 7a & Figure 8). Furthermore, our network shows a rather specific oxidative-stress response of soxSp, also consistent with previous reports (Chubiz et al., 2012). Importantly, our approach misses known interactions, for instance vanillin-marRABp or chloramphenicol-marRABp (Brochado et al., 2018; Hächler et al., 1991). We attribute this to the facts that we used stringent statistical cutoffs to minimize false positive discovery, and comparatively low concentrations aiming at identifying stronger and specific interactions. Thus, we are most likely underestimating CPIs. Nevertheless, ~80% of all CPIs we describe here have not been previously reported (Figure 7b). For instance, we identified tetracycline derivatives, e.g. doxycycline and minocycline, as novel marRABp inducers, beyond the previously reported tetracycline itself (Hächler et al., 1991). Importantly, we identified macrolides (azithromycin, clarithromycin and erythromycin) and antifolates (sulfonamides and trimethoprim) as novel antibiotic classes triggering several of the tested promoters (Figure 8). Beyond antibiotics, we identified the widely consumed food ingredient caffeine as novel marRABp and micFp inducer.

General principles driving transport compound-promoter interactions

Capitalizing on our efforts of assessing promoter activity across environmental cues, we next aimed at uncovering general features driving environment-dependent transport regulation in *E. coli*. Since many of our CPIs involved antibiotics, we questioned whether antimicrobial activity is a pre-requisite for modulating gene expression. Indeed, we observed that our set of 28 compounds instigate, on average, lower minimum growth (OD_{AUC}) when compared to the compounds that did not trigger the tested promoters (Figure 10a). However, also compounds without antimicrobial activity at the concentrations tested (e.g. vanillin, caffeine, growth identical to control at all concentrations tested) are represented among our CPIs, and thus antimicrobial activity is not required to trigger transcriptional changes in transport related genes (Figure 10a).

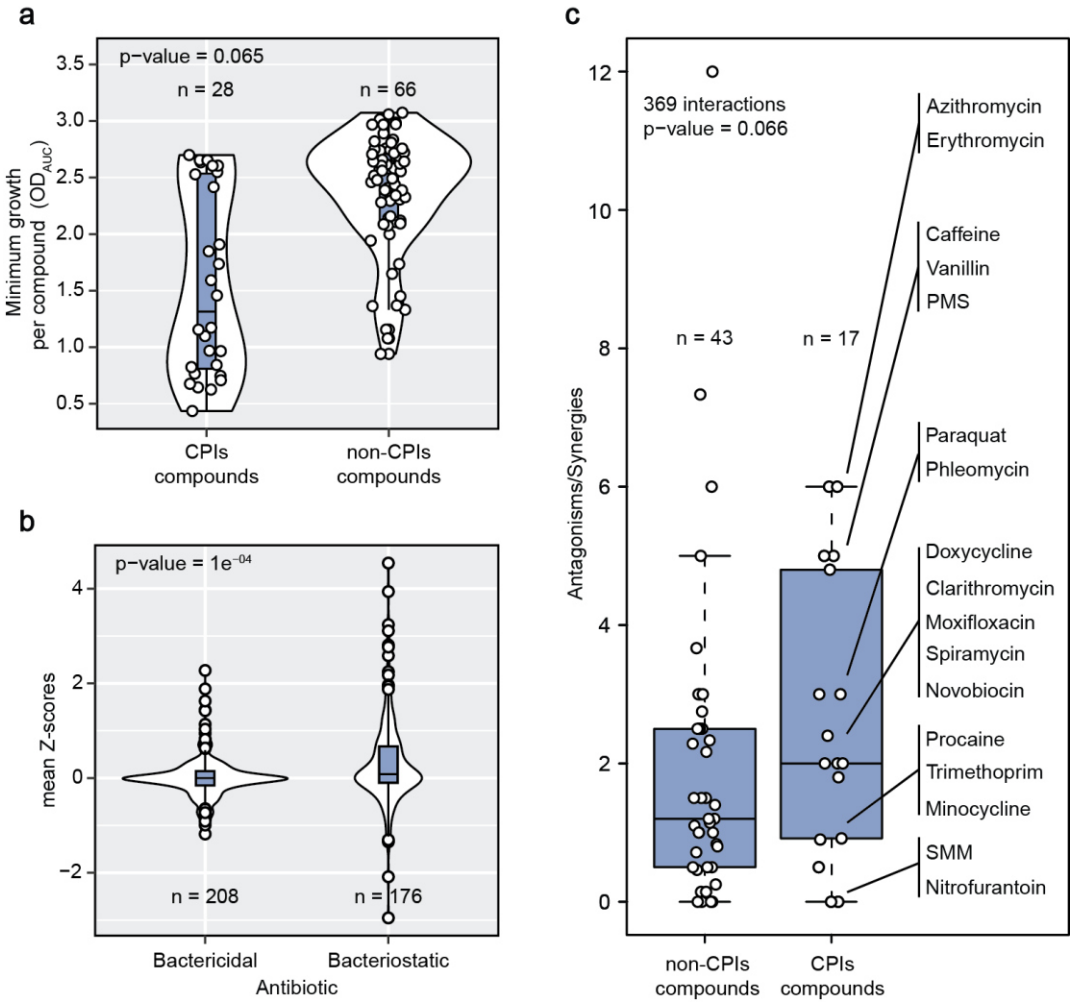

Figure 10: General principles driving transport compound-promoter interactions. a) Most compounds identified within CPIs have antimicrobial effect. Distribution of minimum growth (0.1 quantile of all ODAUC measurements for a given compound, 4 concentrations x 8 strains x 2 replicates = 64 values) of all compounds tested (n_{total} = 94), classified according to whether they are (or not) involved in CPIs. P-value from a double-sided rank sum statistical test between the two distribution depicted in the plot is shown (null-hypothesis is that both distributions are identical). Boxplots indicate 25th, 50th and 75th percentiles, and whiskers extend up to 1.5 times the interquartile range (IQR) from the 25th and 75th percentiles. **b)** Bacteriostatic antibiotics are over-represented within strong CPIs. Mean Z-scores distributions of all tested compound-promoter pairs involving antibiotics (n_{total} = 384), classified according to whether the antibiotic is bactericidal or bacteriostatic. P-value from a double-sided rank sum statistical test between the two distributions depicted in the plot is shown (null-hypothesis is that both distributions are identical). Boxplots indicate 25^{th}, 50^{th} and 75^{th} percentiles, and whiskers extend up to 1.5 x IQR from the 25^{th} and 75^{th} percentiles. **c)** Compounds within CPIs are over-represented among antagonistic drug interactions. Boxplots of ratios antagonisms over synergies (total 369 interactions) for all tested compounds which overlap with our previous work (Brochado et al., 2018) (n_{total} = 60), classified according to whether they are (or not) involved in CPIs. P-value from a one-sided rank sum statistical test is shown. Center, upper and bottom lines represent 50, 75 and 25% percentiles, whiskers extend to 1.5x IQR and points beyond whiskers are represented individually. Figure adapted from manuscript (Binsfeld et al., 2025).

Next, we asked whether the nature of the antibiotic – bactericidal or bacteriostatic – correlates with its ability to trigger transcriptional changes amid the tested promoters. Interestingly, we found that bacteriostatic antibiotics are enriched for extreme Z-scores (Figure 10b). In fact, bacteriostatic antibiotics such as tetracyclines, macrolides or sulfonamides account for half of the 53 CPIs described here. Next, because our previous work showed that antagonism is often associated with decreased intracellular antibiotic concentrations (Brochado et al., 2018), we hypothesized that compounds impacting transport regulation could decrease the concentration of certain antibiotics, and thus exhibit antibiotic antagonism. We combined our results with the data from our previous study, and found that the compounds that are represented in our set of 53 CPIs have indeed a higher chance than other tested compounds to be involved in antagonistic interactions (Figure 10c). Driven by the fact that growth inhibition is a strong trait of the compounds represented in the 53 CPIs (Figure 10a), we probed whether growth alone could explain the extent of promoter induction for any given promoter.

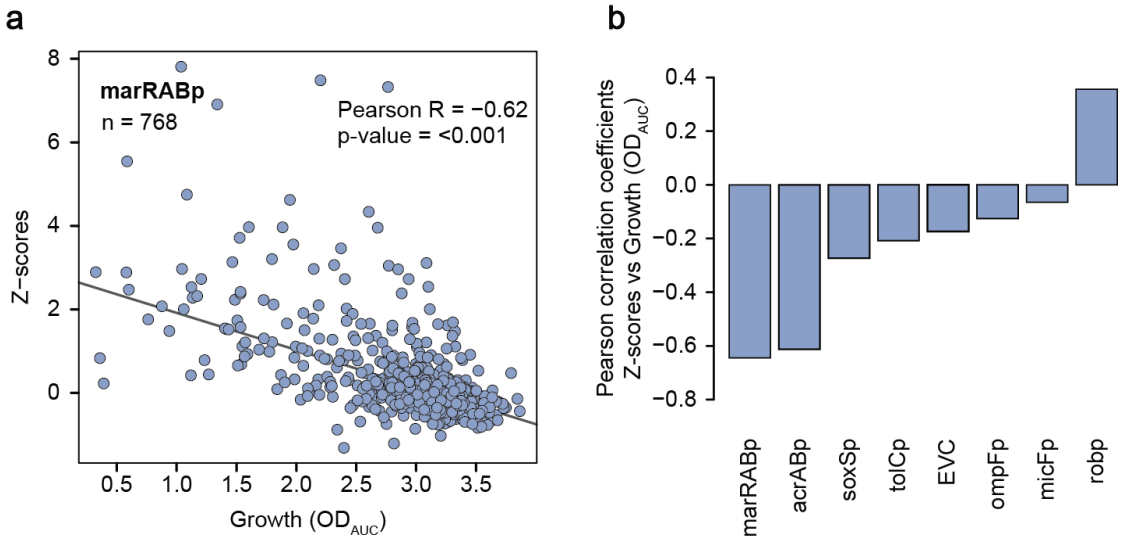

Figure 11: Correlation of promoter activity to growth inhibition. a) marRABp activity inversely correlates with growth. Z-scores of all compound-marRABp tested pairs including water across 4 concentrations and 2 biological replicates (n) are plotted against growth (OD_{AUC}). A strong negative linear relationship is illustrated by the line of best fit (Huber robust model). Correlation p-value (double sided t-test) shown. **b)** Promoter activity is generally not correlated with growth. Pearson correlation coefficients of Z-scores versus growth (OD_{AUC}) for each individual promoter. A strong negative Pearson correlation (>0.6) is only observed for marRABp and acrABp, while robp shows the opposite behavior. Correlation p-value (double sided t-test) < 0.005 for all promoters. Figure adapted from manuscript (Binsfeld et al., 2025).

By assessing correlation of Z-scores versus growth (OD_{AUC}) across all compounds for each individual promoter, we observed strong and significant negative correlation for marRABp and acrABp – meaning that these promoters get progressively stronger activation with increasing inhibitory capacity of the compound at hand (Figure 11a and 11b). This striking observation points towards a generalizable, non-specific, growth-driven response of marRABp across environments, in addition to the widely reported stress-specific response based on de-repression of promoter activity through compound-repressor binding (salicylate-MarR) (Alekshun et al., 2001; Hao et al., 2014).

Among new marRABp inducers, we independently validated that *marRAB* native expression is indeed induced by clarithromycin treatment using RTq-PCR (Figure 12a). In addition, RTq-PCR analysis revealed that sulfamethoxazole also triggers marRABp, although our screening approach was unable to capture it due to stringent cutoffs (Figure 12a). These findings provide a basis for promiscuous marRABp transcriptional activation by structurally diverse compounds, such as salicylate, clarithromycin and sulfamethoxazole (Figure 12b). We then confirmed that concentration-dependent transcriptional activation of marRABp by clarithromycin and sulfamethoxazole remains irrespective of whether its repressor MarR is present or not (Figure 12c and 12d). Even though weaker, the inverse tendency was observed for robp, where reporter expression increases with growth (Figure 11b). This finding increases the scope of previous observations that MarA may directly or indirectly cause *rob* down-regulation (Chubiz et al., 2012; Schneiders and Levy, 2006), as we find they follow this opposite trend across several environmental conditions. For the remaining promoters no comparable correlation was observed, suggesting growth-independent regulation.

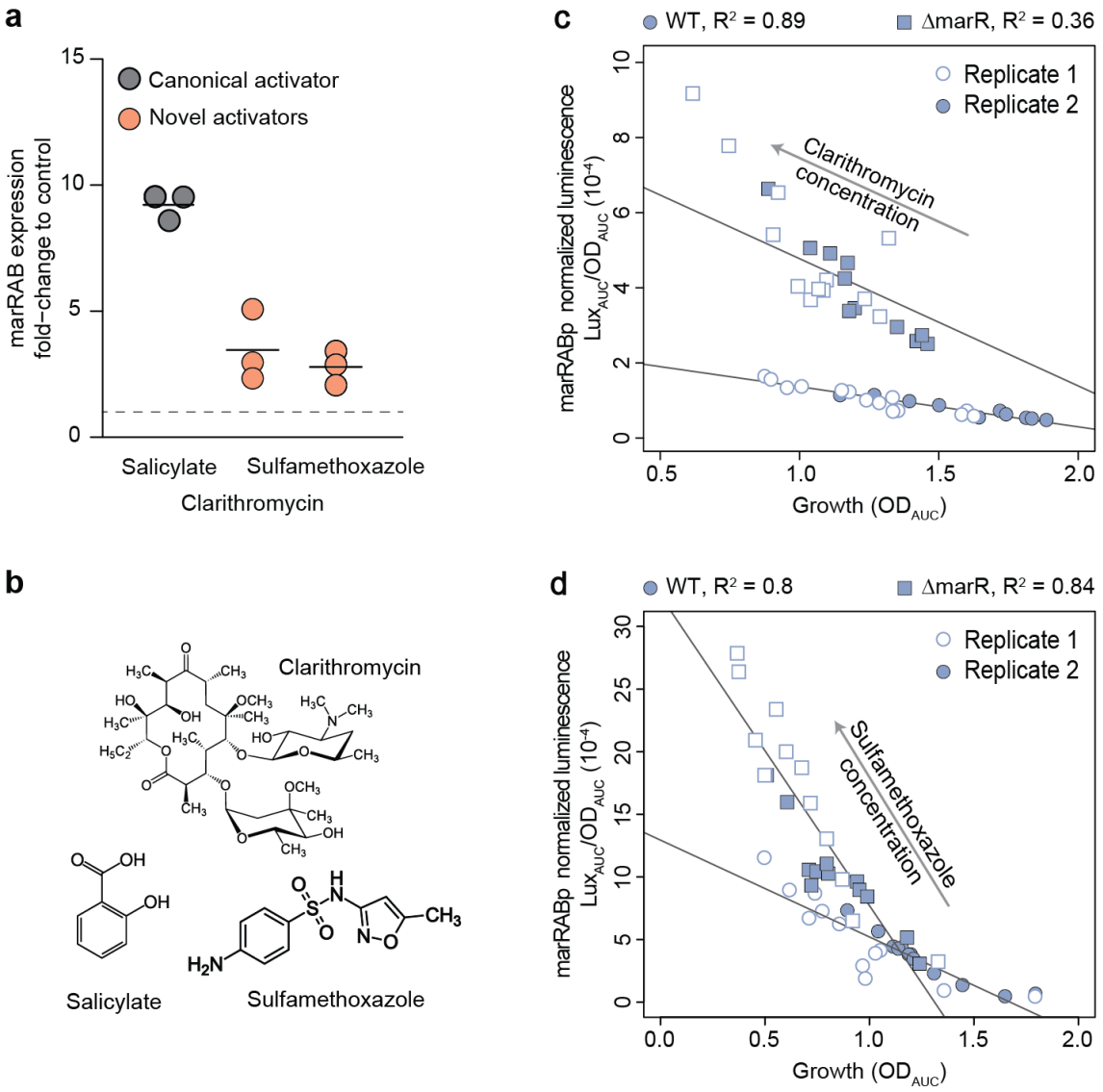

Figure 12: Clarithromycin and sulfamethoxazole are novel inducers of marRABp expression. a) RNA levels of *marA* after treatment with salicylate (positive control), clarithromycin and sulfamethoxazole. Data was double normalized to a non-treated control and to the house-keeping gene *recA* (Methods). Three biological replicates are shown. **b)** Chemical structures of known and novel marRABp inducing compounds. **c)** Induction of marRABp by clarithromycin, as well as its negative correlation with growth remain irrespective of the presence of MarR. Luminescence profiles over growth were measured across a linear range of clarithromycin concentrations from 0 µg/ml to 119.6 µg/ml in wild-type and Δ*marR* background. Growth-normalized luminescence is plotted against growth for two independent biological replicates, and lines-of-best-fit are shown to highlight strong correlation between the two variables. **d)** Induction of marRABp by sulfamethoxazole, as well as its negative correlation with growth, are independent of MarR. Luminescence profiles over growth were measured across a linear range of sulfamethoxazole concentrations from 0 µg/ml to 101.2 µg/ml in wild-type and Δ*marR* background. Growth-normalized luminescence is plotted against growth for two independent biological replicates, and lines-of-best-fit are shown to highlight strong correlation between the two variables. Figure adapted from manuscript (Binsfeld et al., 2025).

Chapter 2) Mapping regulator contributions to compound-promoter interactions

The contents of this chapter have been used in the manuscript “Systematic Characterization of Transport Regulation in *Escherichia coli* across defined environmental cues” and shared as a preprint version on “biorxiv.org” (doi: https://doi.org/10.1101/2024.08.26.609649).
The manuscript was subsequently published at PLOS Biology: “Binsfeld C, et al. (2025) Systematic screen uncovers regulator contributions to chemical cues in *Escherichia coli*. Doi: https://doi.org/10.1371/journal.pbio.3003260, PLoS Biol 23(7): e3003260“.
I constructed the mutant reporter strains, performed the screening experiments and supplied the input data (Scores) for the statistical model. Roberto Olayo-Alarcon, Mara Stadler and Prof. Dr. Christian Müller conceptualized the statistical model. Roberto Olayo-Alarcon programmed the R code to run the statistical model and supplied the coefficients as output data. I further analyzed the data under supervision from Prof. Dr. Ana Rita Brochado. Figures 14 and 15a were produced by Roberto Olayo-Alarcon and we produced Figure 20 together. Figure 15b and 15c were produced by Prof. Dr. Ana Rita Brochado. All other figures in this chapter were produced by me under supervision from Prof. Dr. Ana Rita Brochado. All text in this chapter was produced by me under supervision from Prof. Dr. Ana Rita Brochado with input from Roberto Olayo-Alarcon and Prof. Dr. Christian Müller.

To gain more specific insight into the mar-sox-rob network operational modes – in particular into whether and how regulator-promoter hierarchy changes across environmental cues – we generated individual knockout strains of the regulators *marA*, *soxS* and *rob*, and again probed the 658 compound-promoter pairs with our initial chemical library. Promoter preference towards a given regulator (as seen by loss of reporter activity upon regulator deletion) could already be observed for marRABp, soxSp, acrABp and micFp through altered basal promoter activity without any stress (Figure 13a). In most cases there seems to

be a preference for a single regulator, for instance, acrABp activity decreases only when MarA is absent. Nonetheless, micFp seems to be differently controlled, as its activity decreases in the absence of either MarA or Rob, pointing towards cooperation between these two regulators to sustain *micF* basal expression. Our findings add on previous observations of how the different regulators influence promoter activity (Chubiz et al., 2012; Chubiz and Rao, 2011).

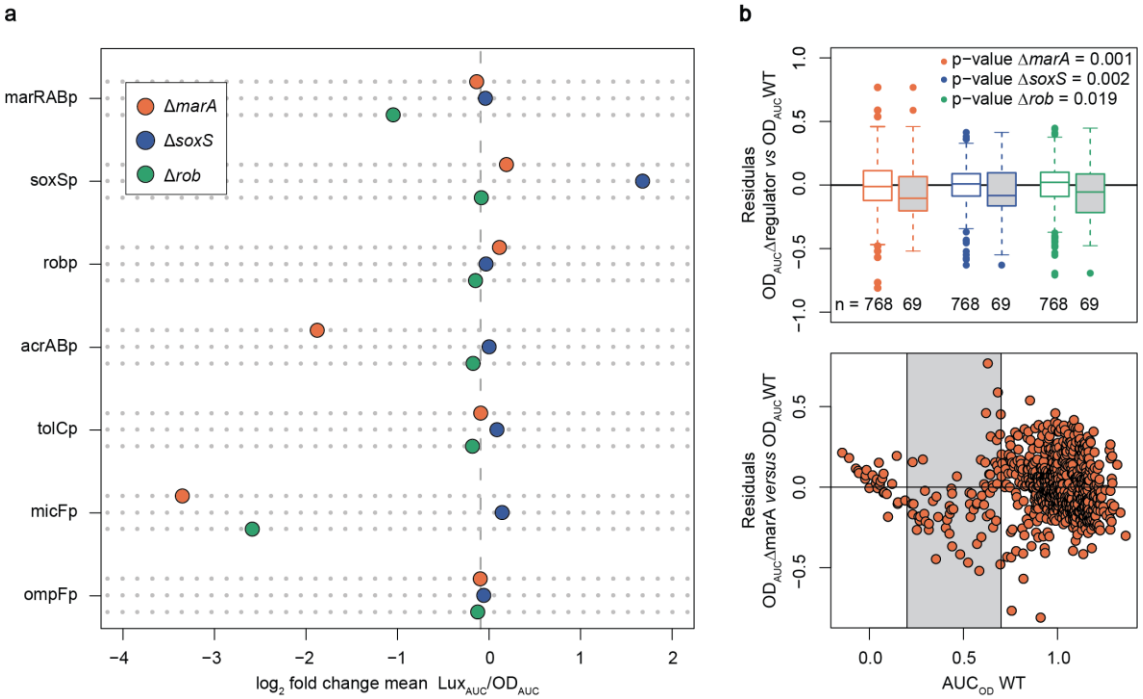

Figure 13: Deletions of *marA*, *soxS* and *rob* alter promoter basal activity and antibiotic susceptibility. a) $\log_2$ fold-change of water-promoter mean normalized luminescence (Lux_{AUC}/OD_{AUC}) of each deletion background in relation to the wild-type are plotted. The dashed line represents the median of $\log_2$ fold-change of water-promoter mean Lux_{AUC}/OD_{AUC} across all promoters, and deletion backgrounds. Water-promoter mean Lux_{AUC}/OD_{AUC} over 16 replicates per reporter (n = 8 x 2 biological replicates = 16). **b)** Deletion of *marA*, *soxS* or *rob* sensitizes bacteria to several compounds at sub-inhibitory concentrations. Top: boxplots of the residuals of the lines-of-best-fit between growth (OD_{AUC}) of the regulator mutants and wild-type for all tested pairs including water (EVC) across all 4 concentrations and 2 biological replicates. Negative residuals represent compounds concentrations to which the regulator mutant is more sensitive than the wild-type. White and gray boxes represent all residuals and a subset of compound concentrations with 0.2 < wild-type OD_{AUC} < 0.7, respectively. The number of data points is indicated below each box plot. Boxplots indicate 25th, 50th and 75th percentiles, and whiskers extend up to 1.5 times the interquartile range (IQR) from the 25th and 75th percentiles. p-value from a one-sided statistical t-test comparing full and subset residuals per mutant are shown. Bottom: Residuals of the lines-of-best-fit between growth (OD_{AUC}) of Δ*marA* and wild-type for all tested pairs including water (EVC) across all 4 concentrations and 2 biological replicates plotted against growth of the wild-type (containing EVC). Gray region corresponds to 0.2 < wild-type OD_{AUC} < 0.7. Figure adapted from manuscript (Binsfeld et al., 2025).

For instance, MarA not only increases acrABp and micFp activity upon overexpression as it has been shown before (Cohen et al., 1988; Okusu et al., 1996), but also determines their basal expression in the absence of any chemical or genetic stress (Figure 13a). In addition, we observed that deletion of either *marA*, *soxS* or *rob* sensitizes *E. coli* towards multiple growth inhibiting compounds, particularly at sub-MIC concentrations (Figure 13b). This highlights that, despite their different responses towards various compounds, the three regulators uniquely contribute to ensure optimal growth. Next, we built a simple statistical model using Lasso regression for hierarchical interactions (Bien et al., 2013) to estimate the contribution of MarA, SoxS and/or Rob to CPIs in our dataset. Briefly, we modeled the transcriptional effect of each compound on a given promoter as a function of compound concentration and regulator presence/absence.The individual regulator and compound concentration contributions to the observed changes in promoter activity are captured in the model coefficients β_j with $j \in \{conc, rob, marA, soxS\}$ (Methods, Figure 14).

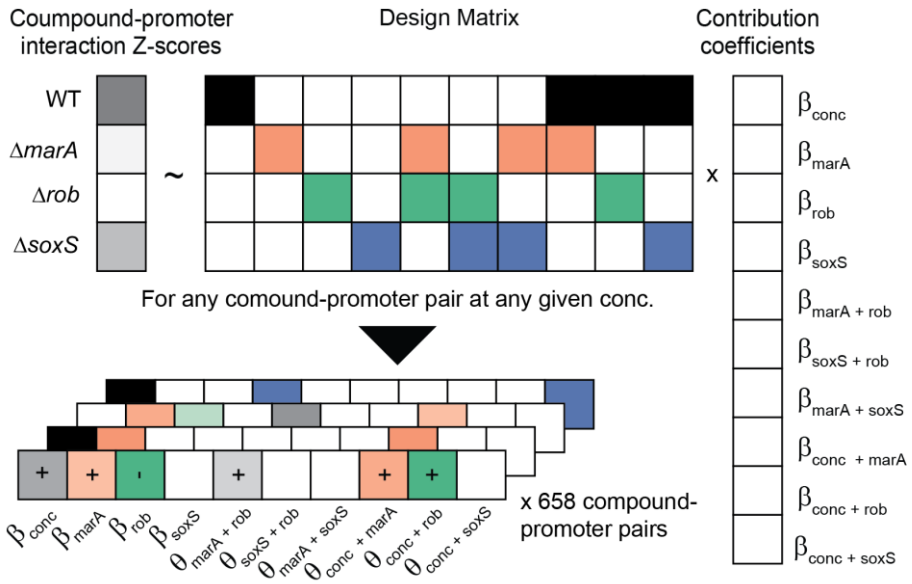

Figure 14: Schematic of the Lasso regression model. Schematic of the statistical model used to estimate regulator contributions to CPIs. Details described in Methods. Figure adapted from manuscript (Binsfeld et al., 2025).

Lasso penalization (Tibshirani, 1996) was used to obtain sparse model coefficients, and as a result, the majority of the values for each β across all modelled CPIs is 0 (or very nearly 0), with positive and negative deviations

reflecting positive or negative contributions to promoter activity in the presence of a given compound (Figure 15a). As our aim was to build an interpretable statistical model, we used all of the available data for each CPI to estimate the corresponding regulator contributions β_j To assess the robustness of these inferred contributions, we performed 10-fold cross-validation and calculated the average out-of-sample R^2 value (Methods).

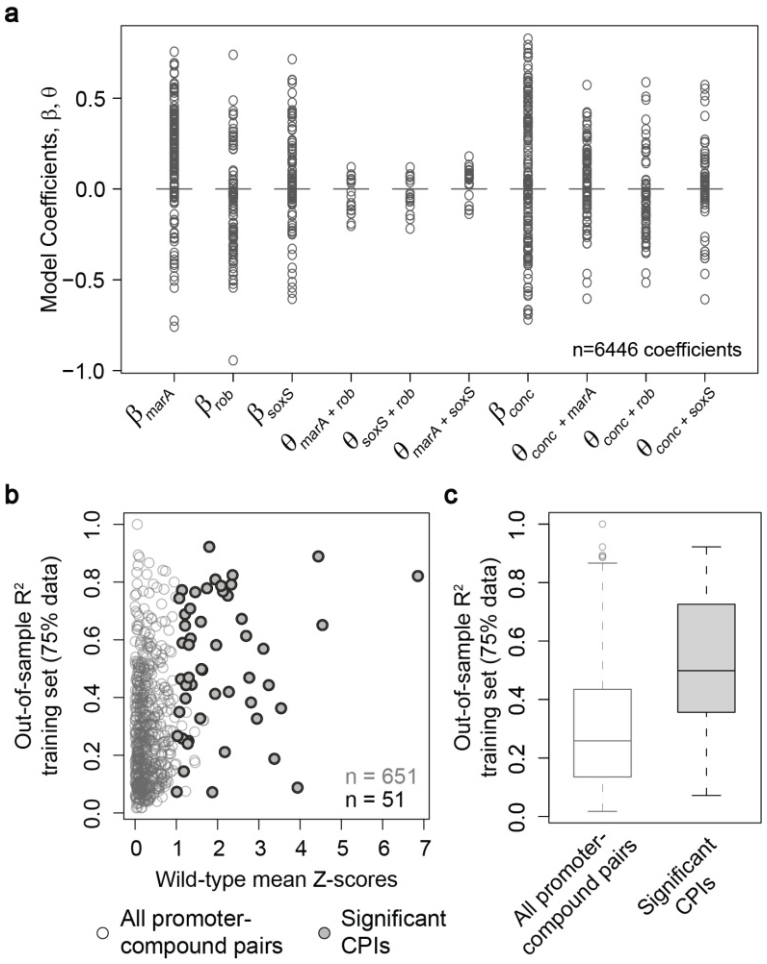

Figure 15: Distributions of coefficients and Out-of-sample R^2 values. a) Boxplots of contribution coefficients β and θ grouped by name. Center, upper and bottom lines represent 50, 75 and 25% percentiles, whiskers extend to 1.5x IQR and points beyond whiskers are represented individually. Due to the nature of the data – very sharply zero-centered – 25^{th}, 50^{th} and 75^{th} overlap. **b)** Scatterplot of out-of-sample R^2 versus wild-type mean Z-scores for all compound-promoter pairs. CPIs are represented with darker color. **c)** CPIs have higher than background out-of-sample R^2. Boxplot of out-of-sample R^2 for all compound-promoter pairs and for CPIs. Center, upper and bottom lines represent 50, 75 and 25% percentiles, whiskers extend to 1.5x IQR and points beyond whiskers are represented individually. Figure adapted from manuscript (Binsfeld et al., 2025).

Higher R^2 values indicate greater robustness and predictive reliability of the estimated regulator contributions. Firstly, the model accurately captures strong compound concentration dependent effects (reflected by large absolute values for β_{conc}, Figure 15a), stressing the added-value of concentration-resolved experiments. We also estimated coefficients for synergistic regulator contributions θ: $\theta_{marA,soxS}$, $\theta_{marA,rob}$ and $\theta_{soxS,rob}$. However, we observed that these are much more modest than single regulator coefficients (Figure 15a), and therefore decided to focus on single regulator contributions (β_{marA}, β_{soxS}, β_{rob}) to the 51 CPIs identified in our initial wild-type dataset (2 CPIs, Phleomycin-marRABp and Phleomycin-acrABp, could not be assessed in the regulator deletion mutants due to very poor growth). As expected, compound promoter pairs with high interactions Z-scores tend to have higher out-of-sample R^2 (Figure 15b), and significant CPIs have indeed higher out-of-sample R^2 than the majority of all pairs (Figure 15c, two-sided rank-sum test p-value < 0.0001).

In order to facilitate interpretation, we computed *multiplied model coefficients* (B*) by multiplying β by the absolute Z-score of the corresponding CPIs in the wild-type. Thus, B* reflect the overall relevance of a regulator towards change in promoter activity by a given compound in the wild-type, since it accounts for the amplitude of the change. B* differs from β in that all B* for weak (or null) compound-promoter interactions scores in the wild type are close to zero (Figure 16a and 16b). Notably, all regulators were found to have both positive and negative contributions to promoter activity depending on the compound-promoter pair (Figure 16a), suggesting a high network cross-talk and plasticity towards the environment. Consistent with its rather specific role in response to oxidative stress, SoxS has the tightest zero-centered coefficient B* distribution, with the least number of strong negative or positive contributions. MarA emerges as the most prominent regulator across all stresses, with the highest number of non-zero contributions, which are positive in most instances (Figure 16a). Interestingly, the far less well characterized Rob plays a more prominent role than SoxS across a variety of stresses, with both positive and negative strong contributions to ~1/3 of all CPIs (Figure 16a).

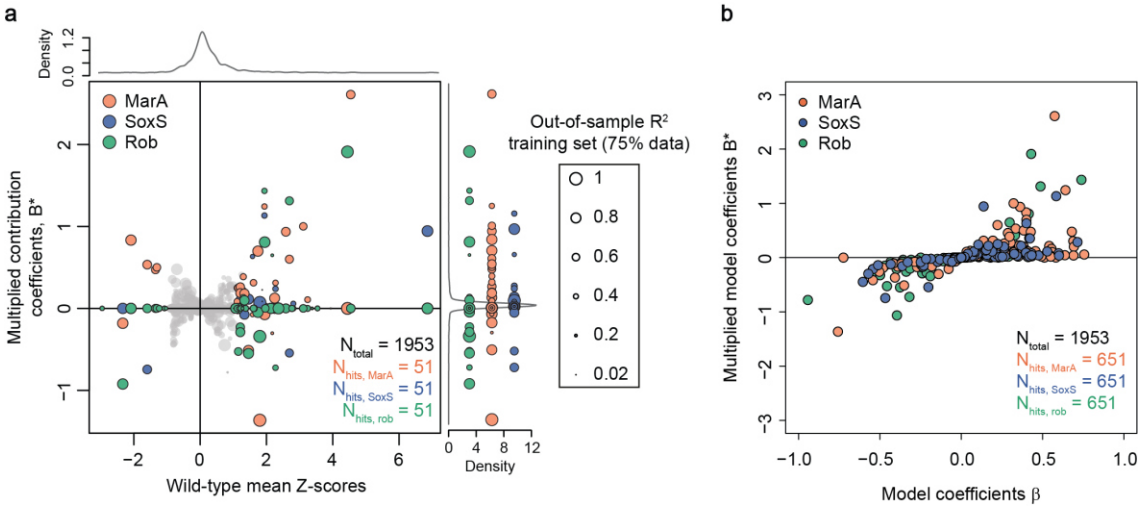

Figure 16: Mapping regulator contributions to compound-promoter interactions. a) Regulator contributions to CPIs are complex and multi-directional. Multiplied coefficients (B*) of MarA, SoxS and Rob of 651 compound-promoter pairs versus wild type mean Z-scores are plotted (n_{total}). Dot size reflects the out-of-sample R^2 of the corresponding compound-promoter pair. Pairs without R^2 are represented with the smallest size. Density distributions of total B* and wild-type mean Z-scores are represented on the top and right side of the main plot, respectively. B* corresponding to 51 significant CPIs are colored according to regulator and projected into the right axis to facilitate visualization. **b)** Scatterplot of multiplied coefficients B* versus model coefficients β of single regulator contributions, colored by regulator. Figure adapted from manuscript (Binsfeld et al., 2025).

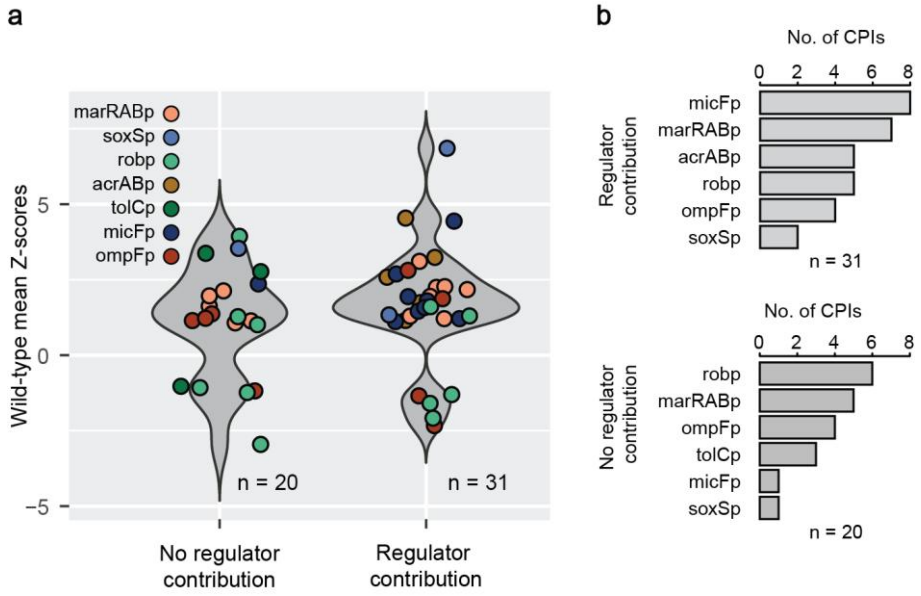

Figure 17: Most CPIs feature contributions of at least one regulator. a) Mean Z-score distributions of 51 CPIs (colored by promoter) classified on whether (or not) they have at least one non-zero B*. **b)** Almost all acrABp and micFp CPIs depend on MarA, SoxS or Rob. Number of CPIs with (B*≠0, upper plot) and without (B*=0, bottom plot) regulator contributions distributed by promoter. Figure adapted from manuscript (Binsfeld et al., 2025).

Overall, our approach captures contributions of MarA, SoxS or Rob to only 31 out of 51 compound-regulator pairs (Figure 17a and 17b). This result is expected, since contributions of other regulatory elements are certainly in place and not taken into account here – e.g. regulation by other transcription factors, such as OmpR or AcrR (Du et al., 2018b). Concomitantly, several CPIs involving ompFp and robp – the first does not even contain a mar-sox-rob box – are not influenced by any of the three tested regulators (Figure 17b). Yet, we quantified MarA, SoxS or Rob contributions to as many interactions involving ompFp, presumably emerging from indirect regulatory network effects. Importantly, the three regulators play a role in pretty much all CPIs involving acrABp and micFp. Among the 31 CPIs for which we could map regulator contributions, only 12 mapped to a single regulator - MarA, SoxS or Rob (Figure 18a). For the remaining 19 CPIs, they can only be fully achieved when two or all three regulators are in place (Figure 18a). A more explicit/functional inspection of regulator contributions to CPIs revealed striking observations. First, the transport-controlling regulatory response to tetracyclines and macrolides is vastly different, despite their common mechanism of action – inhibition of protein synthesis (Figure 18b).

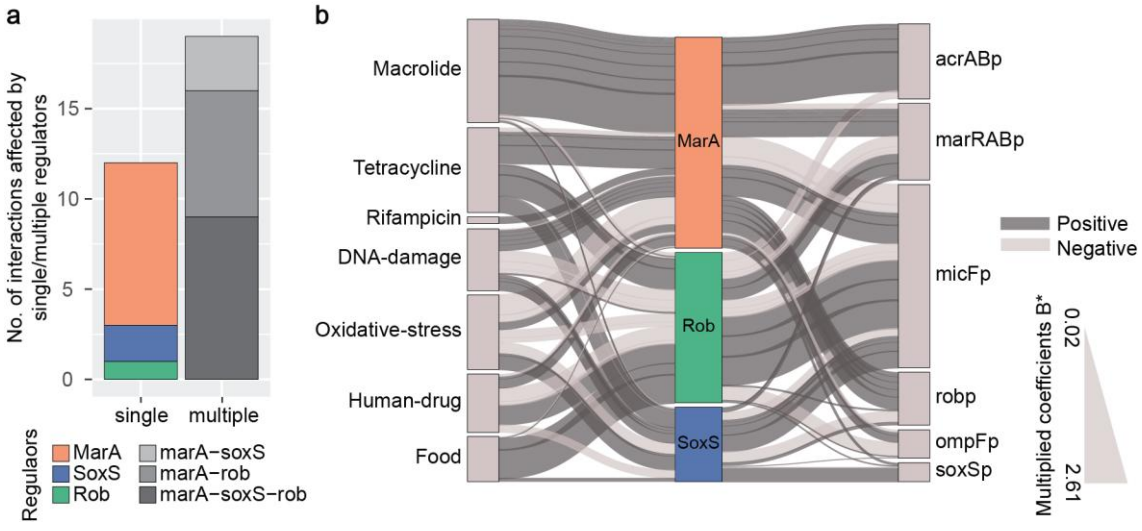

Figure 18: Most CPIs depend on two or all three regulators. a) Number of CPIs depending on single of multiple regulators, colored according to which regulators have B*≠0. **b)** Regulator-CPI network. Regulator contributions to 31 CPIs are shown as edges in a Sankey diagram connecting the compounds (left nodes, grouped according to class or purpose) the promoters (right nodes) via the regulators (middle). Edge thickness and node size represent B*, and the total number of interactions, respectively. Figure adapted from manuscript (Binsfeld et al., 2025).

While response to macrolides seems to be strictly driven by MarA, tetracyclines induce a much more complex response involving all three regulators. Another interesting observation is that acrABp expression is almost exclusively controlled by MarA across all compounds tested, with Rob playing a very minor and even negative role (Figure 18a and Figure 19). Even though MarA control of acrABp is well supported by several studies (Okusu et al., 1996; Ruiz and Levy, 2014, 2010), our results indicate that this is a prevalent regulatory relationship across environments, where SoxS and Rob have minor and rather specific contributions. Interestingly, not all compounds triggering marRABp necessarily trigger acrABp though, so other factors, such as alternative regulation by AcrR might be determinant in these cases.

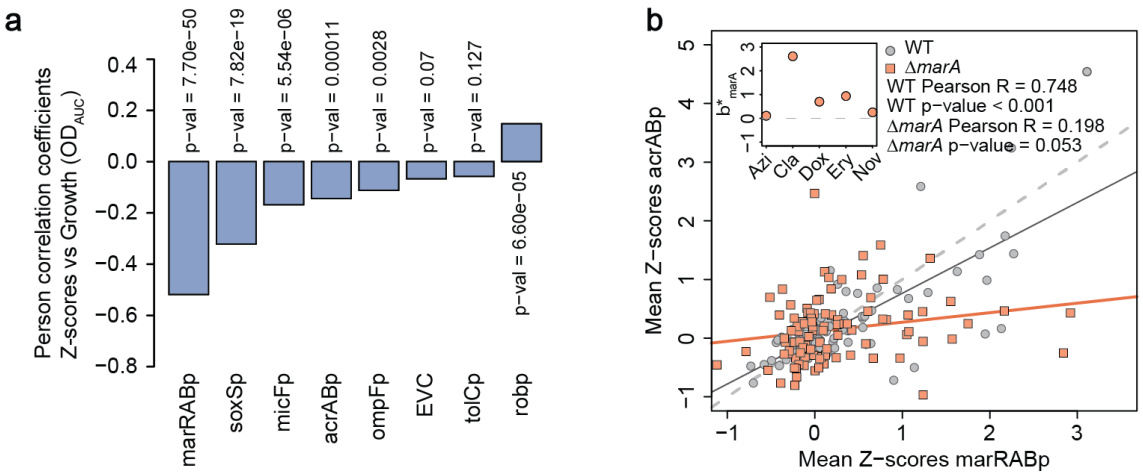

Figure 19: Expression of acrABp is primarily driven by MarA. a) Correlation of acrABp promoter activity with growth is lost upon *marA* deletion. Pearson correlation coefficients of Z-scores versus growth (OD_{AUC}) for each individual promoter in Δ*marA*. Correlation p-value (double sided t-test) shown above bars. **b)** acrABp and marRABp promoter activities are strongly correlated in a MarA-dependent manner. The mean Z-scores of all pairs including water (n=384) of acrABp plotted against marRABp. Correlation p-values (double sided t-test) and Pearson correlation coefficients are shown. Inlay shows β_{marA} to acrABp promoter activity in the wild-type for all CPIs involving acrABp. Figure adapted from manuscript (Binsfeld et al., 2025).

A very different pattern is observed for micFp, where CPIs are the net outcome of a complex regulatory pattern of positive and negative contributions of MarA, SoxS and Rob (Figure 18b). We highlight a few examples where micFp expression is strongly influenced by one (caffeine), two (salicylate) or all three (tetracycline and paraquat) regulators (Figure 20).

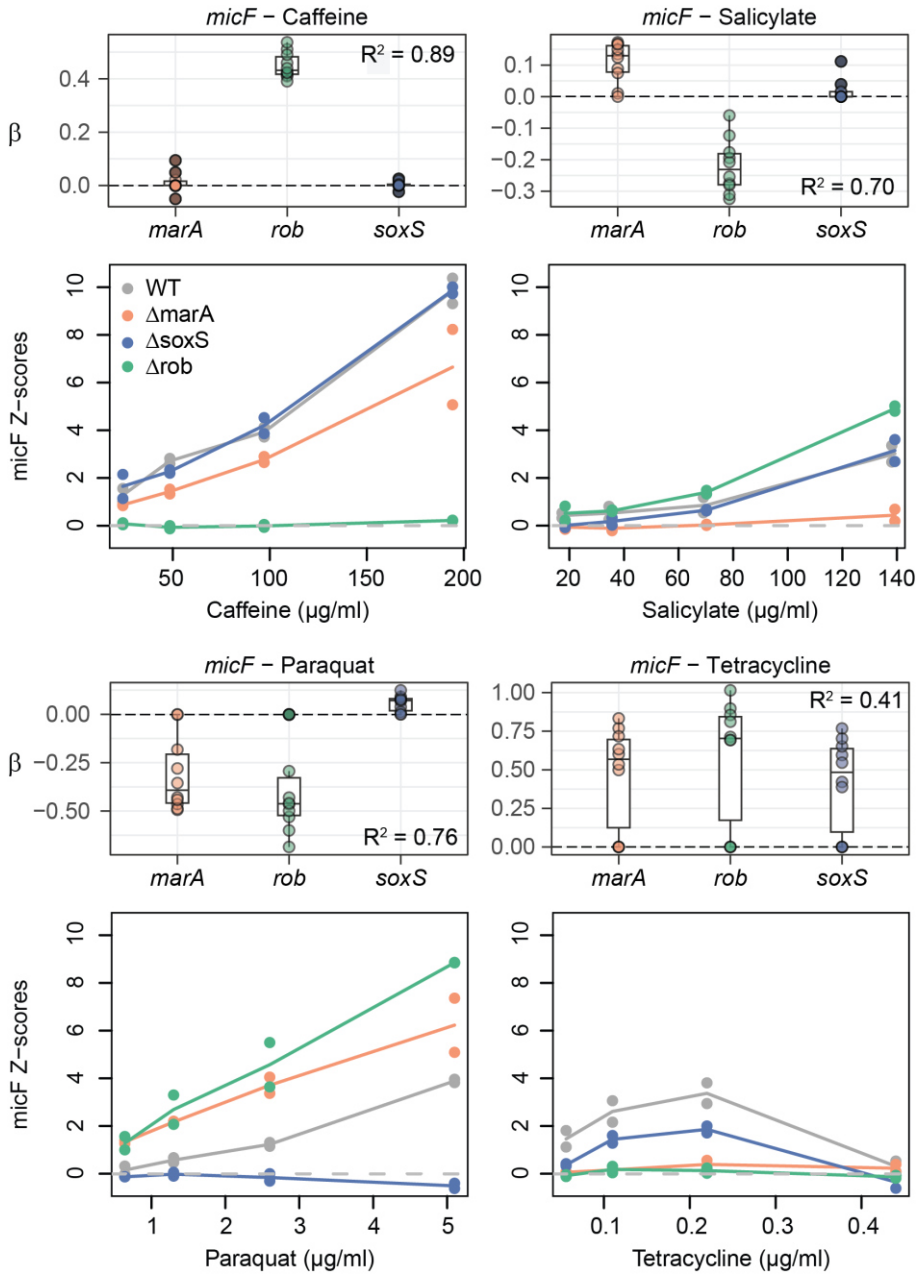

Figure 20: Regulator contributions to specific promoters are compound dependent. β (top) and Z-scores (bottom) of micFp interactions with caffeine, salicylate, paraquat and tetracycline in wild-type and Δ*marA*, Δ*soxS* and Δ*rob*. β corresponds to the regression coefficient quantifying the contribution of each regulator to the observed effect. Lines are colored by strain and indicate mean Z-scores of two biological replicates (dots). Depending on the compound, micFp activity mostly depends on a single (caffeine), on two (salicylate), or on all three regulators (tetracycline and paraquat). Figure adapted from manuscript (Binsfeld et al., 2025).

Our results so far show how *E. coli* diversifies its response to different chemical stresses and, most importantly, provide a quantitative overview on regulator contribution to promoter activity.

Chapter 3) Understanding Rob-dependent induction of micFp expression by caffeine

The contents of this chapter have been used in the manuscript “Systematic Characterization of Transport Regulation in *Escherichia coli* across defined environmental cues” and shared as a preprint version on “biorxiv.org” (doi: https://doi.org/10.1101/2024.08.26.609649).
The manuscript was subsequently published at PLOS Biology: “Binsfeld C, et al. (2025) Systematic screen uncovers regulator contributions to chemical cues in *Escherichia coli*. Doi: https://doi.org/10.1371/journal.pbio.3003260, PLoS Biol 23(7): e3003260“.
All mutant and reporter strains in this chapter were created by me. All experiments except TPP/proteomics were performed by me with help from Manuela Fuchs and Prof. Dr. Franziska Faber for northern blotting. Conceptualization and data analysis were done under supervision of Prof. Dr. Ana Rita Brochado. The TPP/proteomics experiments were conceptualized performed and analyzed by Lucía Pérez Jiménez and Prof. Dr. André Mateus. The TPP/proteomics data was further analyzed by me and Prof. Dr. Ana Rita Brochado performed the GO enrichment analysis. Figures 22c, 26 and 27 were produced by Prof. Dr. Ana Rita Brochado. All other figures and text in this chapter were produced by me under supervision from Prof. Dr. Ana Rita Brochado.

Caffeine induces proteome-wide changes in a Rob-dependent manner

To showcase the potential of our dataset for uncovering new molecular mechanisms, we chose to validate and further investigate the physiological consequences of caffeine-induced increase of *micF* promoter activity – caffeine-micFp interaction (Figure 8). Our choice was anchored to two points: first, it involves caffeine - a widely used food ingredient not previously known to impact transport regulation in prominent enterobacteria. Second, because caffeine-micFp interaction emerges from our dataset as the top CPI being primarily/exclusively controlled by Rob (Figure 20 and Figure 21a), which is by

far the least functionally characterized regulator, in comparison to MarA and SoxS. We started out by validating our initial observation that caffeine triggers *micF* expression. Indeed, MicF small RNA levels increase ~6-fold in the presence of caffeine when compared to no-caffeine control, as measured by Northern blot (Figure 21b). On top of that, we also confirmed that the level of OmpF is significantly decreased in the presence of caffeine (Figure 21c).

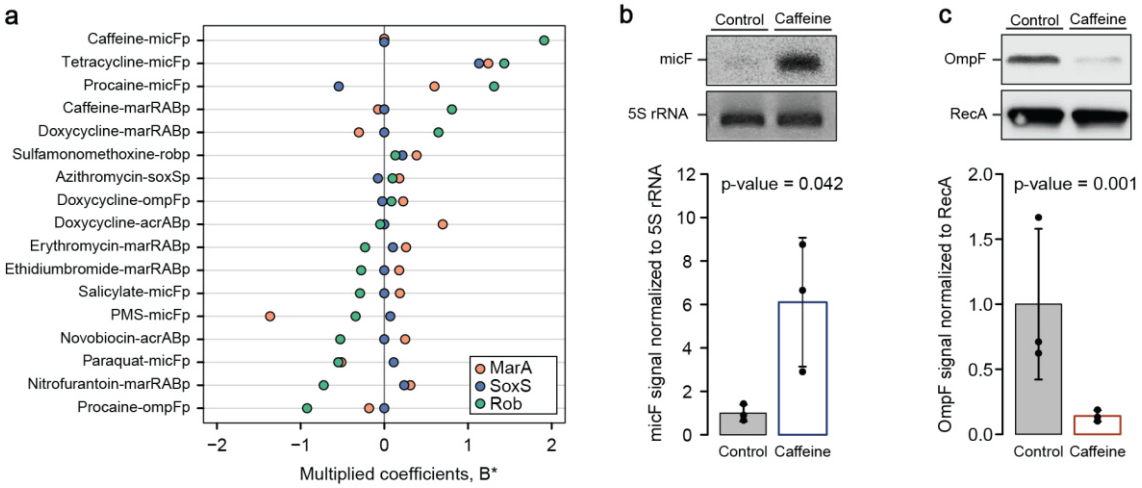

Figure 21: Caffeine is a novel Rob specific inducer of micFp expression. a) Caffeine-micFp interaction is primarily controlled by Rob. B* for all CPIs with non-zero Rob coefficients (n = 17), colored by regulator. **b)** Caffeine increases MicF small RNA levels. Northern blot analysis (top) confirming increased levels of small RNA MicF upon caffeine treatment (1 mM). One out of three biological replicates (quantification at the bottom) is shown. **c)** Caffeine decreases OmpF protein levels. Immunoblot analysis using whole cell lysate and an *E. coli* OmpF specific antibody shows OmpF decreased levels upon caffeine treatment (1 mM). One out of three biological replicates (quantification at the bottom) is shown. Figure adapted from manuscript (Binsfeld et al., 2025).

Furthermore, our screen showed that caffeine-micFp interaction is lost in the absence of Rob, and we confirmed that *rob* complementation reverts this phenotype back to wild-type (Figure 22a). Our next step was towards understanding the mechanism by which caffeine triggers Rob regulatory activity. It has been previously suggested that Rob transcriptional activity is triggered via post-translational modifications upon ligand interaction, either via direct interaction or foci dispersal (Chubiz et al., 2012; Griffith et al., 2009; Shi et al., 2022). Therefore, we first tested whether Rob could directly interact with caffeine *in vitro* using isothermal titration calorimetry (ITC), but no binding was detected (Figure 22b, Methods). Next, we used *in vivo* thermal proteome profiling (TPP (Savitski et al., 2014; Mateus et al., 2018, 2020; Kurzawa et al.,

2020)), aiming to find caffeine-induced protein thermal stability changes that could explain the observed phenotype. In particular, we hypothesized that either direct binding or induction of Rob foci dispersal by caffeine, could cause Rob (de)stabilization *in vivo*. However, no substantial change in stability of Rob (or other proteins) was observed, precluding us to elucidate the mechanism of the caffeine-rob interaction at this stage. Nonetheless, our results show an extensive proteome adjustment in response to caffeine, with change in abundance of >200 proteins.

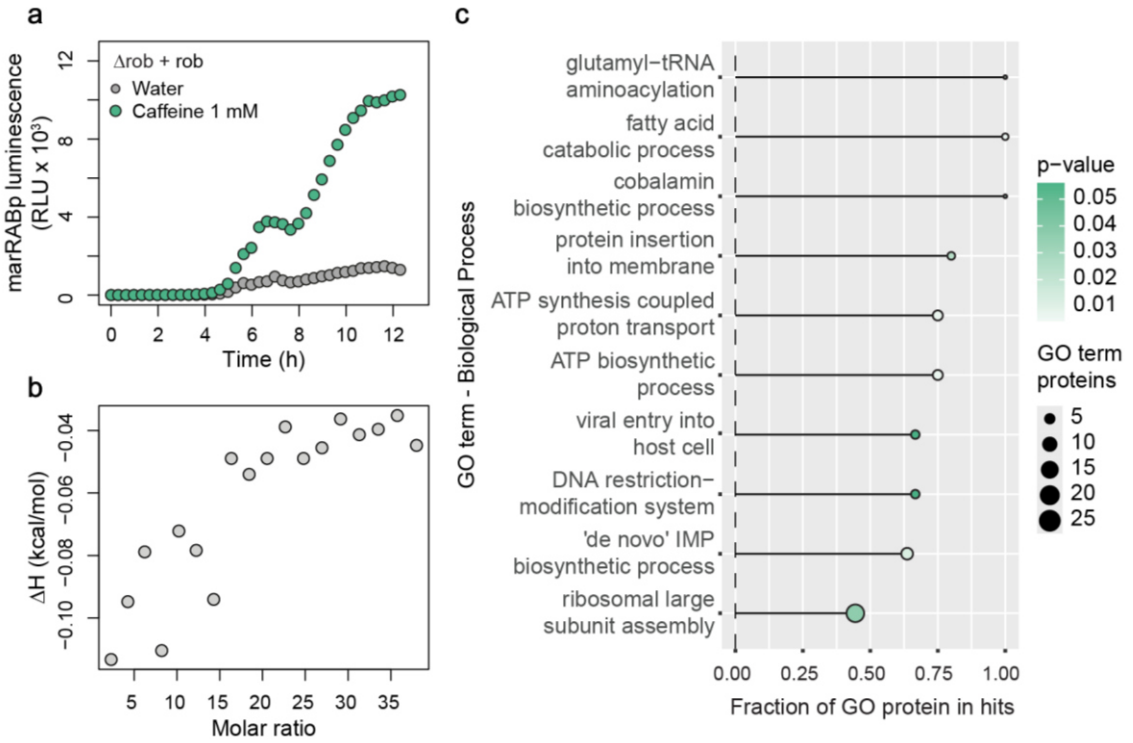

Figure 22: Supporting material for rob-caffeine interaction. a) Complementation of *rob* in the Δ*rob* mutant re-enabled activation of micFp transcriptional activity upon caffeine treatment (as measured by our luminescence reporter), as in the wild-type. Luminescence (RLU) profile over time for micFp basal activity (water) and upon treatment with caffeine in 96-well plates are shown. Average across 3 biological replicates is shown, error bars represent standard deviation. **b)** Caffeine does not interact with Rob. The plot shows a binding isotherm representing the integrated heats (after baseline and dilution correction) over increasing molar ratio of caffeine-Rob, as obtained by ITC. **c)** Gene Ontology enrichment analysis for protein abundance changes upon caffeine treatment in *E. coli*. Figure adapted from manuscript (Binsfeld et al., 2025).

Gene Ontology enrichment analysis (Methods) revealed significant changes in few biological function GO categories (Figure 22c, Methods), of which we found “protein insertion into membrane” of particular relevance. Specifically, the levels

of all detected β-barrel assembly machinery proteins (Bam, 4 out of 5) are decreased upon caffeine treatment (Figure 23a). As the Bam machinery mediates the assembly of OMPs in Gram-negative bacteria, its decrease can potentially impact the levels of all OMPs. Indeed, we observed a strong enrichment of OMPs among all decreased proteins (Figure 23a), thereby suggesting that caffeine could strongly impact membrane permeability way beyond MicF and its targets. Finally, all protein changes upon caffeine treatment are lost in the absence of Rob (deletion mutant, Figure 23b), thereby ultimately establishing Rob as a key regulator of *E. coli* response to caffeine.

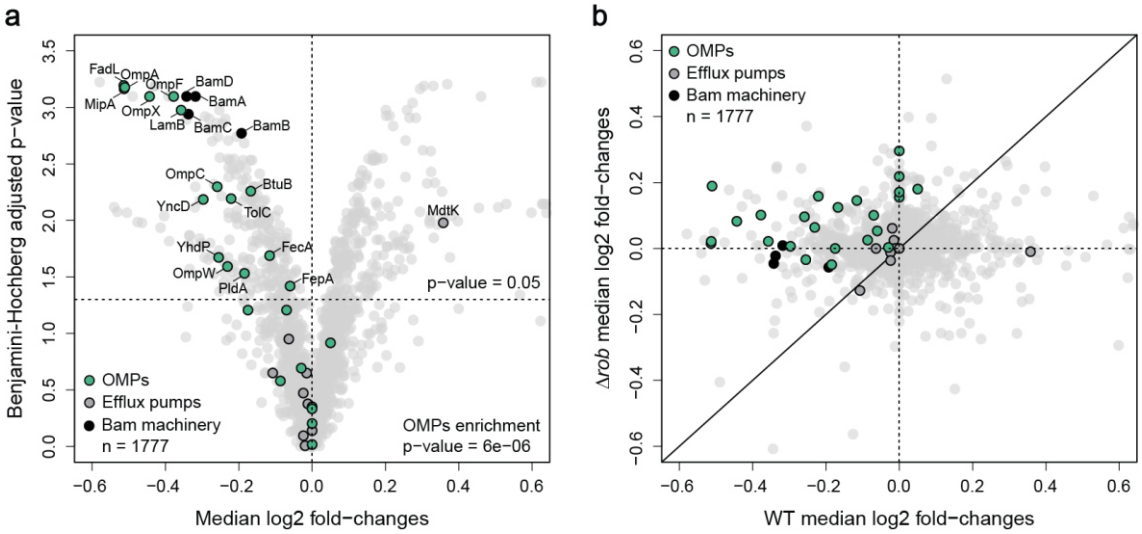

Figure 23: Caffeine induces proteome-wide changes in a Rob-dependent manner. a) Proteome-wide response to caffeine in *E. coli*. Volcano plot showing how -$\log_{10}$(p-value) relates to $\log_2$(fold-change) of caffeine treated compared to untreated cells. The p-values correspond to double-sided rank-sum test between fold-changes of a given protein and those of the entire set of proteins, after Benjamini-Hochberg correction for multiple testing. Median fold-changes across 6 caffeine concentrations at the two lower temperatures are shown (Methods). Horizontal and vertical lines correspond to p-value = 0.05 and $\log_2$(fold-change) = 0, respectively and n refers to the total number of proteins detected. The double-sided Fisher's exact test p-value for enrichment of OMPs among significantly decreased proteins is shown. **b)** Comparison of proteome changes between wild type and Δ*rob* upon caffeine treatment. Horizontal and vertical lines correspond to $\log_2$(fold-change) = 0. The black line represents the 1-to-1 diagonal and n refers to the total number of proteins detected. Median across three replicates treated with increasing caffeine concentrations is shown (Methods). Figure adapted from manuscript (Binsfeld et al., 2025).

Rob-dependent caffeine-micFp interaction underlies species-specific antibiotic antagonisms in *E. coli*

As OmpF is a major entry point for antibiotics in *E. coli*, we hypothesize that caffeine could decrease compound uptake (as we previously showed (Brochado et al., 2018)) in a Rob-dependent manner, thereby causing antibiotic antagonism (Figure 24).

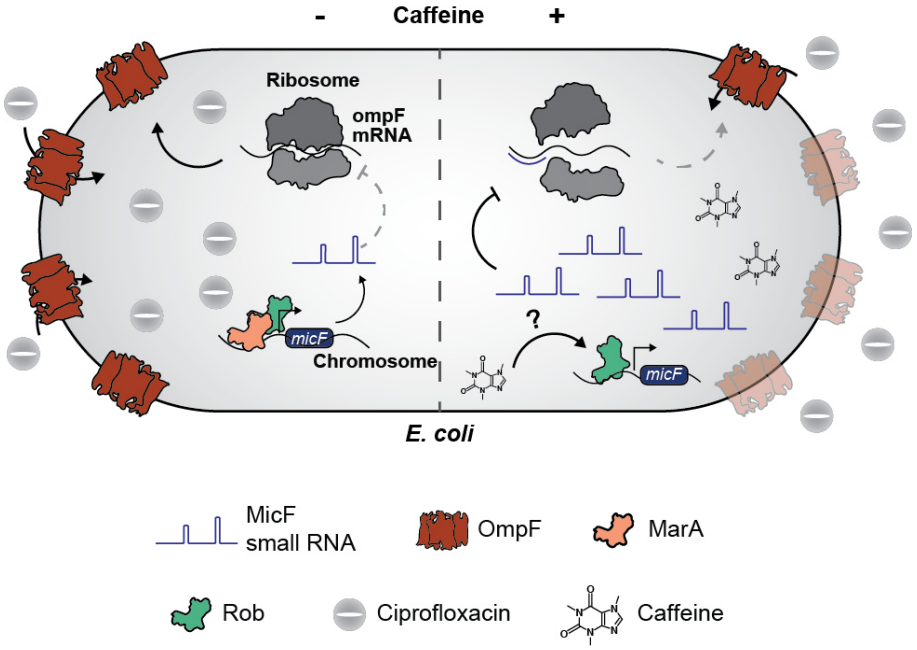

Figure 24: Proposed model for the molecular mechanism of caffeine-ciprofloxacin antagonism. Caffeine triggers expression of MicF small RNA in a Rob-dependent manner, which then binds to the 5'-UTR of *ompF* mRNA to inhibit and decrease OmpF protein levels. This ultimately prevents ciprofloxacin from entering the cell, resulting in caffeine-ciprofloxacin antagonism. Figure adapted from manuscript (Binsfeld et al., 2025).

In order to test this hypothesis, we first re-evaluated the outcome of caffeine combination with ciprofloxacin and amoxicillin, two different antibiotics predominantly taken up through OmpF in *E. coli*, and which our previous work showed to be antagonistic (Brochado et al., 2018). Indeed, a checkerboard assay confirmed the antagonism, showing that the concentration of antibiotics needed to inflict a given inhibitory effect progressively increases with increasing caffeine concentrations (isoboles moving rightward, Figure 25). For instance, amoxicillin IC_{50} (inhibitory concentration of 50%) increases by ~40% in the presence of 55.5 µg/ml of caffeine (Figure 26).

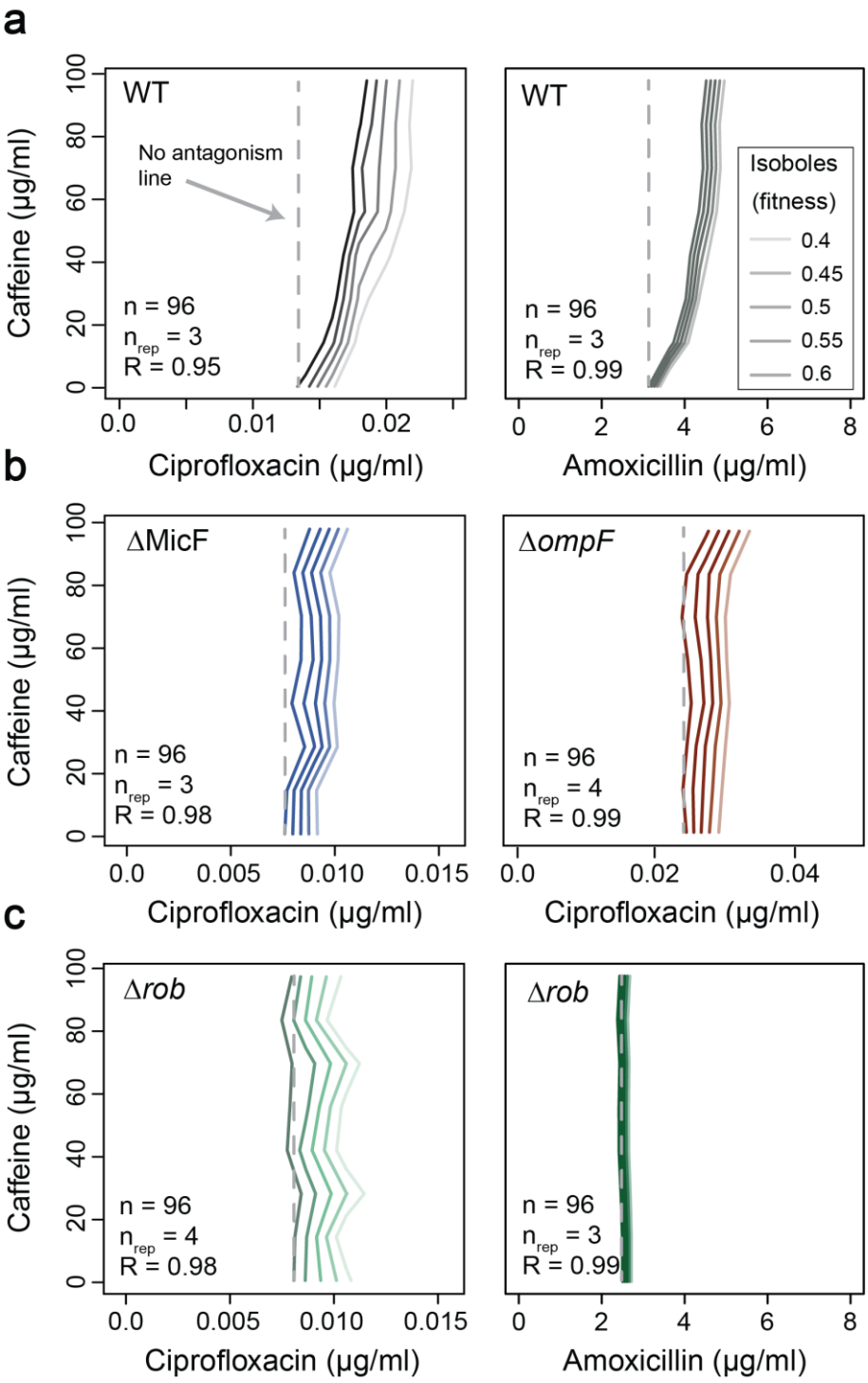

Figure 25: Caffeine-antibiotic antagonisms in *E. coli* are *micF*-, *ompF*- and *rob*-dependent. Isobolograms for caffeine-antibiotic interactions for *E. coli* wild-type (c), Δ*micF* and Δ*ompF* (d) and Δ*rob* (e) are shown. Rightward oriented isoboles indicate antagonism, while upward oriented isoboles indicate no antagonism. A dashed line is plotted for no-antagonism reference for isobole 0.6 for all strains. One out of 3 or 4 biological replicates (n_{rep}) is shown. R is the Pearson correlation between the biological replicates obtained with 96 (n) fitness values used to obtain each checkerboard. Figure adapted from manuscript (Binsfeld et al., 2025).

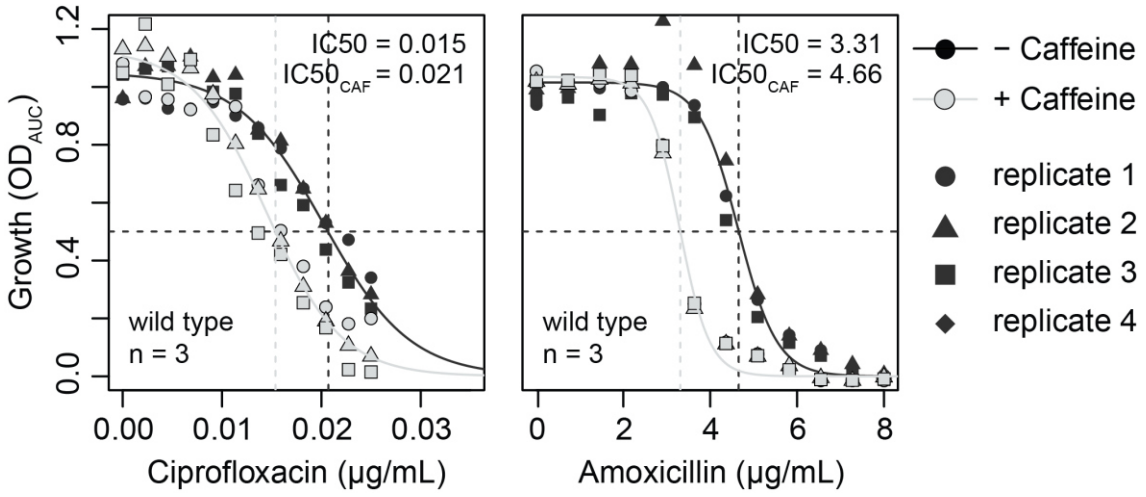

Figure 26: MIC shifts of ciprofloxacin and amoxicillin due to caffeine. Caffeine shifts antibiotic MIC curves towards resistance. MIC curves (growth vs antibiotic concentration) for the wild-type are shown for ciprofloxacin (left) and amoxicillin (right) with and without 55.5 µg/ml caffeine. The data shown is a snapshot of the checkerboard assays (Figure 25) at 0 and 55.5 µg/ml caffeine. Three individual replicates per experiment are shown (dots). The lines represent line-of-best fit of a three-parameter logistic model (Methods) using all replicates with and without caffeine. Dotted vertical and horizontal line represent 50% growth inhibition and corresponding concentration (IC50), respectively. Figure adapted from manuscript (Binsfeld et al., 2025).

Next, we confirmed that deletion of *micF* or *ompF* mostly abolished the caffeine-ciprofloxacin antagonism (straight vertical isoboles), confirming that these two molecular players are key to the antagonism (Figure 25b). Furthermore, we also observed that both caffeine antagonisms with ciprofloxacin and amoxicillin are strictly Rob-dependent, as *rob* deletion equally abolished both antagonisms (Figure 25c). Genetic complementation of *micF, ompF* and *rob* reverted the phenotypes close to wild-type again (Figure 27). Importantly, deletion of *marA*, otherwise also upregulated by caffeine in a Rob-dependent manner, did not affect the caffeine-ciprofloxacin antagonism (Figure 28a, 28b and 28c), further establishing Rob's major role in regulating caffeine response in *E. coli*. Also here, marRABp induction by caffeine was re-established upon complementation of *rob* (Figure 28d). In summary, our results suggest that caffeine is a novel and specific inducer of Rob transcriptional activity and this fully explains the molecular mechanism of antibiotic antagonism in *E. coli*.

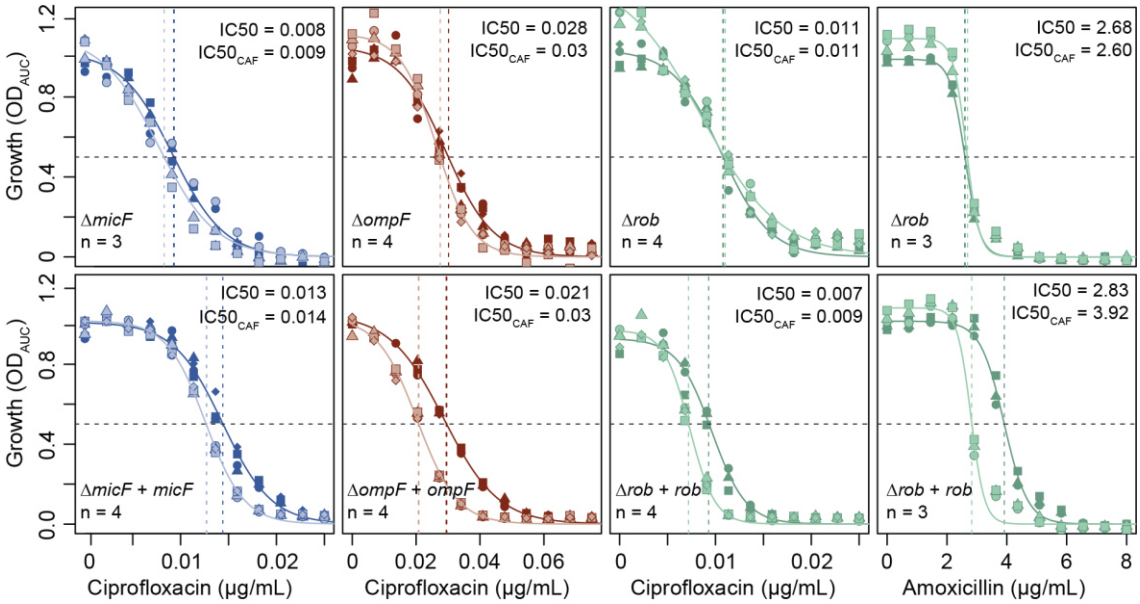

Figure 27: Genetic complementation in deletion mutants reverts caffeine-antagonisms to wild-type levels. Upper panels correspond to ciprofloxacin/amoxicillin MIC curves with and without 55.5 µg/ml caffeine for the depicted deletion mutants, while the lower panels show the corresponding complementation. Data analysis was done as in panel a. The distance between the MIC curves is minimal in the deletion mutants (loss of antagonism), and re-established upon complementation. The data shown for the deletion mutants is a snapshot of the checkerboard assays (Figure 25) at 0 and 55.5 µg/ml caffeine. Figure adapted from manuscript (Binsfeld et al., 2025).

Interestingly, our previous work showed that antagonisms involving caffeine seem to be specific to *E. coli*, as they were not found for the closely related species *Salmonella enterica* Typhimurium (Brochado et al., 2018). Indeed, also here we could confirm that caffeine does not change ciprofloxacin activity against *S.* Typhimurium (Figure 29a). Nonetheless, our previous work also showed that ciprofloxacin antagonism with caffeine occurs for a gut commensal *E. coli* strain (Brochado et al., 2018) as well, suggesting that the mechanism could be more general within *E. coli*. While not extensively assessing this question, we could confirm that the antagonism occurs also in a urinary tract infection *E. coli* isolate (Figure 29b), suggesting that it could be relevant for commensal and pathogenic *E. coli* across different niches in the human host.

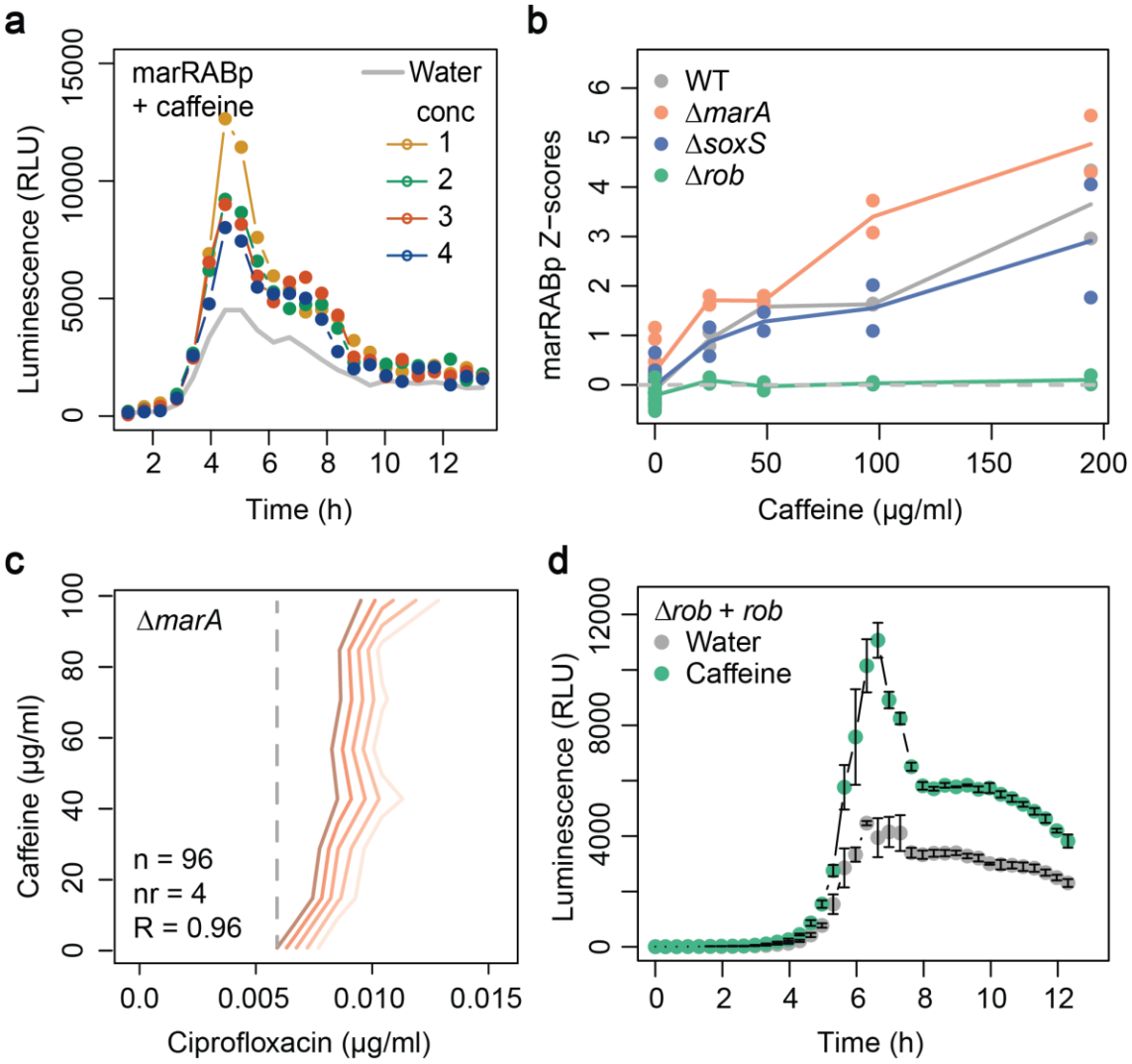

Figure 28: Caffeine induces marRABp in a Rob-dependent manner. a) Luminescence (RLU) profiles of marRABp basal activity (grey) and with increasing concentrations of caffeine (conc, Table 4) over time are shown. One out of two biological replicates is shown. e) Z-scores of caffeine-marRABp interaction showing its dependency on Rob. Lines are colored by strain and indicate mean Z-scores of two biological replicates (dots). f) Deletion of *marA* does not affect the antagonism between ciprofloxacin and caffeine. Isobologram for caffeine-ciprofloxacin for *E. coli* Δ*marA* as done in Figure 25. g) Complementation of *rob* in the Δ*rob* mutant re-enabled activation of marRABp transcriptional activity upon caffeine treatment (as measured by our luminescence reporter), as in the wild-type. Luminescence (RLU) profile over time for marRABp basal activity (water) and upon treatment with caffeine in 96-well plates are shown. Average across 3 biological replicates is shown, error bars represent standard deviation. Figure adapted from manuscript (Binsfeld et al., 2025).

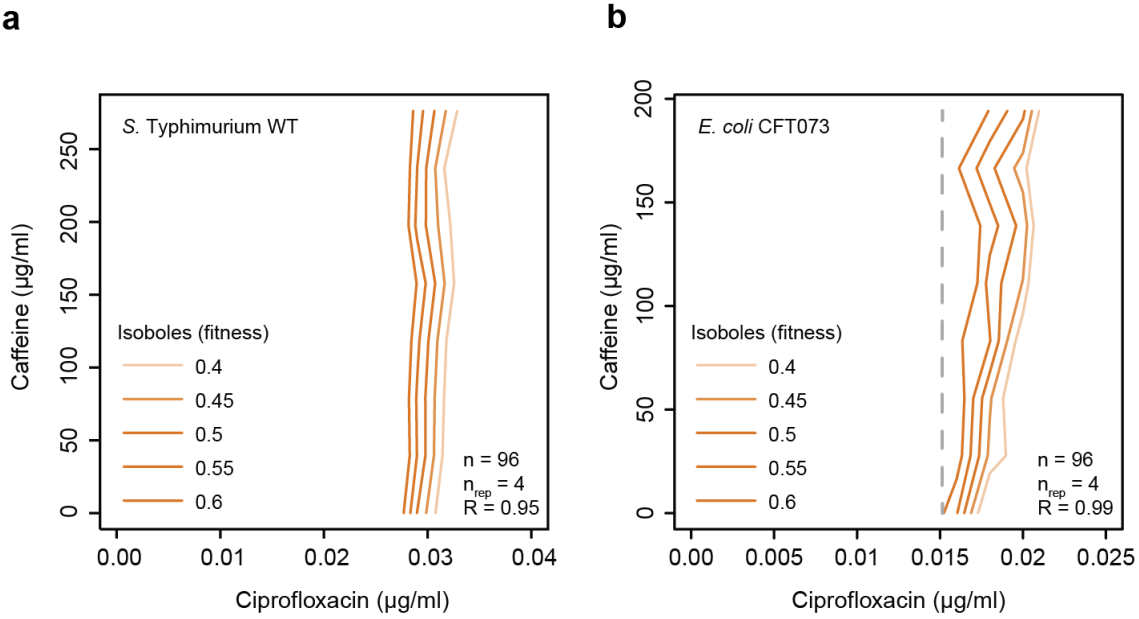

Figure 29: Caffeine-ciprofloxacin antagonism is absent in *S. enterica* but conserved in a clinical *E. coli* isolate. a) Absence of caffeine-ciprofloxacin antagonism in *S.* Typhimurium. Isobologram for caffeine-ciprofloxacin for *S.* Typhimurium. Details as in Figure 25. **b)** Caffeine-ciprofloxacin antagonism against a pathogenic *E. coli* strain. Isobologram for caffeine-ciprofloxacin for *E. coli* CFT073. Details as in Figure 25. Figure adapted from manuscript (Binsfeld et al., 2025).

One possible explanation for the *S.* Typhimurium phenotype could be that, even though all regulators (MarA, SoxS, Rob and MicF) and effectors (MicF and OmpF) are also present in *S.* Typhimurium, their response to caffeine is different than in *E. coli*. Thus, we first assessed if the absence of caffeine antagonism in *S.* Typhimurium could be explained by lack of *micF* transcriptional induction by caffeine. We quickly disproved this hypothesis by using a reporter system to quantify the activity of the *micF* promoter (similar to the *E. coli*), as we observed that, also in *S.* Typhimurium, caffeine treatment increases micFp expression (Figure 30a). In addition, we could also confirm that caffeine treatment reduces the level of OmpF in *S.* Typhimurium (Figure 30b), but not necessarily of other OMPs, as it occurs in *E. coli*. It has been previously suggested that OmpF-mediated uptake is not as determinant for ciprofloxacin activity against *S.* Typhimurium, as it is for *E. coli* (Piddock, 2002). Indeed, we observed that deletion of *ompF* alone (no addition of caffeine) decreases ciprofloxacin sensitivity in *E. coli*, but not in *S.* Typhimurium (Figure 30c and 30d), suggesting that lack of conservation of antagonism with caffeine is likely due to different antibiotic uptake mechanisms between the two species.

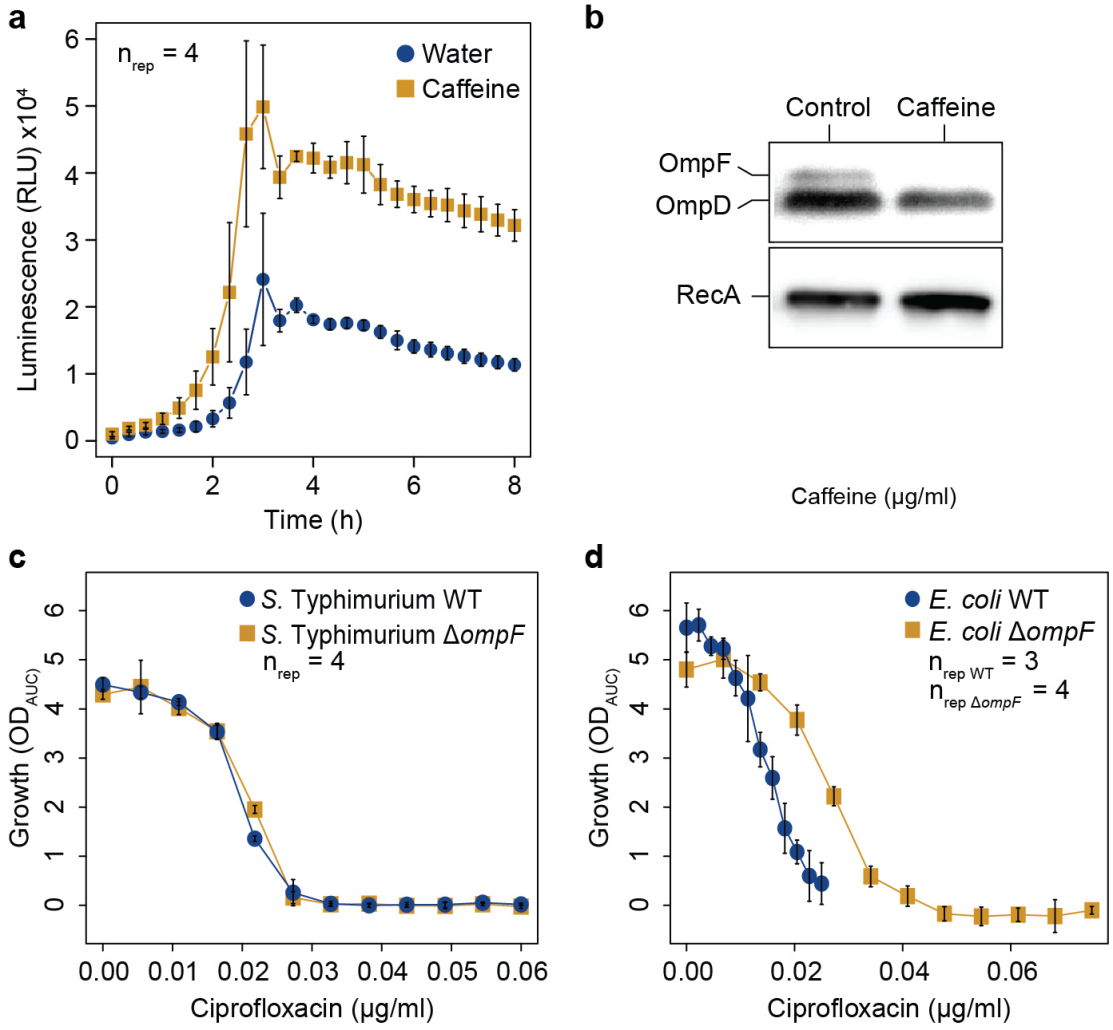

Figure 30: Caffeine-ciprofloxacin antagonism is absent in *S.* Typhimurium despite conserved regulatory mechanism. a) Caffeine induces micFp activity in *S.* Typhimurium. Luminescence profiles of *S.* Typhimurium micFp reporter strain over time +/- caffeine (2 mM). Mean luminescence (dots) and standard deviations (error bars) over 4 biological replicates. **b)** Caffeine does not inhibit growth of *E. coli* or *S.* Typhimurium. Caffeine MIC curves (growth vs caffeine concentration) of *E. coli* and *S.* Typhimurium wild-type strains. Mean growth (OD_{AUC}, dots) and standard deviations (error bars) over 3 and 4 biological replicates for *E. coli* and *S.* Typhimurium, respectively. **c)** Ciprofloxacin MIC is not altered upon OmpF deletion in *S.* Typhimurium. Ciprofloxacin MIC curves (growth vs antibiotic concentration) of *S.* Typhimurium wild-type and Δ*ompF.* Mean growth (OD_{AUC}, dots) and standard deviations (error bars) over 4 replicates. Inlay: Immunoblot analysis using total protein extractions and an OmpF polyclonal antibody shows OmpF decreased levels upon caffeine treatment (2 mM). One out of 3 biological replicates is shown. **d)** Ciprofloxacin MIC decreases upon OmpF deletion in *S.* Typhimurium. Ciprofloxacin MIC curves (growth vs antibiotic concentration) of *E. coli* wild-type and Δ*ompF.* Mean growth (OD_{AUC}, dots) and standard deviations (error bars) over 3 or 4 biological replicates. Figure adapted from manuscript (Binsfeld et al., 2025).

Altogether, this example illustrates how challenging it is to predict final outcome of CPIs on drug transport across species, even closely related ones for which the regulatory response to the environmental cues is conserved.

Discussion

The content of this chapter has partially been used in the manuscript “Systematic Characterization of Transport Regulation in *Escherichia coli* across defined environmental cues” and shared as a preprint version on “biorxiv.org” (doi: https://doi.org/10.1101/2024.08.26.609649). Several passages have been expanded with original content by myself.
The manuscript was subsequently published at PLOS Biology: “Binsfeld C, et al. (2025) Systematic screen uncovers regulator contributions to chemical cues in *Escherichia coli*. Doi: https://doi.org/10.1371/journal.pbio.3003260, PLoS Biol 23(7): e3003260“. The Discussion was written by me under supervision from Prof. Dr. Ana Rita Brochado with input from Roberto Olayo-Alarcon and Prof. Dr. Christian Müller regarding the statistical model and from Lucía Pérez Jiménez and Prof. Dr. André Mateus regarding TPP/proteomics, respectively.

Transport across the bacterial cell envelope has been subject of study for decades, with important constituents like AcrAB-TolC and OmpF, and also central regulators such as MarA, SoxS and Rob being extensively characterized (Chubiz, 2023; Du et al., 2018b). Despite vast molecular evidence on how each of these proteins plays a role in a complex regulatory cascade, we mostly lack comprehensive approaches that provide general overviews on how all the different players come together to orchestrate a coordinated response. Here we provide an integrative systematic approach to assess the transcriptional response of a small set of transport-related genes to environmental cues (CPIs), while quantitatively assessing regulator contributions to each response. Such an approach enabled not only the discovery of new CPIs, such as caffeine-micFp and macrolides-marRABp, but most importantly, allowed us to disentangle the relative contribution of each central regulator to the observed phenotype. Our results endow several previous observations, such as that not all compounds being effectively effluxed (Du et al., 2018b; Pagès et al., 2008; Ricci et al., 2023) are capable of inducing expression of efflux genes, or that transport regulation underlies antibiotic antagonism (Brochado et al., 2018). Importantly, we provide a set of new general findings suggesting a paradigm

change in our perception of how *E. coli* controls its transport. For instance, *marA* regulation is mostly investigated in the presence of salicylate, which releases *marA* transcriptional repression by binding MarR (Alekshun et al., 2001). However, other compounds seem to regulate *marA* in a growth dependent manner, even in the absence of MarR. While this has been described for salicylate and tetracycline (Hächler et al., 1991; Cohen et al., 1993b; Martin and Rosner, 1995) and observed by us for many protein biosynthesis inhibitors and folate inhibitors (Figure 8), so far no mechanism has been identified. The promoter region of the *marRAB* operon features (potential) binding sites for multiple global transcriptional regulators, including CpxR, Cra, Crp, Fis and Nac, which – with the exception of CpxR – are all directly connected to regulation of central carbon metabolism and adaptation to growth conditions (Martin and Rosner, 1997; Ruiz and Levy, 2010; Shimada et al., 2011; Weatherspoon-Griffin et al., 2014; Aquino et al., 2017). Curiously, preliminary experiments point towards CpxR being central for the induction of marRABp by clarithromycin but not other identified inducers from our screening, suggesting there is not just one single mechanism that explains how marRABp reacts to growth inhibition. Deletion of the other regulators mentioned above did not affect any of the biosynthesis inhibitor-marRABp pairs induction. However, deletion of any of these global regulators affects dozens to hundreds of genes and therefore results have to be verified carefully.

Another interesting finding is that ~1/3 of all CPIs depend on Rob. This is well beyond what is generally described or perceived, and indicates that a much better understanding of Rob-dependent regulation is crucial to fully comprehend transport transcriptional control. Interestingly, almost all CPIs involving Rob also involve MarA, or MarA and SoxS (Figure 18a), which certainly renders full functional characterization more challenging. Exceptionally, our data suggests that Rob alone seems to have complete control of caffeine response in *E. coli* way beyond transcription where we observed significant changes in the abundance of >200 proteins, including several OMPs, in a Rob-dependent manner. Despite several attempts, we were not yet able to decipher the molecular mechanism by which caffeine triggers Rob transcriptional activity and its downstream effects. Similarly, at this stage it is still unclear how exactly

caffeine induces such a proteome-wide adjustment via a single regulator. Studying interactions of Rob with compounds such as caffeine is especially difficult since methods relying on protein purification seem to automatically render Rob active (Rosner et al., 2002; Griffith et al., 2009). This could be one explanation why we were not able to detect physical binding of caffeine to Rob using ITC (Figure 22). This basically restricts us to use *in vivo* methodologies, such as the 2-D TPP approach we chose to better understand the impact of caffeine on *E. coli*. However, also here we did not detect any stability changes of Rob in response to caffeine. In an attempt to find proteins that could lie upstream of Rob in a signal cascade, we searched for proteins stabilized by caffeine in both wild-type and Δ*rob* backgrounds and found ArcA and IbpB as candidates. However, neither deletion did affect induction of robp by caffeine. Finally, it is very interesting that a compound such as caffeine, which does not inhibit growth in a meaningful way at the concentrations used, causes downregulation of most outer membrane proteins, albeit to a limited extent (Figure 23). Furthermore, this effect appears to depend completely on Rob, which is not known to have such a vast impact on the outer membrane. Parts of the Rob regulon are genes involved in remodeling of LPS and fatty acids, which could perhaps provide a signal that ultimately also affects the composition of outer membrane proteins via the BAM machinery. This aspect of the Rob regulon needs to be understood better and could increase the importance and roles attributed to Rob. Beyond caffeine and Rob, we readily acknowledge that other regulators than those we selected will most certainly also play a role in controlling the transcriptional response of the promoters we selected, and also that the compounds we used will most certainly inflict wider transcriptional changes than those we monitored. Nonetheless, this study, even if limited to 7 promoters, shows the potential of our approach to generate valuable insight into the extensive cross-talk of complex transcriptional regulatory networks.

A second aspect to highlight is the potential of our dataset for mining molecular mechanisms. We showcased it by exposing how caffeine-micFp interaction underlies caffeine-antibiotic antagonism through impaired antibiotic uptake, in a Rob-dependent manner. Even if caffeine causes only a modest increase in antibiotic resistance (up to~40%), this finding features the potential impact of

the immediate environment for treatment efficacy through transport modulation, and supports future predictive design of drug combinations. As we did not do any experiments in animal models and did not strictly adhere to standard methodologies when it comes to assessing MICs, it is difficult to judge whether our findings about caffeine related antagonisms have clinical relevance or not. However, for this project these experiments would have been out of scope and did not align with our focus to gain mechanistic insights into transport-related drug interactions. Nonetheless, future studies focusing on systematically assessing combinations of antibiotics with other antibiotics and non-antibiotics in a clinical background will surely be necessary to translate findings from basic research into clinical practice. Studies in this direction could also utilize more specialized drug libraries, for example focusing on compounds found in the ecological niches of the bacteria, specific infection or tissue sites, or a broader range of human targeted drugs.

Given the ever increasing evidence of transport's prevalent role in the bacterial response to harsh environments, for instance in modulating the impact of human-targeted-drugs in gut microbes (Maier et al., 2018), or potentially contributing to bioaccumulation within the gut microbiota thereby modulating drug action on the host (Klünemann et al., 2021), the scope of our findings and approach goes well beyond *E. coli* or even enterobacteria. Nonetheless, our data indicate that the ultimate physiological consequences of (even) conserved compound-promoter interactions are not necessarily conserved across species. More specifically, we showed that even if caffeine-micFp interaction, and the subsequent decrease in OmpF levels are conserved between *S.* Typhimurium and *E. coli*, this is not sufficient to yield caffeine antagonism in *S.* Typhimurium. Several reasons could explain this phenomenon, for instance the presence and alternative regulation by caffeine of additional outer membrane porins in *S.* Typhimurium, or a more prevalent role of efflux versus uptake (Li et al., 2015b; Maher and Hassan, 2023; Piddock, 2002). Based on these findings, we foresee a challenging, but unavoidable and important task in mapping key determinants of transport functions across different bacteria. Nonetheless, our data supports that caffeine antagonisms extend to commensal pathogenic *E. coli* strains, advocating for further investigation of its potential relevance in host contexts.

Outlook

Several aspects of this project are still not completed and have more potential for novel discoveries. As mentioned before, CpxR appears to be crucial for the induction of marRABp by clarithromycin. To this end, further experiments need to be conducted to determine how clarithromycin affects CpxR activity. In a broader sense, it would be interesting to screen the whole genome for genes that break the interaction between protein synthesis inhibitors and marRABp. This could be achieved by conjugation of the respective reporter plasmids to the whole KEIO collection and a subsequent screening in liquid media. This could provide additional insight about whether the induction of marRABp reacts to, e.g., altered growth conditions/growth rate or the specific effects of protein inhibition. Another experiment in this direction could be to monitor activity of marRABp under artificially controlled growth rates by modulating e.g. temperature or nutrient levels.

Even though it is difficult to determine how Rob activity is induced by caffeine, there are still a few possibilities to be explored. Transcriptomics experiments of cells treated with caffeine in wild-type and D*micF* backgrounds have been performed and await analysis. This dataset could provide further candidates that react to caffeine and direct a signal towards Rob to change its activity. Furthermore, this dataset could provide insights into how the extensive reorganisation of the outer membrane in response to caffeine is orchestrated. To test if there are other proteins interacting with Rob, one could use the His-tagged Rob protein used for purification to perform crosslinking and pull-down assays. Finally, similar to the approach above, one could conjugate a micFp reporter plasmid into the KEIO collection to screen for mutants that break the micFp-caffeine interaction.

Materials and Methods

The contents of this chapter have been used in the manuscript “Systematic Characterization of Transport Regulation in *Escherichia coli* across defined environmental cues” and shared as a preprint version on “biorxiv.org” (doi: https://doi.org/10.1101/2024.08.26.609649).
The manuscript was subsequently published at PLOS Biology: “Binsfeld C, et al. (2025) Systematic screen uncovers regulator contributions to chemical cues in *Escherichia coli*. Doi: https://doi.org/10.1371/journal.pbio.3003260, PLoS Biol 23(7): e3003260“.
The materials and methods section was written by me under supervision from Prof. Dr. Ana Rita Brochado with the exception of the paragraph about the statistical model which was produced by Roberto Olayo-Alarcon and Prof. Dr. Christian Müller. Lucía Pérez Jiménez and Prof. Dr. André Mateus provided input on the paragraph about TPP/proteomics.

Growth medium, reporter plasmids and strain construction

A summary of all strains used in this study can be found in Table 1. *Escherichia coli* BW25113 and *Salmonella enterica* subsp. *enterica* ser. Typhimurium 14028S were used as wild-type strains (WT) and cultured in Lysogeny Broth (LB Lennox) adjusted to pH 7.5 at 37°C. The medium was supplemented with kanamycin (50 µg/ml, CatNo. K1876-5G, Sigma-Aldrich-Merck), carbenicillin (100 µg/ml, CatNo. Cay20871-5, Biomol) or spectinomycin (100 µg/ml, CatNo. S4014-5G, Sigma-Aldrich-Merck) when selection was required for strain construction.

All plasmids constructed in this study are listed in Table 2. Reporter plasmids for *E. coli* were assembled by restriction-ligation using enzymes EcoRI and XhoI (SalI in case of acrABp, CatNos. R3101S, R0146S, R3138S, NEB) to linearize the backbone vector pTU175-LUX. T4 DNA ligase (CatNo. M0202S NEB) was used for plasmid assembly following supplier instructions. Reporter plasmids for *S.* Typhimurium were assembled using Gibson Assembly, using XhoI for plasmid linearization. Vector pTU175-LUX is a low copy plasmid with a pSC101

origin of replication constructed from pTU175(Uehara et al., 2010). by insertion of an oriT, a spectinomycin resistance cassette and the full luxCDABE operon (amplified from Plasmid #44918, AddGene) with a putative RBS for basal expression – used as **e**mpty **v**ector **c**ontrol, EVC. The pASCOT-LUX vector is a variant of pTU175-LUX with a carbenicillin resistance cassette instead of spectinomycin used for *Salmonella*. DNA inserts were digested with the respective restriction enzymes and assembled into the plasmid backbone utilizing T4 DNA ligase according to a standard protocol (NEB). Plasmids were transformed into *E. coli* BW25113 and *Salmonella* Typhimurium 14028S by transformation (TSS transformation) and electroporation, respectively. The protein expression vector for purification of Rob-6xHis was created by insertion of a PCR fragment containing *rob* into pET28a using restriction-ligation as mentioned above with Hind-III and NcoI (CatNos. R3104S, R3193S NEB). The plasmid was subsequently transformed into *E. coli* BL21 (DE3).
Deletions of Δ*marA*, Δ*soxS* and Δ*ompF* were derived from the KEIO collection in case of *E. coli* (Baba et al., 2006) or a similar knockout-library in case of *S.* Typhimurium (Porwollik et al., 2014). Mutations were confirmed using PCR and transduced into wild type BW25113 or ST14028s using P1 and P22 phage, respectively. Deletion of *rob* in *E. coli* was done with Lambda RED recombineering according to the protocol of Datsenko and Wanner (Datsenko and Wanner, 2000), similar to how the KEIO collection strains were created. Kanamycin resistance cassettes were subsequently removed using the pCP20 plasmid.

Genetic complementation of Δ*rob* and Δ*ompF* were achieved by assembling PCR products of wild type *rob* and *ompF* with 500 bp of respective promoter regions into the pKD13 backbone using Gibson Assembly (Gibson et al., 2009). PCR fragments containing respective genes, kanamycin cassette and FRT sites were then transferred to the native locus of respective deletion strains using Lambda RED recombineering (Datsenko and Wanner, 2000). Positive clones were selected using kanamycin as a selection marker and gene insertions were subsequently transferred into clean backgrounds using P1 transduction, followed by excision of the kanamycin cassette using plasmid pCP20. Deletion of *micF* was complemented using a version of the pTU175 vector, where the

luxCDABE operon was replaced by *micF* with its respective 500bp promoter region. The resulting pTU175-*micF*-comp was transformed into the Δ*micF* deletion background using TSS transformation (Chung et al., 1989).

Compound-promoter screens

The compound-promoter screen for *E. coli* BW25113 (wild type, as well as Δ*marA*, Δ*soxS* and Δ*rob* backgrounds) containing each reporter plasmid – arcABp, marRABp, soxSp, robp, micFp, ompFp, tolCp and EVC - was done in black 384 well-plates with clear bottom (CatNo. 781097, Greiner-Bio One, Germany), in 40 µl LB Lennox. The compound library contains 94 diverse compounds purchased from Biomol (Germany), MP Biomedicals (Germany), or Sigma-Aldrich-Merck (solvents, concentrations and purchase details listed in Table 4). The highest screening concentration of compounds with antimicrobial activity was adjusted to MIC for antimicrobials, 500 µM for most non-antimicrobials, and up to 1 mM for small compounds with similarity to canonical inducers (positive controls, e.g. salicylate, Table 4). Four working concentrations were achieved through 1:2 serial dilutions using a Biomek i7 liquid handler (Beckman Coulter, Figure 31). Precultures were grown overnight and diluted to an $OD_{600\ nm}$ of 1 (WT) or 0.1 (deletion backgrounds) and used to inoculate 384 well plates using a Singer Rotor+ replicator (Singer Instruments, UK), resulting in further ~1:600 dilution and starting OD of ~0.003 and ~0.0003. Transparent breathable membranes (Breathe-Easy®, Sigma-Aldrich-Merck) were used to seal plates, which were then incubated at 37°C, shaking at 800 rpm using a Cytomat 2 incubator (Thermo Scientific). Growth ($OD_{600\ nm}$) and reporter activity (luminescence) were measured in 30-minute intervals over 12 hours in a Synergy H1 plate reader (Agilent, USA). The screen was performed in biological duplicates, resulting in 768 growth and luminescence curves per strain. Data analysis was performed using R (version 4.2.2). A representation of the analysis pipeline can be found in Figure 31. Baseline-correction of growth curves was done by subtraction of initial $OD_{600\ nm}$ before growth onset (time 1-2 hours). Area under the curve was calculated for growth (OD_{AUC}) and luminescence (Lux_{AUC}) curves between 0 and 8 h in case of the wild type and between 1 and 9 h for the deletion background strains to account for the differences in inoculum size mentioned above. This eight-hour interval covers

lag phase, exponential phase and transition into stationary phase assuming regular, non-stressed growth – using water instead of any compound.

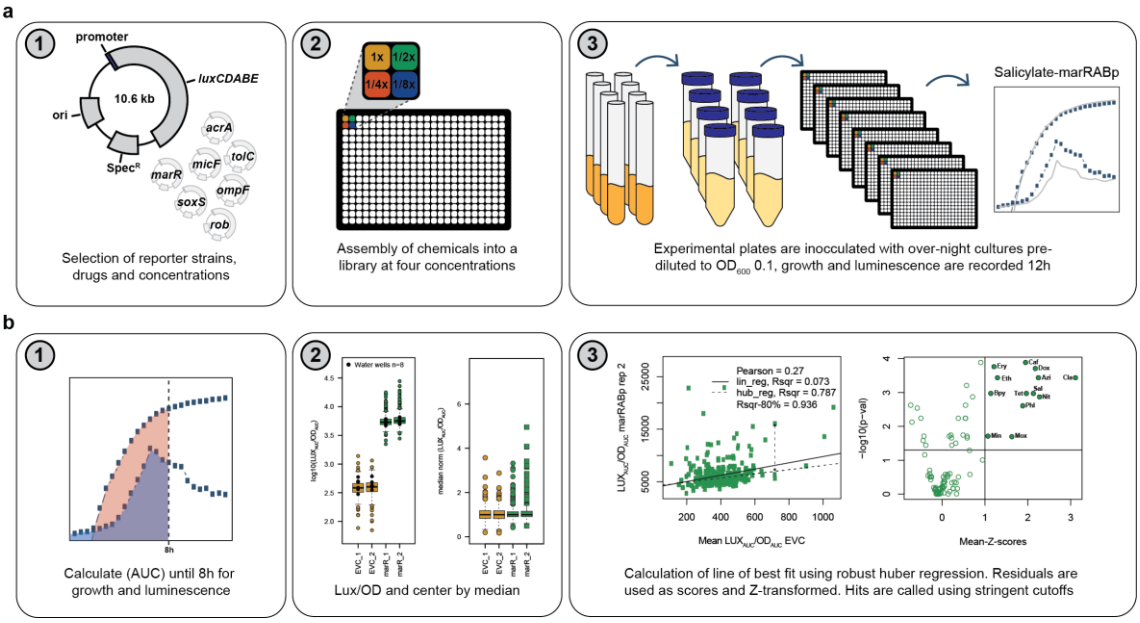

Figure 31: Schematic representation of the screen workflow and data processing.
a) Schematic screen workflow. Details described in methods. **b)** Schematic of data processing. Details described in methods. Figure adapted from manuscript (Binsfeld et al., 2025).

Non-growing samples (less than 10% of median OD_{AUC} across all compounds, reporters and concentrations) were removed from further analysis (250-419 wells out of 6144 wells total, depending on strain background), and luminescence was then normalized by growth (Lux_{AUC}/OD_{AUC}). Based on the premise that most compounds in the library do not induce/inhibit expression of any of the promoters, compound-promoter interactions were defined to be the deviation (residuals) of the line-of-best fit (Huber robust linear regression) (Huber, 1981) of normalized luminescence between a given promoter and the EVC. This method allows to better control for possible non-specific transcriptional effects of each compound, as we observed that normalized luminescence for EVC can in fact change across compounds/concentrations. Importantly, we observed that the robust linear fits had reasonably high R^2, indicating that this approach captures and corrects well non-specific effects, and positive and negative deviations (residuals) reflect compounds which increase or decrease promoter expression, respectively. The interaction scores (residuals) were subsequently Z-transformed (Z-scores) to allow comparability

of promoters of varying signal intensity. Finally, significant compound-promoter interactions were called based a double cut-off on mean Z-score of all compound concentrations and replicates for each compound-promoter pair (±1) and Benjamini-Hochberg (Benjamini and Hochberg, 1995) adjusted double sided rank-sum test p-value (<0.05) comparing the Z-scores distributions of each compound-promoter to water-promoter. Most Mean Z-scores are calculated with all 8 values (4 concentrations x 2 replicates), while in some cases data of up to three concentrations was removed due to poor growth as detailed earlier. However, phleomycin is the only case calculated with only 2 values (3 out of 4 concentrations over-killed) and there is no case where a compound was completely removed in the wild-type background. In all deletion backgrounds phleomycin became lethal at all four concentrations and was removed entirely as the only drug.

DNA and RNA quantification by qPCR and RT-qPCR

To confirm plasmid copy number stability after treatment with protein biosynthesis inhibitors, overnight cultures of *E. coli* BW25113 harboring plasmids pTU175-Lux-EVC or pBR322 were diluted 1:100 in fresh LB medium and grown at 37°C with agitation until exponential phase ($OD_{600\ nm}$ ~0.4). Chloramphenicol was added to half of the cultures to a final concentration of 2 µg/ml followed by further cultivation for 30 minutes. Total DNA was extracted using the Monarch Genomic DNA Purification Kit (NEB) using the manufacturer's instructions. All experiments were conducted in three biological replicates. Relative plasmid number fold changes were estimated by comparison with a non-treated control. All DNA oligos used in this study are listed in Table 3.

To confirm induction of *marA* after treatment with salicylate clarithromycin and sulfamethoxazole, overnight cultures of wild-type *E. coli* BW25113 were diluted 1:100 in fresh LB medium and grown at 37°C with agitation until exponential phase ($OD_{600\ nm}$ ~0.4). Salicylate, clarithromycin and sulfamethoxazole were added to cultures to a final concentration of 1 mM, 40 µM and 0.8 mM, respectively, while controls were left untreated, followed by further cultivation for

30 minutes. Total RNA was extracted using the Monarch Total RNA Miniprep Kit (NEB) using the manufacturer's instructions. Luna Universal One-Step RT-qPCR Kit (NEB) was used to prepare cDNA and as reagent for RT-qPCR according to the manufacturer's instructions. All experiments were conducted in at least three biological replicates and relative expression levels were estimated as previously described (Livak and Schmittgen, 2001), using *gyrA* expression as reference.

Lasso regression for estimation of regulator contributions of compound-promoter interactions

Firstly, the interaction scores gathered from the different genetic backgrounds were quantile normalized to account for baseline changes in expression due to regulator deletions. These normalized scores were then further pre-processed to consider the baseline values obtained from exposure to water through a soft-thresholding approach. Namely, we subtract the value of the water-promoter score from compound-promoter scores gathered in the same genetic background. In cases where the compound-promoter score is lower than the corresponding water-promoter score, the compound-promoter score is set to 0. These normalized and *water-thresholded* scores are then centered and scaled prior to modelling.

Once pre-processed, we modelled the scores for a given CPI as a function of compound concentration and genetic background, resulting in a design matrix X = $[X_{conc}, X_{rob}, X_{marA}, X_{soxS}]$ with dimensions $n \times 4$ (n being the number of samples). Compound concentration is a discrete variable ($X_{conc} \in \{1,2,4,8\}^n$), while genetic background is represented as a binary variable to indicate regulator presence/absence ($X_{rob,}\, X_{marA}, X_{soxS} \in \{0,1\}^n$). We also include all pairwise interactions between the variables in X in our model. In this way, our model can be stated as:

$$\mathrm{Y} = \beta_0 + \sum_{j}^{4} \beta_j X_j + \frac{1}{2} \sum_{j \neq k}^{4} \boldsymbol{\theta}_{jk} X_j X_k + \varepsilon$$

where $Y \in \mathbb{R}^n$ is the vector of pre-processed interaction scores for a given CPI, β_0 is a CPI-specific intercept, β_j is the effect that variable $j \in \{conc, rob, marA, soxS\}$ has on Y, $\boldsymbol{\theta}_{jk}$ captures the pairwise interaction effect between variables j and k, where $j, k \in \{conc, rob, marA, soxS\}$ and $j \neq k$, and ε models technical and biological noise.

To select for a parsimonious model, we estimate model coefficients via regularized maximum-likelihood estimation with lasso penalization (Bien et al., 2012; Tibshirani, 1996). Furthermore, we restrict non-zero interaction terms $\boldsymbol{\theta}_{jk}$ to only be present if both associated individual effects β_j and β_k are also non-zero (strong hierarchy). This restriction prioritizes explaining Y in terms of main effects β, and interactions are only included if the response cannot be solely captured by linear additive effects. Given that the log-likelihood of our model is

$$l(\beta_0, \beta, \theta) = ||Y - \beta_0 - X\beta - \frac{1}{2} X\boldsymbol{\theta}X^T||_2^2$$

the complete optimization problem for the hierarchical interaction model is:

$$min_{\beta,\boldsymbol{\theta}}\, l(\beta_0, \beta, \theta) + \lambda \left||\beta|\right|_1 + \frac{\lambda}{2}\left||\boldsymbol{\theta}|\right|_1$$
$$\text{s.t. } \boldsymbol{\theta} = \boldsymbol{\theta}^T, \qquad ||\,\boldsymbol{\theta}_j||_1 \leq \left|\beta_j\right|$$

where $\lambda > 0$ is the lasso penalization parameter that controls the sparsity of coefficients β and $\boldsymbol{\theta}$.

We solve this optimization problem using the efficient implementation provided in the R package `hierNet` (version 1.9)(Bien et al., 2012). The optimal value for λ was determined through 4-fold cross validation. We selected the λ value that was within one standard error of the λ that minimized the cross validation error. In this way, the nature of the individual effects that drug concentration and regulator presence have on changes in gene expression in response to a given chemical stressor are captured in the sign and magnitude of the coefficients β.

Interaction coefficients θ, potentially reflecting added synergistic effects, were negligible compared to concentration or single regulator coefficients, and were therefore excluded from further analysis.

Regulator contribution coefficients (β) to compound-promoter pairs were then multiplied by the absolute of mean Z-scores of the wild type – multiplied coefficients B* – thereby reflecting the strength of the compound-promoter interactions in wild type, in addition to regulator contribution. This approach facilitates interpretation and enables better understanding of regulator contributions to strong compound-promoter interactions in the wild type.
We performed a 10-fold cross-validation to provide a robustness measurement of each compound-promoter pair's regulator contributions using a "out-of-sample R^2" metric. In this procedure, the data for each compound-promoter pair was randomly divided into a training set (75% of the data) and a testing set (25% of the data). The model was trained on the training set, and its out-of-sample performance was evaluated on the testing set. The average R^2 per compound-promoter pair was estimated considering the results from folds where the ground-truth test set values had a variance > 0 (i.e. more than one unique value). For compound-promoter pairs for which all contribution coefficients are invariably zero, R^2 cannot be estimated.

Determination of Minimum Inhibitory Concentration (MIC)

Compound Minimum Inhibitory Concentration (MIC) against *E. coli* and *Salmonella* strains was quantified using liquid growth assays in LB-Lennox in microtiter plates in preparation for screening or checker board assays. The assay was performed in 96-well plates in 100 µl, and conditions similar to those used in the screening approach described above. Drugs were diluted linearly in 11 equal steps, allowing for finely resolved quantification of antimicrobial efficacy. Growth curves were analysed similar to those from the screening approach, and growth after 8h was approximated by OD_{AUC}.

MIC curves were generated to assess complementation of *micF*, *ompF* and *rob* in the respective deletion genetic backgrounds. We used our checkerboard

assays to select a suitable caffeine concentration where antagonism was observed for the wild type: at 55.5 µg/ml caffeine the ciprofloxacin and amoxicillin MIC curves are shifted towards higher concentrations (ED Fig 5a). We then followed the procedure described above (in 384 well-plates, 40 µl) for obtaining MIC curves for ciprofloxacin and amoxicillin with the complemented mutants in the presence and absence of 55.5 µg/ml caffeine. The MIC curves were estimated as previously described (Brenzinger et al., 2024) by fitting a three-parameter logistic model to the drug dosage response curves using the R-package drc (Ritz et al., 2015), using $OD_{AUC,8h}$ as proxy for growth.

Isothermal Titration Calorimetry

Purification and subsequent ITC of Rob-6xHis with caffeine were carried out essentially as described previously (Chubiz et al., 2012). Briefly, Rob was expressed in *E. coli* BL21 (DE3) from a pET28a plasmid harboring the *E.* coli Rob open reading frame, fused to a C-terminal 6xHis-tag. 4x 2 l cultures in LB medium were grown at 37°C to an OD_{600} of 0.6 and expression was induced by addition of 1 mM isopropyl β-D-1-thiogalactopyranoside (IPTG), followed by protein expression at 18°C overnight. Pellets were harvested by centrifugation and resuspended in lysis buffer (50 mM Tris-HCl pH 8.0, 200 mM NaCl, 10 mM imidazole, 1 mM TCEP, 10% glycerol, protease inhibitors, DNase), followed by lysis via sonication and centrifugation at 4°C at 30000 xg for 30 min. The soluble lysate was then loaded onto 5 ml Ni-NTA agarose beads. After intensive washing of the beads, the Rob protein was eluted with IMAC elution buffer (20 mM Tris-HCl pH 8.0, 200 mM NaCl, 250 mM imidazole, 1 mM TCEP, 10% glycerol). As a second purification step, target protein containing IMAC eluates were pooled and subjected to size-exclusion chromatography on a HiLoad Superdex 75 16/600 pg column, equilibrated to SEC buffer (200 mM NaCl, 20 mM Tris-HCl pH 8.0, 10% glycerol, 1 mM DTT). SEC peak eluates were pooled and concentrated to 14.35 mg/ml. Samples were aliquoted, frozen in liquid nitrogen and stored at -80°C.

Isothermal titration calorimetry (ITC) experiments were done using a MicroCal PEAQ-ITC titration calorimeter (Malvern) equilibrated to 25°C. Rob was adjusted to 50 µM in dialysis buffer (20 mM HEPES, 200 mM NaCl, pH 8). Caffeine solutions were prepared fresh in the same buffer to a final concentration of 10 mM. The experimental parameters used with the PEAQ-ITC system were 18 times 2 µl injections at 4 seconds duration, 150 seconds spacing, 750 rpm stirring speed, and a reference power of 10 µcal/s.

Proteomics

In vivo two-dimensional thermal proteome profiling (2D-TPP) with wild type *E. coli* BW25113 and Δ*marA* backgrounds was performed as previously described (Mateus et al., 2020, 2018) with a caffeine concentration gradient ranging from 0 - 400 µM (0, 4.1 µM,10.2 µM, 25.6 µM, 64 µM, 160 µM, 400 µM). A single culture of mid-exponential cells was split before treatment. Protein digestion, peptide labelling, MS-based proteomics and data analysis for assessment of protein thermal stability changes were performed as previously described (Kurzawa et al., 2020; Mateus et al., 2020, 2018). Caffeine-induced changes in protein abundance without temperature denaturation were calculated as the median fold-change across all caffeine concentrations (4.1 µM - 400 µM) at the lowest two temperatures (42°C, 45.4°C, n = 12). Benjamini-Hochberg adjusted double-sided rank-sum test was used to compare the fold-change distributions of each protein to the background (entire dataset). Gene Ontology (GO) analysis (for biological process) was performed to identify functional enrichment among significantly abundant proteins (p-value < 0.05) in *E. coli*. Gene annotations were obtained from EcoCyc (https://ecocyc.org). Statistical enrichment analysis among all detected proteins (n=1177) was performed using Fisher's exact test. No correction for multiple testing was done, as the p-values were generally high (low risk for false positives), and a correction would deem all changes non-significant, thereby increasing the risk for false negatives. Thus, GO terms with a p-value < 0.05 were considered significantly enriched.

Quantification of OmpF levels by Western Blot

E. coli and *S. enterica* OmpF levels were quantified by Western blotting. Caffeine treated and untreated cultures were prepared in three biological replicates each by 1:100 dilution of over-night cultures in 20 mL LB-medium and grown at 37°C and 180 rpm shaking. Caffeine was added to half of the flasks at a concentration of 1 mM, while the other half of the flasks served as a negative control. Cultures were grown until OD_{600} of ~0.8, followed by pelleting via centrifugation (10 min, 4000g, 4°C). Pellets were resuspendet in 200 µl 4% SDS solution, heated to 95°C for 5 min and stored at -80°C until used. The Pierce™ BCA Protein Assay Kit (Fisher Scientific, Germany) was used to calculate total protein concentration of all samples according to the manufacturer's instructions. Samples were adjusted to 4 µg/µl protein with 4% SDS solution and mixed in equal parts with 2x Laemmli buffer containing 2-mercaptoethanol. Aliquots containing 20 µg of total protein (10 µl) were boiled for 5 min at 95°C to denature any proteins. Samples were separated by SDS-PAGE on a 10% gel at 80 V for 3.5 h and transferred to a PVDF membrane via Trans-Blot® Turbo™ system (BioRad), according to the manufacturer's instructions. A specific rabbit αOmpF antibody (kindly provided by Joel Selkrig, Aachen, Germany) and a rabbit αRecA antibody (ab63797, Abcam) were used as primary antibodies at dilutions of 1:20000 and 1:5000, respectively, to detect OmpF and RecA on the PVDF membrane. For both primary antibodies, we used an HRP-coupled secondary antibody (A0545, Sigma), and Pierce™ ECL Western Blotting-Substrate (Thermo Scientific) to visualise OmpF using an chemiluminescence imager (Intas Science Imaging Instruments GmbH, Germany).

Quantification of MicF small RNA by Northern blotting

Bacterial cultures were grown to exponential phase (OD_{600} ~0.4) and treated with 1 mM caffeine for 30 minutes or left untreated as negative control. Samples were then mixed with 0.2 volumes of STOP solution (95% ethanol, 5% phenol) and snap-frozen in liquid nitrogen to prevent RNA degradation. Total RNA was extracted using the hot phenol method. Cell pellets were thawed and resuspended in 65°C lysis buffer (40 mM EDTA pH 8, 200 mM NaCl, 0.5%

SDS, 100 mM Tris-HCl pH 7.5), incubated for 5 minutes at 65°C in a water bath and subsequently mixed with acidic phenol (ROTI Aqua-Phenol, Roth). Samples were mixed thoroughly by vortexing, snap-frozen in liquid nitrogen and centrifuged for 10 minutes. The upper aqueous phase was then mixed with the same volume of chloroform-isoamyl alcohol (24:1) and mixed again by vortexing. The resulting upper phase was then mixed with 1/10th volume of 3M sodium acetate (pH 4.5) and one volume isopropanol to precipitate total RNA for 30 minutes on ice. Supernatants were subsequently removed, pellets dried and resuspended in RNAse free water. Northern blotting, radioactive labelling of DNA oligonucleotides, hybridization and signal detection were all performed as previously described (Fuchs et al., 2023). Signals were subsequently analysed using ImageJ software (Schindelin et al., 2012; Schneider et al., 2012).

Checkerboard Assays

Quantification of interactions between caffeine and ciprofloxacin and/or amoxicillin was performed using checkerboard assays. In brief, a checkerboard assay resembles a two-dimensional MIC assay, with two different drugs being combined across concentration gradients. The assays were performed in 96- or 384-well plates in biological quadruplicates and conditions similar to the screening described above. Growth inhibitory effect (OD_{AUC} after 8h) was determined in a series of 7 (vertical dilution series) equally spaced concentrations for caffeine and 11 (horizontal dilution series) equally spaced concentrations for the antibiotic. Concentrations were adapted for *E. coli*, *S. enterica*, and respective deletion mutants (Δ*rob*, Δ*micF*, Δ*marA* and Δ*ompF*). Fitness was calculated by normalization of OD_{AUC} of each well with the no-drug control. Lines of equal fitness (isoboles) were estimated by the contours derived from drug-interaction-surfaces. Provided that caffeine alone does not show inhibitory effects at the concentrations tested, antagonism with ciprofloxacin or amoxicillin is reflected by increased concentrations of ciprofloxacin or amoxicillin needed to inflict a given inhibitory effect with increasing concentrations of caffeine (isoboles moving rightward, Figure 25).

Table 1: Bacterial strains used throughout this thesis

Name	Species	Strain	Genotype	BSL	Origin	Resistance
AB10001	E. coli	BW25113	Δ(araD-araB)567, ΔlacZ4787(::rrnB-3), λ-, rph-1, Δ(rhaD-rhaB)568, hsdR514	S1	Typas	none
AB10005	E. coli	DH5α	F– endA1 glnV44 thi-1 recA1 relA1 gyrA96 deoR nupG purB20 φ80dlacZΔM15 Δ(lacZYA-argF)U169, hsdR17(rK– mK+), λ–	S1	Typas	none
AB10013	S. enterica Typhimurium	14028S	-	S2	Typas	none
AB30003	E. coli	BW25113	ΔompF	S1	This study	none
AB30004	E. coli	BW25113	ΔmarA	S1	This study	none
AB30043	E. coli	BW25113	pTU175-pMicF-lux rep	S1	This study	Spectinomycin
AB30045	E. coli	BW25113	pTU175-pTolC-lux rep	S1	This study	Spectinomycin
AB30046	E. coli	BW25113	pTU175-pOmpF-lux rep	S1	This study	Spectinomycin
AB30067	E. coli	BW25113	pTU175-pMarR-lux rep	S1	This study	Spectinomycin
AB30068	E. coli	BW25113	pTU175-pSoxS-lux rep	S1	This study	Spectinomycin
AB30069	E. coli	BW25113	pTU175-pRob-lux rep	S1	This study	Spectinomycin
AB30070	E. coli	BW25113	pTU175-pAcrAB-lux rep	S1	This study	Spectinomycin
AB30081	E. coli	BW25113	pTU175-EVC-lux rep	S1	This study	Spectinomycin
AB30084	S. enterica Typhimurium	14028S	pASCoT-LuxCDABE	S2	This study	Ampicillin
AB30127	S. enterica Typhimurium	14028S	pASCoT-pMicF-Lux	S2	This study	Ampicillin
AB30212	E. coli	BW25113	ΔmicF	S1	This study	none
AB30219	E. coli	BW25113	Δrob	S1	This study	none
AB30257	E. coli	BW25113	ΔmarR pTU175 EVC	S1	This study	Spectinomycin
AB30258	E. coli	BW25113	ΔmarR pTU175 pmarRAB	S1	This study	Spectinomycin
AB30305	E. coli	BW25113	ΔsoxS	S1	This study	none
AB30306	E. coli	BW25113	ΔsoxS pTU175 EVC	S1	This study	Spectinomycin
AB30307	E. coli	BW25113	ΔsoxS pTU175 ptolC	S1	This study	Spectinomycin
AB30308	E. coli	BW25113	ΔmarA pTU175 EVC	S1	This study	Spectinomycin

AB30309	E. coli	BW25113	ΔmarA pTU175 pmicF	S1	This study	Spectinomycin
AB30310	E. coli	BW25113	ΔmarA pTU175 pompF	S1	This study	Spectinomycin
AB30311	E. coli	BW25113	ΔmarA pTU175 pacrA	S1	This study	Spectinomycin
AB30312	E. coli	BW25113	ΔmarA pTU175 ptolC	S1	This study	Spectinomycin
AB30332	E. coli	BW25113	ΔmarA pTU175-pmarRAB	S1	This study	Spectinomycin
AB30333	E. coli	BW25113	ΔmarA pTU175-psoxS	S1	This study	Spectinomycin
AB30334	E. coli	BW25113	ΔmarA pTU175-prob	S1	This study	Spectinomycin
AB30335	E. coli	BW25113	ΔsoxS pTU175-pacrAB	S1	This study	Spectinomycin
AB30336	E. coli	BW25113	ΔsoxS pTU175-pmarRAB	S1	This study	Spectinomycin
AB30337	E. coli	BW25113	ΔsoxS pTU175-psoxS	S1	This study	Spectinomycin
AB30338	E. coli	BW25113	ΔsoxS pTU175-prob	S1	This study	Spectinomycin
AB30339	E. coli	BW25113	ΔsoxS pTU175-pmicF	S1	This study	Spectinomycin
AB30340	E. coli	BW25113	ΔsoxS pTU175-pompF	S1	This study	Spectinomycin
AB30341	E. coli	BW25113	Δrob pTU175-EVC	S1	This study	Spectinomycin
AB30342	E. coli	BW25113	Δrob pTU175-pacrAB	S1	This study	Spectinomycin
AB30343	E. coli	BW25113	Δrob pTU175-ptolC	S1	This study	Spectinomycin
AB30344	E. coli	BW25113	Δrob pTU175-pmarRAB	S1	This study	Spectinomycin
AB30345	E. coli	BW25113	Δrob pTU175-psoxS	S1	This study	Spectinomycin
AB30346	E. coli	BW25113	Δrob pTU175-prob	S1	This study	Spectinomycin
AB30347	E. coli	BW25113	Δrob pTU175-pmicF	S1	This study	Spectinomycin
AB30348	E. coli	BW25113	Δrob pTU175-pompF	S1	This study	Spectinomycin
AB30463	S. enterica Typhimurium	14028S	ΔompF	S2	This study	none
AB10027	E. coli	CFT073	-	S2	DSMZ	none
AB20127	E. coli	DH5α	F– endA1 glnV44 thi-1 recA1 relA1 gyrA96 deoR nupG purB20 φ80dlacZΔM15 Δ(lacZYA-argF)U169, hsdR17(rK– mK+), λ–	S1	Jörg Vogel	Ampicillin
AB20206	E. coli	BL21	F– ompT gal dcm lon hsdSB(rB– mB–) [malB+]K-12(λS)	S1	This study	Kanamycin
AB30538	E. coli	BW25113	rob::rob	S1	This	none

					study	
AB30539	E. coli	BW25113	ΔmicF pTU175-MicF-comp	S1	This study	Spectinomycin
AB30536	E. coli	BW25113	ompF::ompF	S1	This study	none
AB30543	E. coli	BW25113	rob::rob pTU175-pmarRAB-lux rep	S1	This study	Spectinomycin
AB30542	E. coli	BW25113	rob::rob pTU175-pMicF-lux rep	S1	This study	Spectinomycin

Table 2: Plasmids and plasmid carrying strains used throughout this thesis

Name	Strain	Plasmid Name	Plasmid backbone	Primers used	Source
AB20011	E. Coli Top10	pTU175-luxCDABE	pTU175-luxCDABE	-	Typas Lab, EMBL Heidelberg
AB20041	E. Coli DH5α	pTU175-marRAB	pTU175-luxCDABE	29 & 30	This study
AB20043	E. Coli DH5α	pTU175-acrAB	pTU175-luxCDABE	57 & 58	This study
AB20044	E. Coli DH5α	pTU175-soxS	pTU175-luxCDABE	43 & 44	This study
AB20045	E. Coli DH5α	pTU175-rob	pTU175-luxCDABE	47 & 48	This study
AB20048	E. Coli DH5α	pTU175-ompF	pTU175-luxCDABE	53 & 54	This study
AB20049	E. Coli DH5α	pTU175-micF	pTU175-luxCDABE	51 & 52	This study
AB20051	E. Coli DH5α	pTU175-tolC	pTU175-luxCDABE	31 & 32	This study
AB20086	E. Coli DH5α	pASCoT-luxCDABE	pTU175-luxCDABE	-	Brochado Lab
AB20118	E. Coli DH5α	pASCoT-micF	pASCoT-luxCDABE	99 & 181	This study
AB20008	E. coli DH5a	pKD13	pKD13	-	Westermann Lab
AB20046	E. coli Top10	pKD46	pKD46	-	Westermann Lab
AB20055	E. coli DH5a	pCp20	pCP20	-	Westermann Lab
AB20127	E. coli DH5a	pBR322	pBR322	-	Typas Lab, EMBL Heidelberg

AB20003	E. coli BL21	pET-28a	pET-28a	-	Typas Lab, EMBL Heidelberg
AB20206	E. coli BL21	pET-28a-Rob	pET-28a	658 & 659	This study
AB20277	E. coli DH5a	pKD13-rob	pKD13	1121 & 1122	This study
AB20279	E. coli DH5a	pKD13-ompF	pKD13	1125 & 1126	This study
AB20284	E. coli DH5a	pTU175-micF-comp	pTU175-luxCDABE	1161 & 1162	This study

Table 3: DNA oligonucleotides used throughout this thesis

Number	Primer name	sequence
29	RL_pTU175_Lux_pMarRAB-fwd	TGTCGG**GAATTC**tctgttgcggaaagagcatcc
30	RL_pTU175_Lux_pMarRAB-rev	TGGTCT**CTCGAG**attagttgccctggcaagtaattagttgc
31	RL_pTU175_Lux_TolC-fwd	TGTCGG**GAATTC**atcatcccggcaaccatctcc
32	RL_pTU175_Lux_TolC-rev	TGGTCT**CTCGAG**ttgcattccttgtggtgaagcag
43	RL_pTU175_Lux_pSoxS-fwd	TGTCGG**GAATTC**agcggtcgcccgggttacg
44	RL_pTU175_Lux_pSoxS-rev	TGGTCT**CTCGAG**aaatctgcctcttttcagtgttcagttcg
47	RL_pTU175_Lux_pRob-fwd	TGTCGG**GAATTC**ccgtttttaatacgatccgacagttcaatcg
48	RL_pTU175_Lux_pRob-rev	TGGTCT**CTCGAG**aaaatatcctcatcctttcaacaacgagcacc
51	RL_pTU175_Lux_pMicF-fwd	TGTCGG**GAATTC**aggtctggtcgccatctacatc
52	RL_pTU175_Lux_pMicF-rev	TGGTCT**CTCGAG**gggagttattctagttgcgagtgaagg
53	RL_pTU175_Lux_pOmpF-fwd	TGTCGG**GAATTC**cgatcatcctgttacggaatattacattgc
54	RL_pTU175_Lux_pOmpF-rev	TGGTCT**CTCGAG**tatttattaccctcatggttttttttatgacacctgc
57	RL_pTU175_Lux_pAcrAB-fwd	TGTCGG**GAATTC**acaaattcgcatttgtggaatataatctcc
58	RL_pTU175_Lux_pAcrAB-rev	TGGTCT**GTCGAC**atgtaaacctcgagtgtccg
99	SB5 MicF fw	CGGCGCAGTATGAAGATCTCGAGTAGGTCTGGTCGCCATCGC
181	ST pMicF rev	GGTACCGTTGTGGTCTCggtcactattttagttgcgaatg
591	dRob_KanFRT_fwd	tccaattacctgatgtcaggtgctcgttgttgaaaggatgaggatattttgtgtaggctggagctgcttc
592	dRob_KanFRT_rev	gggacatctcgcatctggacgcccctgcattagatgagctgcagcgttaaattccggggatccgtcgacc
580	5S-rRNA_Nblot_probe	CTACGGCGTTTCACTTCTGAGTTC

524	micF_Nblot_probe	GGGGTAAACAGACATTCAGA
658	Rob-6xHis_fwd	GATATACCatggatcaggccggcattattcg
659	Rob-6xHis_rev	GGCCGCAAGCTTacgacggatcggaatcagcag
1161	GA_pTU-micF-comp_fwd	GCATCGGCGGCGCAGTATGAAGATCTCGAGAG GTCTGGTCGCCATCTACATC
1162	GA_pTU-micF-comp_rev	CAG CTA TCG ATC CAT GGG GCC CGC GGC CGC AAA AAA AAC CGA ATG CGA GGC ATC
1121	pKD13_rob_fwd	gagaatagga acttcgaact gcaggtcgac ttaacgacgg atcggaatca gcag
1122	pKD13_rob_rev	gtcaaacatg agaattaatt ccggggatcc ccgtttttaa tacgatccga cagttcaatc
1125	pKD13_ompF_fwd	gagaatagga acttcgaact gcaggtcgac ttagaactgg taaacgatac ccacagc
1126	pKD13_ompF_rev	gtcaaacatg agaattaatt ccggggatcc cgatcatcct gttacggaat attacattgc

Table 4: Compounds used for reporter screening

Drug	**Highest conc (µM)**	**Highest conc (µg/ml)**	**Supplier**	**Cat. No**
Water	0.000	0.000	-	-
1-Methyluric acid	1000.000	91.070	Sigma	M6885-100MG
2,3-DHBA	1000.000	154.120	Sigma	126209-5G
2'-2'-Bipyridyl	500.000	78.090	Sigma	D216305-10G
4-Aminobenzoic acid	500.000	68.570	Sigma	A9878-5G
4-aminosalicylic acid	1000.000	153.140	Sigma	A79604-100G
A22	5.000	1.358	Sigma	SML0471-10MG
Acetylsalicylic acid	1000.000	180.160	Sigma	A5376-100G
Adrenalin	500.000	109.835	Sigma	E4642-5G
Amikacin	1.000	0.586	Sigma	PHR1654-1G
Amoxicillin	5.500	2.010	Sigma	A8523-5G
Azithromycin	3.000	2.247	Biomol	LKT-A9834.500
Aztreonam	0.100	0.044	MP Biomedicals	215041501
Bacitracin	200.000	284.538	Sigma	11702-5G
Benzalkonium	40.000	14.881	Sigma	B6295-100G
Berberine	500.000	168.183	Sigma	14050-10G
Bleomycin	0.200	0.303	Biomol	Cay13877-

				10
Butyrate	500.000	55.045	Sigma	8202360250
Caffeine	1000.000	194.190	Sigma	C0750-5G
Catechin	500.000	145.135	Sigma	C1251-5G
CCCP	25.000	5.116	Sigma	C2759-250MG
Cefaclor	2.500	0.920	Sigma	C6895-100MG
Cefotaxime	0.020	0.010	Sigma	C7039-100MG
Cefsulodin	25.000	13.863	Sigma	C8145-250MG
Cerulenin	45.000	10.047	Sigma	C2389-5MG
Cetirizine dihydrochloride	500.000	230.905	Sigma	C3618-50MG
Chloramphenicol	3.000	0.969	MP Biomedicals	219032105
Chlorhexidine	1.000	0.505	Sigma	282227-1G
Cidofovir	500.000	139.595	Sigma	C5874-10MG
Ciprofloxacin	0.030	0.010	Sigma	17850-5G-F
Clarithromycin	40.000	29.918	Sigma	C9742-100MG
Clindamycin	4.500	2.076	Biomol	LKT-C4532.50
Colistin	0.300	0.380	Sigma	PHR1605
Curcumin	500.000	184.193	Biomol	Cay81025
Cycloserine D	75.000	7.657	Sigma	C6880-1G
Deoxycholic acid	500.000	196.285	Sigma	30960-25G
Dopamine	500.000	94.820	Sigma	H8502-5G
Doxorubicin	4.000	2.320	Biomol	Cay15007-50
Doxycycline	1.000	0.513	Sigma	D9891-1G
EDTA	500.000	146.120	Carl Roth	8040.2
EGCG	50.000	22.919	Sigma	E4143-50MG
Erythromycin	20.000	14.679	Sigma	E5389-1G
Estradiol	500.000	136.190	Sigma	E8875-1G
Ethidiumbromide	500.000	197.147	Sigma	E1510-10ML
Fosfomycin	0.500	0.091	Sigma	P5396-1G
Fusidic acid	200.000	107.738	Sigma	F0881-1G

Gentamicin	2.000	1.033	Sigma	G1914-250MG
Hydrocortisone	500.000	181.230	Sigma	H4001-1G
Ibuprofen	500.000	103.140	Sigma	I7905-1G
Imipenem	0.500	0.159	Biomol	Cay16039-25
Indole	1000.000	117.150	Sigma	I3408-25G
Levofloxacin	0.100	0.036	Sigma	28266-1G-F
Lithocholic acid	500.000	188.285	Sigma	L6250-10G
Loperamide	250.000	256.753	Sigma	PHR-1162-1G
Water	0.000	0.000	-	-
Mecillinam	0.200	0.065	Sigma	33447-100MG
Meropenem	0.200	0.088	Sigma	M2574-10MG
Metformin	1000.000	165.620	Biomol	Cay13118-5
Metronidazole	5.000	0.856	Sigma	M3761-5G
Minocycline	1.000	0.494	Biomol	Cay14454-50
Mitomycin C	1.500	0.501	Biomol	Cay11435-5
Moxifloxacin	0.200	0.088	Sigma	SML1581-50MG
Nitrofurantoin	15.000	3.572	Sigma	N7878-10G
Noradrenalin	500.000	159.630	Sigma	A0937-1G
Novobiocin	30.000	19.038	Sigma	74675-5G
Omeprazole	500.000	172.700	Biomol	Cay14880-100
Oxacillin	10.000	4.234	Sigma	28221-1G
Paraquat	20.000	5.143	Sigma	36541-100MG
Penicillin G	10.000	3.725	Sigma	P8721-25MU
Phleomycin	3.500	4.996	Biomol	Cay15549-10
Piperacillin	0.500	0.270	Sigma	P8396-1G
Piperine	500.000	142.670	Sigma	W290904-100G-K
PMS	30.000	9.190	Sigma	P9625-1G
Polymyxin B	0.200	0.277	Sigma	P0972-1MU

Procaine	45000.000	10633.950	Sigma	P9879-50G
Progesterone	500.000	157.230	Sigma	P8783-1G
Pseudomonic acid	4.000	2.003	Biomol	Cay23238-50
Puromycin	45.000	24.499	Biomol	Cay13884-100
Quercetin	500.000	151.120	Sigma	Q4951-10G
Quinine	1000.000	324.420	Sigma	22620-5G
Rifampicin	10.000	8.229	Sigma	R3501-1G
Salicylate	1000.000	138.120	Sigma	247588-100G
Serotonine	500.000	106.340	Biomol	Cay14332-100
Sodium urate	1000.000	227.301	Sigma	U2875-5G
Spectinomycin	10.000	4.954	Sigma	S4014-5G
Spiramycin	25.000	21.076	Sigma	S9132-1G
Sulfamethoxazole	100.000	25.330	Biomol	Cay23613-25
Sulfamonomethoxine	200.000	56.060	Sigma	S0508-250MG
Testosterone	500.000	144.210	Sigma	86500-1G
Tetracycline	1.000	0.444	Sigma	87128-25G
Thiourea	500.000	38.060	Sigma	T8656-100G
Tobramycin	2.000	0.935	Sigma	T4014-100MG
Trimethoprim	2.000	0.581	Sigma	T7883-5G
Tunicamycin	25.000	21.125	Sigma	T7765-5MG
Vanillin	1000.000	152.149	Sigma	V1104-2G
Verapamil	500.000	227.301	Biomol	Cay14288-5

Acknowledgements

First of all, I would like to thank Ana for taking me in as her first PhD student and for the enthusiasm and scientific curiosity that you employ to all of our projects. Despite many of the difficult circumstances we faced in the last few years you always supported us, which I am very grateful for.

Next, I would like to thank the entire Brochado lab, who similarly always supported me throughout the last years and created a great atmosphere. I really enjoyed working alongside all of you and wish you all the best.

Finally, I would also like to say thank you to Liv and my family, who always cheered me on when I felt stressed or upset about work. I am immensely grateful for all of your support.

References

Alekshun, M.N., Levy, S.B., 1999. Alteration of the repressor activity of MarR, the negative regulator of the Escherichia coli marRAB locus, by multiple chemicals in vitro. J Bacteriol 181, 4669–72. https://doi.org/10.1128/JB.181.15.4669-4672.1999

Alekshun, M.N., Levy, S.B., Mealy, T.R., Seaton, B.A., Head, J.F., 2001. The crystal structure of MarR, a regulator of multiple antibiotic resistance, at 2.3 angstrom resolution. Nature Structural Biology 8, 710–714. https://doi.org/Doi 10.1038/90429

Amábile-Cuevas, C.F., Demple, B., 1991. Molecular characterization of the soxRS genes of Escherichia coli: two genes control a superoxide stress regulon. Nucleic Acids Res 19, 4479–4484. https://doi.org/10.1093/nar/19.16.4479

Andersen, J., Delihas, N., 1990. micF RNA binds to the 5' end of ompF mRNA and to a protein from Escherichia coli. Biochemistry 29, 9249–56. https://doi.org/10.1021/bi00491a020

Andersen, J., Forst, S.A., Zhao, K., Inouye, M., Delihas, N., 1989. The function of micF RNA. micF RNA is a major factor in the thermal regulation of OmpF protein in Escherichia coli. J Biol Chem 264, 17961–17970.

Andersson, D.I., Hughes, D., 2014. Microbiological effects of sublethal levels of antibiotics. Nat Rev Microbiol 12, 465–478. https://doi.org/10.1038/nrmicro3270

Andersson, D.I., Nicoloff, H., Hjort, K., 2019. Mechanisms and clinical relevance of bacterial heteroresistance. Nat Rev Microbiol 17, 479–496. https://doi.org/10.1038/s41579-019-0218-1

Aquino, P., Honda, B., Jaini, S., Lyubetskaya, A., Hosur, K., Chiu, J.G., Ekladious, I., Hu, D., Jin, L., Sayeg, M.K., Stettner, A.I., Wang, J., Wong, B.G., Wong, W.S., Alexander, S.L., Ba, C., Bensussen, S.I., Bernstein, D.B., Braff, D., Cha, S., Cheng, D.I., Cho, J.H., Chou, K., Chuang, J., Gastler, D.E., Grasso, D.J., Greifenberger, J.S., Guo, C., Hawes, A.K., Israni, D.V., Jain, S.R., Kim, J., Lei, J., Li, H., Li, D., Li, Q., Mancuso, C.P., Mao, N., Masud, S.F., Meisel, C.L., Mi, J., Nykyforchyn, C.S., Park, M., Peterson, H.M., Ramirez, A.K., Reynolds, D.S., Rim, N.G., Saffie, J.C., Su, H., Su, W.R., Su, Y., Sun, M., Thommes, M.M., Tu, T., Varongchayakul, N., Wagner, T.E., Weinberg, B.H., Yang, R., Yaroslavsky, A., Yoon, C., Zhao, Y., Zollinger, A.J., Stringer, A.M., Foster, J.W., Wade, J., Raman, S., Broude, N., Wong, W.W., Galagan, J.E., 2017. Coordinated regulation of acid resistance in Escherichia coli. BMC Systems Biology 11, 1. https://doi.org/10.1186/s12918-016-0376-y

Ariza, R.R., Li, Z., Ringstad, N., Demple, B., 1995. Activation of multiple antibiotic resistance and binding of stress-inducible promoters by Escherichia coli Rob protein. J Bacteriol 177, 1655–61. https://doi.org/10.1128/jb.177.7.1655-1661.1995

Azam, T.A., Hiraga, S., Ishihama, A., 2000. Two types of localization of the DNA-binding proteins within the Escherichia coli nucleoid. Genes to Cells 5, 613–626. https://doi.org/10.1046/j.1365-2443.2000.00350.x

References

Baba, T., Ara, T., Hasegawa, M., Takai, Y., Okumura, Y., Baba, M., Datsenko, K.A., Tomita, M., Wanner, B.L., Mori, H., 2006. Construction of Escherichia coli K-12 in-frame, single-gene knockout mutants: the Keio collection. Mol Syst Biol 2, 2006 0008. https://doi.org/10.1038/msb4100050

Babu, M., Díaz-Mejía, J.J., Vlasblom, J., Gagarinova, A., Phanse, S., Graham, C., Yousif, F., Ding, H., Xiong, X., Nazarians-Armavil, A., Alamgir, M., Ali, M., Pogoutse, O., Pe'er, A., Arnold, R., Michaut, M., Parkinson, J., Golshani, A., Whitfield, C., Wodak, S.J., Moreno-Hagelsieb, G., Greenblatt, J.F., Emili, A., 2011. Genetic Interaction Maps in Escherichia coli Reveal Functional Crosstalk among Cell Envelope Biogenesis Pathways. PLOS Genetics 7, e1002377. https://doi.org/10.1371/journal.pgen.1002377

Barbosa, T.M., Levy, S.B., 2000. Differential Expression of over 60 Chromosomal Genes in *Escherichia coli* by Constitutive Expression of MarA. J Bacteriol 182, 3467–3474. https://doi.org/10.1128/JB.182.12.3467-3474.2000

Batchelor, E., Walthers, D., Kenney, L.J., Goulian, M., 2005. The Escherichia coli CpxA-CpxR Envelope Stress Response System Regulates Expression of the Porins OmpF and OmpC. Journal of Bacteriology 187, 5723–5731. https://doi.org/10.1128/jb.187.16.5723-5731.2005

Benjamini, Y., Hochberg, Y., 1995. Controlling the False Discovery Rate: A Practical and Powerful Approach to Multiple Testing. Journal of the Royal Statistical Society Series B: Statistical Methodology 57, 289–300. https://doi.org/10.1111/j.2517-6161.1995.tb02031.x

Bennik, M.H.J., Pomposiello, P.J., Thorne, D.F., Demple, B., 2000. Defining a *rob* Regulon in *Escherichia coli* by Using Transposon Mutagenesis. J Bacteriol 182, 3794–3801. https://doi.org/10.1128/JB.182.13.3794-3801.2000

Bien, J., Taylor, J., Tibshirani, R., 2013. A lasso for hierarchical interactions. Ann. Statist. 41. https://doi.org/10.1214/13-AOS1096

Bien, J., Taylor, J., Tibshirani, R., 2012. A lasso for hierarchical interactions. https://doi.org/10.48550/ARXIV.1205.5050

Binsfeld, C., Olayo-Alarcon, R., Pérez Jiménez, L., Wartel, M., Stadler, M., Mateus, A., Müller, C., Brochado, A.R., 2025. Systematic screen uncovers regulator contributions to chemical cues in Escherichia coli. PLoS Biol 23, e3003260. https://doi.org/10.1371/journal.pbio.3003260

Brauner, A., Fridman, O., Gefen, O., Balaban, N.Q., 2016. Distinguishing between resistance, tolerance and persistence to antibiotic treatment. Nat Rev Microbiol 14, 320–330. https://doi.org/10.1038/nrmicro.2016.34

Brenzinger, S., Airoldi, M., Ogunleye, A.J., Jugovic, K., Amstalden, M.K., Brochado, A.R., 2024. The Vibrio cholerae CBASS phage defence system modulates resistance and killing by antifolate antibiotics. Nat Microbiol, 5 9, 251–262. https://doi.org/10.1038/s41564-023-01556-y

Brochado, A.R., Telzerow, A., Bobonis, J., Banzhaf, M., Mateus, A., Selkrig, J., Huth, E., Bassler, S., Zamarreno Beas, J., Zietek, M., Ng, N., Foerster, S., Ezraty, B., Py, B., Barras, F., Savitski, M.M., Bork, P., Gottig, S., Typas, A., 2018. Species-specific activity of antibacterial drug combinations. Nature, 5 559, 259–263. https://doi.org/10.1038/s41586-018-0278-9

Butland, G., Babu, M., Díaz-Mejía, J.J., Bohdana, F., Phanse, S., Gold, B., Yang, W., Li, J., Gagarinova, A.G., Pogoutse, O., Mori, H., Wanner, B.L., Lo, H., Wasniewski, J., Christopoulos, C., Ali, M., Venn, P., Safavi-Naini, A., Sourour, N., Caron, S., Choi, J.-Y., Laigle, L., Nazarians-Armavil, A., Deshpande, A., Joe, S., Datsenko, K.A., Yamamoto, N., Andrews, B.J., Boone, C., Ding, H., Sheikh, B., Moreno-Hagelsieb, G., Greenblatt, J.F., Emili, A., 2008. eSGA: E. coli synthetic genetic array analysis. Nat Methods 5, 789–795. https://doi.org/10.1038/nmeth.1239

Chait, R., Craney, A., Kishony, R., 2007. Antibiotic interactions that select against resistance. Nature 446, 668–671. https://doi.org/10.1038/nature05685

Chen, S., Zhang, A., Blyn, L.B., Storz, G., 2004. MicC, a second small-RNA regulator of Omp protein expression in Escherichia coli. J Bacteriol 186, 6689–6697. https://doi.org/10.1128/JB.186.20.6689-6697.2004

Choi, U., Lee, C.-R., 2019. Distinct Roles of Outer Membrane Porins in Antibiotic Resistance and Membrane Integrity in Escherichia coli. Front. Microbiol. 10, 953. https://doi.org/10.3389/fmicb.2019.00953

Chubiz, L.M., 2023. The Mar, Sox, and Rob Systems. EcoSal Plus eesp00102022. https://doi.org/10.1128/ecosalplus.esp-0010-2022

Chubiz, L.M., Glekas, G.D., Rao, C.V., 2012. Transcriptional cross talk within the mar-sox-rob regulon in Escherichia coli is limited to the rob and marRAB operons. J Bacteriol 194, 4867–75. https://doi.org/10.1128/JB.00680-12

Chubiz, L.M., Rao, C.V., 2011. Role of the mar-sox-rob regulon in regulating outer membrane porin expression. J Bacteriol 193, 2252–60. https://doi.org/10.1128/JB.01382-10

Chung, C.T., Niemela, S.L., Miller, R.H., 1989. One-step preparation of competent Escherichia coli: transformation and storage of bacterial cells in the same solution. Proc. Natl. Acad. Sci. U.S.A. 86, 2172–2175. https://doi.org/10.1073/pnas.86.7.2172

Cohen, S.P., Hächler, H., Levy, S.B., 1993a. Genetic and functional analysis of the multiple antibiotic resistance (mar) locus in Escherichia coli. Journal of Bacteriology 175, 1484–1492. https://doi.org/10.1128/jb.175.5.1484-1492.1993

Cohen, S.P., Levy, S.B., Foulds, J., Rosner, J.L., 1993b. Salicylate induction of antibiotic resistance in Escherichia coli: activation of the mar operon and a mar-independent pathway. J Bacteriol 175, 7856–7862. https://doi.org/10.1128/jb.175.24.7856-7862.1993

Cohen, S.P., McMurry, L.M., Levy, S.B., 1988. marA locus causes decreased expression of OmpF porin in multiple-antibiotic-resistant (Mar) mutants of Escherichia coli. J Bacteriol 170, 5416–22. https://doi.org/10.1128/jb.170.12.5416-5422.1988

Cox, G., Wright, G.D., 2013. Intrinsic antibiotic resistance: Mechanisms, origins, challenges and solutions. International Journal of Medical Microbiology 303, 287–292. https://doi.org/10.1016/j.ijmm.2013.02.009

Coyer, J., Andersen, J., Forst, S.A., Inouye, M., Delihas, N., 1990. micF RNA in ompB mutants of Escherichia coli: different pathways regulate micF RNA levels in response to osmolarity and temperature change. J Bacteriol 172, 4143–50. https://doi.org/10.1128/jb.172.8.4143-4150.1990

Darby, E.M., Trampari, E., Siasat, P., Gaya, M.S., Alav, I., Webber, M.A., Blair, J.M.A., 2023. Molecular mechanisms of antibiotic resistance revisited. Nat Rev Microbiol 21, 280–295. https://doi.org/10.1038/s41579-022-00820-y

Datsenko, K.A., Wanner, B.L., 2000. One-step inactivation of chromosomal genes in Escherichia coli K-12 using PCR products. Proc Natl Acad Sci U S A 97, 6640–6645. https://doi.org/10.1073/pnas.120163297

Delcour, A.H., 2009. Outer Membrane Permeability and Antibiotic Resistance. Biochim Biophys Acta 1794, 808–816. https://doi.org/10.1016/j.bbapap.2008.11.005

Du, D., Wang-Kan, X., Neuberger, A., van Veen, H.W., Pos, K.M., Piddock, L.J.V., Luisi, B.F., 2018a. Multidrug efflux pumps: structure, function and regulation. Nat Rev Microbiol 16, 523–539. https://doi.org/10.1038/s41579-018-0048-6

Du, D., Wang-Kan, X., Neuberger, A., van Veen, H.W., Pos, K.M., Piddock, L.J.V., Luisi, B.F., 2018b. Multidrug efflux pumps: structure, function and regulation. Nat Rev Microbiol 16, 523–539. https://doi.org/10.1038/s41579-018-0048-6

Eguchi, Y., Ishii, E., Hata, K., Utsumi, R., 2011. Regulation of Acid Resistance by Connectors of Two-Component Signal Transduction Systems in Escherichia coli. Journal of Bacteriology 193, 1222–1228. https://doi.org/10.1128/jb.01124-10

Eguchi, Y., Itou, J., Yamane, M., Demizu, R., Yamato, F., Okada, A., Mori, H., Kato, A., Utsumi, R., 2007. B1500, a small membrane protein, connects the two-component systems EvgS/EvgA and PhoQ/PhoP in Escherichia coli. Proceedings of the National Academy of Sciences 104, 18712–18717. https://doi.org/10.1073/pnas.0705768104

Eguchi, Y., Okada, T., Minagawa, S., Oshima, T., Mori, H., Yamamoto, K., Ishihama, A., Utsumi, R., 2004. Signal Transduction Cascade between EvgA/EvgS and PhoP/PhoQ Two-Component Systems of Escherichia coli. Journal of Bacteriology 186, 3006–3014. https://doi.org/10.1128/jb.186.10.3006-3014.2004

Eguchi, Y., Oshima, T., Mori, H., Aono, R., Yamamoto, K., Ishihama, A., Utsumi, R., 2003. Transcriptional regulation of drug efflux genes by EvgAS, a two-component system in Escherichia coli. Microbiology (Reading) 149, 2819–2828. https://doi.org/10.1099/mic.0.26460-0

Eguchi, Y., Utsumi, R., 2014. Alkali metals in addition to acidic pH activate the EvgS histidine kinase sensor in Escherichia coli. J Bacteriol 196, 3140–3149. https://doi.org/10.1128/JB.01742-14

Ejim, L., Farha, M.A., Falconer, S.B., Wildenhain, J., Coombes, B.K., Tyers, M., Brown, E.D., Wright, G.D., 2011. Combinations of antibiotics and nonantibiotic drugs enhance antimicrobial efficacy. Nat Chem Biol 7, 348–350. https://doi.org/10.1038/nchembio.559

Elkins, C.A., Nikaido, H., 2002. Substrate specificity of the RND-type multidrug efflux pumps AcrB and AcrD of Escherichia coli is determined predominantly by two large periplasmic loops. J Bacteriol 184, 6490–6498. https://doi.org/10.1128/JB.184.23.6490-6499.2002

Fernández, L., Hancock, R.E.W., 2012. Adaptive and Mutational Resistance: Role of Porins and Efflux Pumps in Drug Resistance. Clinical

Microbiology Reviews 25, 661–681. https://doi.org/10.1128/cmr.00043-12

Fisher, R.A., Gollan, B., Helaine, S., 2017. Persistent bacterial infections and persister cells. Nat Rev Microbiol 15, 453–464. https://doi.org/10.1038/nrmicro.2017.42

Fuchs, M., Lamm-Schmidt, V., Lenče, T., Sulzer, J., Bublitz, A., Wackenreuter, J., Gerovac, M., Strowig, T., Faber, F., 2023. A network of small RNAs regulates sporulation initiation in *Clostridioides difficile*. The EMBO Journal 42, e112858. https://doi.org/10.15252/embj.2022112858

Gerken, H., Charlson, E.S., Cicirelli, E.M., Kenney, L.J., Misra, R., 2009. MzrA: a novel modulator of the EnvZ/OmpR two-component regulon. Molecular Microbiology 72, 1408–1422. https://doi.org/10.1111/j.1365-2958.2009.06728.x

Gibson, D.G., Young, L., Chuang, R.-Y., Venter, J.C., Hutchison, C.A., Smith, H.O., 2009. Enzymatic assembly of DNA molecules up to several hundred kilobases. Nat Methods 6, 343–345. https://doi.org/10.1038/nmeth.1318

Gogol, E.B., Rhodius, V.A., Papenfort, K., Vogel, J., Gross, C.A., 2011. Small RNAs endow a transcriptional activator with essential repressor functions for single-tier control of a global stress regulon. Proc Natl Acad Sci U S A 108, 12875–12880. https://doi.org/10.1073/pnas.1109379108

Goh, E.-B., Yim, G., Tsui, W., McClure, J., Surette, M.G., Davies, J., 2002. Transcriptional modulation of bacterial gene expression by subinhibitory concentrations of antibiotics. Proceedings of the National Academy of Sciences 99, 17025–17030. https://doi.org/10.1073/pnas.252607699

Greenberg, J.T., Monach, P., Chou, J.H., Josephy, P.D., Demple, B., 1990. Positive control of a global antioxidant defense regulon activated by superoxide-generating agents in Escherichia coli. Proceedings of the National Academy of Sciences 87, 6181–6185. https://doi.org/10.1073/pnas.87.16.6181

Griffith, K.L., Fitzpatrick, M.M., Keen, E.F., Wolf, R.E., 2009. Two functions of the C-terminal domain of Escherichia coli Rob: mediating “sequestration-dispersal” as a novel off-on switch for regulating Rob’s activity as a transcription activator and preventing degradation of Rob by Lon protease. J Mol Biol 388, 415–30. https://doi.org/10.1016/j.jmb.2009.03.023

Griffith, K.L., Shah, I.M., E. Wolf Jr, R., 2004. Proteolytic degradation of Escherichia coli transcription activators SoxS and MarA as the mechanism for reversing the induction of the superoxide (SoxRS) and multiple antibiotic resistance (Mar) regulons. Molecular Microbiology 51, 1801–1816. https://doi.org/10.1046/j.1365-2958.2003.03952.x

Gu, M., Imlay, J.A., 2011. The SoxRS response of Escherichia coli is directly activated by redox-cycling drugs rather than by superoxide. Mol Microbiol 79, 1136–1150. https://doi.org/10.1111/j.1365-2958.2010.07520.x

Hächler, H., Cohen, S.P., Levy, S.B., 1991. marA, a regulated locus which controls expression of chromosomal multiple antibiotic resistance in Escherichia coli. J Bacteriol 173, 5532–5538. https://doi.org/10.1128/jb.173.17.5532-5538.1991

Hao, Z., Lou, H., Zhu, R., Zhu, J., Zhang, D., Zhao, B.S., Zeng, S., Chen, X., Chan, J., He, C., Chen, P.R., 2014. The multiple antibiotic resistance

regulator MarR is a copper sensor in Escherichia coli. Nat Chem Biol 10, 21–28. https://doi.org/10.1038/nchembio.1380
Helaine, S., Conlon, B.P., Davis, K.M., Russell, D.G., 2024. Host stress drives tolerance and persistence: The bane of anti-microbial therapeutics. Cell Host & Microbe 32, 852–862. https://doi.org/10.1016/j.chom.2024.04.019
Hidalgo, E., Demple, B., 1994. An iron-sulfur center essential for transcriptional activation by the redox-sensing SoxR protein. EMBO J 13, 138–146. https://doi.org/10.1002/j.1460-2075.1994.tb06243.x
Huber, P.J., 1981. Robust Statistics, 1st ed, Wiley Series in Probability and Statistics. Wiley. https://doi.org/10.1002/0471725250
Husain, F., Nikaido, H., 2010. Substrate path in the AcrB multidrug efflux pump of Escherichia coli. Mol Microbiol 78, 320–330. https://doi.org/10.1111/j.1365-2958.2010.07330.x
Hutchings, M.I., Truman, A.W., Wilkinson, B., 2019. Antibiotics: past, present and future. Current Opinion in Microbiology 51, 72–80. https://doi.org/10.1016/j.mib.2019.10.008
Jair, K.W., Yu, X., Skarstad, K., Thöny, B., Fujita, N., Ishihama, A., Wolf, R.E., 1996. Transcriptional activation of promoters of the superoxide and multiple antibiotic resistance regulons by Rob, a binding protein of the Escherichia coli origin of chromosomal replication. Journal of Bacteriology 178, 2507–2513. https://doi.org/10.1128/jb.178.9.2507-2513.1996
Karakonstantis, S., Kritsotakis, E.I., Gikas, A., 2019. Pandrug-resistant Gram-negative bacteria: a systematic review of current epidemiology, prognosis and treatment options. Journal of Antimicrobial Chemotherapy dkz401. https://doi.org/10.1093/jac/dkz401
Kitagawa, M., Ara, T., Arifuzzaman, M., Ioka-Nakamichi, T., Inamoto, E., Toyonaga, H., Mori, H., 2005. Complete set of ORF clones of Escherichia coli ASKA library (a complete set of E. coli K-12 ORF archive): unique resources for biological research. DNA Res 12, 291–299. https://doi.org/10.1093/dnares/dsi012
Klünemann, M., Andrejev, S., Blasche, S., Mateus, A., Phapale, P., Devendran, S., Vappiani, J., Simon, B., Scott, T.A., Kafkia, E., Konstantinidis, D., Zirngibl, K., Mastrorilli, E., Banzhaf, M., Mackmull, M.-T., Hövelmann, F., Nesme, L., Brochado, A.R., Maier, L., Bock, T., Periwal, V., Kumar, M., Kim, Y., Tramontano, M., Schultz, C., Beck, M., Hennig, J., Zimmermann, M., Sévin, D.C., Cabreiro, F., Savitski, M.M., Bork, P., Typas, A., Patil, K.R., 2021. Bioaccumulation of therapeutic drugs by human gut bacteria. Nature 597, 533–538. https://doi.org/10.1038/s41586-021-03891-8
Kurzawa, N., Becher, I., Sridharan, S., Franken, H., Mateus, A., Anders, S., Bantscheff, M., Huber, W., Savitski, M.M., 2020. A computational method for detection of ligand-binding proteins from dose range thermal proteome profiles. Nat Commun 11, 5783. https://doi.org/10.1038/s41467-020-19529-8
Lee, J.O., Cho, K.-S., Kim, O.B., 2014. Overproduction of AcrR increases organic solvent tolerance mediated by modulation of SoxS regulon in Escherichia coli. Appl Microbiol Biotechnol 98, 8763–8773. https://doi.org/10.1007/s00253-014-6024-9

Li, X.-Z., Plésiat, P., Nikaido, H., 2015a. The Challenge of Efflux-Mediated Antibiotic Resistance in Gram-Negative Bacteria. Clin Microbiol Rev 28, 337–418. https://doi.org/10.1128/CMR.00117-14

Li, X.-Z., Plésiat, P., Nikaido, H., 2015b. The Challenge of Efflux-Mediated Antibiotic Resistance in Gram-Negative Bacteria. Clinical Microbiology Reviews 28, 337–418. https://doi.org/10.1128/cmr.00117-14

Liochev, S.I., Fridovich, I., 1992. Fumarase C, the stable fumarase of Escherichia coli, is controlled by the soxRS regulon. Proc Natl Acad Sci U S A 89, 5892–5896. https://doi.org/10.1073/pnas.89.13.5892

Livak, K.J., Schmittgen, T.D., 2001. Analysis of Relative Gene Expression Data Using Real-Time Quantitative PCR and the 2−ΔΔCT Method. Methods 25, 402–408. https://doi.org/10.1006/meth.2001.1262

Ma, D., Alberti, M., Lynch, C., Nikaido, H., Hearst, J.E., 1996. The local repressor AcrR plays a modulating role in the regulation of acrAB genes of Escherichia coli by global stress signals. Molecular Microbiology 19, 101–112. https://doi.org/10.1046/j.1365-2958.1996.357881.x

Maher, C., Hassan, K.A., 2023. The Gram-negative permeability barrier: tipping the balance of the in and the out. mBio 14, e01205-23. https://doi.org/10.1128/mbio.01205-23

Maier, L., Pruteanu, M., Kuhn, M., Zeller, G., Telzerow, A., Anderson, E.E., Brochado, A.R., Fernandez, K.C., Dose, H., Mori, H., Patil, K.R., Bork, P., Typas, A., 2018. Extensive impact of non-antibiotic drugs on human gut bacteria. Nature 555, 623–628. https://doi.org/10.1038/nature25979

Martin, R.G., Gillette, W.K., Rhee, S., Rosner, J.L., 1999. Structural requirements for marbox function in transcriptional activation of mar/sox/rob regulon promoters in Escherichia coli: sequence, orientation and spatial relationship to the core promoter. Molecular Microbiology 34, 431–441. https://doi.org/10.1046/j.1365-2958.1999.01599.x

Martin, R.G., Gillette, W.K., Rosner, J.L., 2000. Promoter discrimination by the related transcriptional activators MarA and SoxS: differential regulation by differential binding. Mol Microbiol 35, 623–34. https://doi.org/10.1046/j.1365-2958.2000.01732.x

Martin, R.G., Jair, K.W., Wolf, R.E., Rosner, J.L., 1996. Autoactivation of the marRAB multiple antibiotic resistance operon by the MarA transcriptional activator in Escherichia coli. Journal of Bacteriology 178, 2216–2223. https://doi.org/10.1128/jb.178.8.2216-2223.1996

Martin, R.G., Rosner, J.L., 2002. Genomics of the marA/soxS/rob regulon of Escherichia coli: identification of directly activated promoters by application of molecular genetics and informatics to microarray data. Mol Microbiol 44, 1611–1624. https://doi.org/10.1046/j.1365-2958.2002.02985.x

Martin, R.G., Rosner, J.L., 1997. Fis, an accessorial factor for transcriptional activation of the mar (multiple antibiotic resistance) promoter of Escherichia coli in the presence of the activator MarA, SoxS, or Rob. Journal of Bacteriology 179, 7410–7419. https://doi.org/10.1128/jb.179.23.7410-7419.1997

Martin, R.G., Rosner, J.L., 1995. Binding of purified multiple antibiotic-resistance repressor protein (MarR) to mar operator sequences. Proc Natl Acad Sci U S A 92, 5456–60. https://doi.org/10.1073/pnas.92.12.5456

Masi, M., Réfregiers, M., Pos, K.M., Pagès, J.-M., 2017. Mechanisms of envelope permeability and antibiotic influx and efflux in Gram-negative bacteria. Nat Microbiol 2, 17001. https://doi.org/10.1038/nmicrobiol.2017.1

Mateus, A., Bobonis, J., Kurzawa, N., Stein, F., Helm, D., Hevler, J., Typas, A., Savitski, M.M., 2018. Thermal proteome profiling in bacteria: probing protein state in vivo. Mol Syst Biol 14, e8242. https://doi.org/10.15252/msb.20188242

Mateus, A., Hevler, J., Bobonis, J., Kurzawa, N., Shah, M., Mitosch, K., Goemans, C.V., Helm, D., Stein, F., Typas, A., Savitski, M.M., 2020. The functional proteome landscape of Escherichia coli. Nature 588, 473–478. https://doi.org/10.1038/s41586-020-3002-5

Michán, C., Manchado, M., Pueyo, C., 2002. SoxRS Down-Regulation of *rob* Transcription. J Bacteriol 184, 4733–4738. https://doi.org/10.1128/JB.184.17.4733-4738.2002

Mitchell, A.M., Silhavy, T.J., 2019. Envelope stress responses: balancing damage repair and toxicity. Nat Rev Microbiol 17, 417–428. https://doi.org/10.1038/s41579-019-0199-0

Mizuno, T., Chou, M.Y., Inouye, M., 1984. A unique mechanism regulating gene expression: translational inhibition by a complementary RNA transcript (micRNA). Proc Natl Acad Sci U S A 81, 1966–1970. https://doi.org/10.1073/pnas.81.7.1966

Mizuno, T., Mizushima, S., 1990. Signal transduction and gene regulation through the phosphorylation of two regulatory components: the molecular basis for the osmotic regulation of the porin genes. Molecular Microbiology 4, 1077–1082. https://doi.org/10.1111/j.1365-2958.1990.tb00681.x

Murray, C.J.L., Ikuta, K.S., Sharara, F., Swetschinski, L., Robles Aguilar, G., Gray, A., Han, C., Bisignano, C., Rao, P., Wool, E., Johnson, S.C., Browne, A.J., Chipeta, M.G., Fell, F., Hackett, S., Haines-Woodhouse, G., Kashef Hamadani, B.H., Kumaran, E.A.P., McManigal, B., Achalapong, S., Agarwal, R., Akech, S., Albertson, S., Amuasi, J., Andrews, J., Aravkin, A., Ashley, E., Babin, F.-X., Bailey, F., Baker, S., Basnyat, B., Bekker, A., Bender, R., Berkley, J.A., Bethou, A., Bielicki, J., Boonkasidecha, S., Bukosia, J., Carvalheiro, C., Castañeda-Orjuela, C., Chansamouth, V., Chaurasia, S., Chiurchiù, S., Chowdhury, F., Clotaire Donatien, R., Cook, A.J., Cooper, B., Cressey, T.R., Criollo-Mora, E., Cunningham, M., Darboe, S., Day, N.P.J., De Luca, M., Dokova, K., Dramowski, A., Dunachie, S.J., Duong Bich, T., Eckmanns, T., Eibach, D., Emami, A., Feasey, N., Fisher-Pearson, N., Forrest, K., Garcia, C., Garrett, D., Gastmeier, P., Giref, A.Z., Greer, R.C., Gupta, V., Haller, S., Haselbeck, A., Hay, S.I., Holm, M., Hopkins, S., Hsia, Y., Iregbu, K.C., Jacobs, J., Jarovsky, D., Javanmardi, F., Jenney, A.W.J., Khorana, M., Khusuwan, S., Kissoon, N., Kobeissi, E., Kostyanev, T., Krapp, F., Krumkamp, R., Kumar, A., Kyu, H.H., Lim, C., Lim, K., Limmathurotsakul, D., Loftus, M.J., Lunn, M., Ma, J., Manoharan, A., Marks, F., May, J., Mayxay, M., Mturi, N., Munera-Huertas, T., Musicha, P., Musila, L.A., Mussi-Pinhata, M.M., Naidu, R.N., Nakamura, T., Nanavati, R., Nangia, S., Newton, P., Ngoun, C., Novotney, A., Nwakanma, D., Obiero, C.W., Ochoa, T.J., Olivas-Martinez, A., Olliaro, P., Ooko, E., Ortiz-Brizuela, E.,

Ounchanum, P., Pak, G.D., Paredes, J.L., Peleg, A.Y., Perrone, C., Phe, T., Phommasone, K., Plakkal, N., Ponce-de-Leon, A., Raad, M., Ramdin, T., Rattanavong, S., Riddell, A., Roberts, T., Robotham, J.V., Roca, A., Rosenthal, V.D., Rudd, K.E., Russell, N., Sader, H.S., Saengchan, W., Schnall, J., Scott, J.A.G., Seekaew, S., Sharland, M., Shivamallappa, M., Sifuentes-Osornio, J., Simpson, A.J., Steenkeste, N., Stewardson, A.J., Stoeva, T., Tasak, N., Thaiprakong, A., Thwaites, G., Tigoi, C., Turner, C., Turner, P., Van Doorn, H.R., Velaphi, S., Vongpradith, A., Vongsouvath, M., Vu, H., Walsh, T., Walson, J.L., Waner, S., Wangrangsimakul, T., Wannapinij, P., Wozniak, T., Young Sharma, T.E.M.W., Yu, K.C., Zheng, P., Sartorius, B., Lopez, A.D., Stergachis, A., Moore, C., Dolecek, C., Naghavi, M., 2022. Global burden of bacterial antimicrobial resistance in 2019: a systematic analysis. The Lancet 399, 629–655. https://doi.org/10.1016/S0140-6736(21)02724-0

Naghavi, M., Vollset, S.E., Ikuta, K.S., Swetschinski, L.R., Gray, A.P., Wool, E.E., Robles Aguilar, G., Mestrovic, T., Smith, G., Han, C., Hsu, R.L., Chalek, J., Araki, D.T., Chung, E., Raggi, C., Gershberg Hayoon, A., Davis Weaver, N., Lindstedt, P.A., Smith, A.E., Altay, U., Bhattacharjee, N.V., Giannakis, K., Fell, F., McManigal, B., Ekapirat, N., Mendes, J.A., Runghien, T., Srimokla, O., Abdelkader, A., Abd-Elsalam, S., Aboagye, R.G., Abolhassani, H., Abualruz, H., Abubakar, U., Abukhadijah, H.J., Aburuz, S., Abu-Zaid, A., Achalapong, S., Addo, I.Y., Adekanmbi, V., Adeyeoluwa, T.E., Adnani, Q.E.S., Adzigbli, L.A., Afzal, M.S., Afzal, S., Agodi, A., Ahlstrom, A.J., Ahmad, A., Ahmad, S., Ahmad, T., Ahmadi, A., Ahmed, A., Ahmed, H., Ahmed, I., Ahmed, M., Ahmed, S., Ahmed, S.A., Akkaif, M.A., Al Awaidy, S., Al Thaher, Y., Alalalmeh, S.O., AlBataineh, M.T., Aldhaleei, W.A., Al-Gheethi, A.A.S., Alhaji, N.B., Ali, A., Ali, L., Ali, S.S., Ali, W., Allel, K., Al-Marwani, S., Alrawashdeh, A., Altaf, A., Al-Tammemi, A.B., Al-Tawfiq, J.A., Alzoubi, K.H., Al-Zyoud, W.A., Amos, B., Amuasi, J.H., Ancuceanu, R., Andrews, J.R., Anil, A., Anuoluwa, I.A., Anvari, S., Anyasodor, A.E., Apostol, G.L.C., Arabloo, J., Arafat, M., Aravkin, A.Y., Areda, D., Aremu, A., Artamonov, A.A., Ashley, E.A., Asika, M.O., Athari, S.S., Atout, M.M.W., Awoke, T., Azadnajafabad, S., Azam, J.M., Aziz, S., Azzam, A.Y., Babaei, M., Babin, F.-X., Badar, M., Baig, A.A., Bajcetic, M., Baker, S., Bardhan, M., Barqawi, H.J., Basharat, Z., Basiru, A., Bastard, M., Basu, S., Bayleyegn, N.S., Belete, M.A., Bello, O.O., Beloukas, A., Berkley, J.A., Bhagavathula, A.S., Bhaskar, S., Bhuyan, S.S., Bielicki, J.A., Briko, N.I., Brown, C.S., Browne, A.J., Buonsenso, D., Bustanji, Y., Carvalheiro, C.G., Castañeda-Orjuela, C.A., Cenderadewi, M., Chadwick, J., Chakraborty, S., Chandika, R.M., Chandy, S., Chansamouth, V., Chattu, V.K., Chaudhary, A.A., Ching, P.R., Chopra, H., Chowdhury, F.R., Chu, D.-T., Chutiyami, M., Cruz-Martins, N., Da Silva, A.G., Dadras, O., Dai, X., Darcho, S.D., Das, S., De La Hoz, F.P., Dekker, D.M., Dhama, K., Diaz, D., Dickson, B.F.R., Djorie, S.G., Dodangeh, M., Dohare, S., Dokova, K.G., Doshi, O.P., Dowou, R.K., Dsouza, H.L., Dunachie, S.J., Dziedzic, A.M., Eckmanns, T., Ed-Dra, A., Eftekharimehrabad, A., Ekundayo, T.C., El Sayed, I., Elhadi, M., El-Huneidi, W., Elias, C., Ellis, S.J., Elsheikh, R., Elsohaby, I., Eltaha, C., Eshrati, B., Eslami, M., Eyre, D.W., Fadaka, A.O., Fagbamigbe, A.F., Fahim, A., Fakhri-Demeshghieh, A., Fasina, F.O.,

Fasina, M.M., Fatehizadeh, A., Feasey, N.A., Feizkhah, A., Fekadu, G., Fischer, F., Fitriana, I., Forrest, K.M., Fortuna Rodrigues, C., Fuller, J.E., Gadanya, M.A., Gajdács, M., Gandhi, A.P., Garcia-Gallo, E.E., Garrett, D.O., Gautam, R.K., Gebregergis, M.W., Gebrehiwot, M., Gebremeskel, T.G., Geffers, C., Georgalis, L., Ghazy, R.M., Golechha, M., Golinelli, D., Gordon, M., Gulati, S., Gupta, R.D., Gupta, S., Gupta, V.K., Habteyohannes, A.D., Haller, S., Harapan, H., Harrison, M.L., Hasaballah, A.I., Hasan, I., Hasan, R.S., Hasani, H., Haselbeck, A.H., Hasnain, M.S., Hassan, I.I., Hassan, S., Hassan Zadeh Tabatabaei, M.S., Hayat, K., He, J., Hegazi, O.E., Heidari, M., Hezam, K., Holla, R., Holm, M., Hopkins, H., Hossain, M.M., Hosseinzadeh, M., Hostiuc, S., Hussein, N.R., Huy, L.D., Ibáñez-Prada, E.D., Ikiroma, A., Ilic, I.M., Islam, S.M.S., Ismail, F., Ismail, N.E., Iwu, C.D., Iwu-Jaja, C.J., Jafarzadeh, A., Jaiteh, F., Jalilzadeh Yengejeh, R., Jamora, R.D.G., Javidnia, J., Jawaid, T., Jenney, A.W.J., Jeon, H.J., Jokar, M., Jomehzadeh, N., Joo, T., Joseph, N., Kamal, Z., Kanmodi, K.K., Kantar, R.S., Kapisi, J.A., Karaye, I.M., Khader, Y.S., Khajuria, H., Khalid, N., Khamesipour, F., Khan, A., Khan, M.J., Khan, M.T., Khanal, V., Khidri, F.F., Khubchandani, J., Khusuwan, S., Kim, M.S., Kisa, A., Korshunov, V.A., Krapp, F., Krumkamp, R., Kuddus, M., Kulimbet, M., Kumar, D., Kumaran, E.A.P., Kuttikkattu, A., Kyu, H.H., Landires, I., Lawal, B.K., Le, T.T.T., Lederer, I.M., Lee, M., Lee, S.W., Lepape, A., Lerango, T.L., Ligade, V.S., Lim, C., Lim, S.S., Limenh, L.W., Liu, C., Liu, Xiaofeng, Liu, Xuefeng, Loftus, M.J., M Amin, H.I., Maass, K.L., Maharaj, S.B., Mahmoud, M.A., Maikanti-Charalampous, P., Makram, O.M., Malhotra, K., Malik, A.A., Mandilara, G.D., Marks, F., Martinez-Guerra, B.A., Martorell, M., Masoumi-Asl, H., Mathioudakis, A.G., May, J., McHugh, T.A., Meiring, J., Meles, H.N., Melese, A., Melese, E.B., Minervini, G., Mohamed, N.S., Mohammed, S., Mohan, S., Mokdad, A.H., Monasta, L., Moodi Ghalibaf, A., Moore, C.E., Moradi, Y., Mossialos, E., Mougin, V., Mukoro, G.D., Mulita, F., Muller-Pebody, B., Murillo-Zamora, E., Musa, S., Musicha, P., Musila, L.A., Muthupandian, S., Nagarajan, A.J., Naghavi, P., Nainu, F., Nair, T.S., Najmuldeen, H.H.R., Natto, Z.S., Nauman, J., Nayak, B.P., Nchanji, G.T., Ndishimye, P., Negoi, I., Negoi, R.I., Nejadghaderi, S.A., Nguyen, Q.P., Noman, E.A., Nwakanma, D.C., O'Brien, S., Ochoa, T.J., Odetokun, I.A., Ogundijo, O.A., Ojo-Akosile, T.R., Okeke, S.R., Okonji, O.C., Olagunju, A.T., Olivas-Martinez, A., Olorukooba, A.A., Olwoch, P., Onyedibe, K.I., Ortiz-Brizuela, E., Osuolale, O., Ounchanum, P., Oyeyemi, O.T., P A, M.P., Paredes, J.L., Parikh, R.R., Patel, J., Patil, S., Pawar, S., Peleg, A.Y., Peprah, P., Perdigão, J., Perrone, C., Petcu, I.-R., Phommasone, K., Piracha, Z.Z., Poddighe, D., Pollard, A.J., Poluru, R., Ponce-De-Leon, A., Puvvula, J., Qamar, F.N., Qasim, N.H., Rafai, C.D., Raghav, P., Rahbarnia, L., Rahim, F., Rahimi-Movaghar, V., Rahman, M., Rahman, M.A., Ramadan, H., Ramasamy, S.K., Ramesh, P.S., Ramteke, P.W., Rana, R.K., Rani, U., Rashidi, M.-M., Rathish, D., Rattanavong, S., Rawaf, S., Redwan, E.M.M., Reyes, L.F., Roberts, T., Robotham, J.V., Rosenthal, V.D., Ross, A.G., Roy, N., Rudd, K.E., Sabet, C.J., Saddik, B.A., Saeb, M.R., Saeed, U., Saeedi Moghaddam, S., Saengchan, W., Safaei, M., Saghazadeh, A., Saheb Sharif-Askari, N., Sahebkar, A., Sahoo, S.S.,

Sahu, M., Saki, M., Salam, N., Saleem, Z., Saleh, M.A., Samodra, Y.L., Samy, A.M., Saravanan, A., Satpathy, M., Schumacher, A.E., Sedighi, M., Seekaew, S., Shafie, M., Shah, P.A., Shahid, S., Shahwan, M.J., Shakoor, S., Shalev, N., Shamim, M.A., Shamshirgaran, M.A., Shamsi, A., Sharifan, A., Shastry, R.P., Shetty, M., Shittu, A., Shrestha, S., Siddig, E.E., Sideroglou, T., Sifuentes-Osornio, J., Silva, L.M.L.R., Simões, E.A.F., Simpson, A.J.H., Singh, A., Singh, S., Sinto, R., Soliman, S.S.M., Soraneh, S., Stoesser, N., Stoeva, T.Z., Swain, C.K., Szarpak, L., T Y, S.S., Tabatabai, S., Tabche, C., Taha, Z.M.-A., Tan, K.-K., Tasak, N., Tat, N.Y., Thaiprakong, A., Thangaraju, P., Tigoi, C.C., Tiwari, K., Tovani-Palone, M.R., Tran, T.H., Tumurkhuu, M., Turner, P., Udoakang, A.J., Udoh, A., Ullah, N., Ullah, S., Vaithinathan, A.G., Valenti, M., Vos, T., Vu, H.T.L., Waheed, Y., Walker, A.S., Walson, J.L., Wangrangsimakul, T., Weerakoon, K.G., Wertheim, H.F.L., Williams, P.C.M., Wolde, A.A., Wozniak, T.M., Wu, F., Wu, Z., Yadav, M.K.K., Yaghoubi, S., Yahaya, Z.S., Yarahmadi, A., Yezli, S., Yismaw, Y.E., Yon, D.K., Yuan, C.-W., Yusuf, H., Zakham, F., Zamagni, G., Zhang, H., Zhang, Z.-J., Zielińska, M., Zumla, A., Zyoud, S.H.H., Zyoud, S.H., Hay, S.I., Stergachis, A., Sartorius, B., Cooper, B.S., Dolecek, C., Murray, C.J.L., 2024. Global burden of bacterial antimicrobial resistance 1990–2021: a systematic analysis with forecasts to 2050. The Lancet S0140673624018671. https://doi.org/10.1016/S0140-6736(24)01867-1

Nichols, R.J., Sen, S., Choo, Y.J., Beltrao, P., Zietek, M., Chaba, R., Lee, S., Kazmierczak, K.M., Lee, K.J., Wong, A., Shales, M., Lovett, S., Winkler, M.E., Krogan, N.J., Typas, A., Gross, C.A., 2011. Phenotypic Landscape of a Bacterial Cell. Cell 144, 143–156.

Nikaido, E., Yamaguchi, A., Nishino, K., 2008. AcrAB Multidrug Efflux Pump Regulation in Salmonella enterica serovar Typhimurium by RamA in Response to Environmental Signals *. Journal of Biological Chemistry 283, 24245–24253. https://doi.org/10.1074/jbc.M804544200

Nikaido, H., 2003. Molecular basis of bacterial outer membrane permeability revisited. Microbiol Mol Biol Rev 67, 593–656. https://doi.org/10.1128/MMBR.67.4.593-656.2003

Nishino, K., Yamaguchi, A., 2001. Analysis of a Complete Library of Putative Drug Transporter Genes in *Escherichia coli*. J Bacteriol 183, 5803–5812. https://doi.org/10.1128/JB.183.20.5803-5812.2001

Nunoshiba, T., Hidalgo, E., Amabile Cuevas, C.F., Demple, B., 1992a. Two-stage control of an oxidative stress regulon: the Escherichia coli SoxR protein triggers redox-inducible expression of the soxS regulatory gene. J Bacteriol 174, 6054–60. https://doi.org/10.1128/jb.174.19.6054-6060.1992

Nunoshiba, T., Hidalgo, E., Amabile Cuevas, C.F., Demple, B., 1992b. Two-stage control of an oxidative stress regulon: the Escherichia coli SoxR protein triggers redox-inducible expression of the soxS regulatory gene. J Bacteriol 174, 6054–60. https://doi.org/10.1128/jb.174.19.6054-6060.1992

Nunoshiba, T., Hidalgo, E., Li, Z., Demple, B., 1993. Negative autoregulation by the Escherichia coli SoxS protein: a dampening mechanism for the soxRS redox stress response. Journal of Bacteriology 175, 7492–7494. https://doi.org/10.1128/jb.175.22.7492-7494.1993

Okusu, H., Ma, D., Nikaido, H., 1996. AcrAB efflux pump plays a major role in the antibiotic resistance phenotype of Escherichia coli multiple-antibiotic-resistance (Mar) mutants. J Bacteriol 178, 306–308. https://doi.org/10.1128/jb.178.1.306-308.1996

Pagès, J.-M., James, C.E., Winterhalter, M., 2008. The porin and the permeating antibiotic: a selective diffusion barrier in Gram-negative bacteria. Nat Rev Microbiol 6, 893–903. https://doi.org/10.1038/nrmicro1994

Parker, A., Gottesman, S., 2016. Small RNA Regulation of TolC, the Outer Membrane Component of Bacterial Multidrug Transporters. J Bacteriol 198, 1101–1113. https://doi.org/10.1128/JB.00971-15

Piddock, L.J.V., 2002. Fluoroquinolone resistance in Salmonella serovars isolated from humans and food animals1. FEMS Microbiology Reviews 26, 3–16. https://doi.org/10.1111/j.1574-6976.2002.tb00596.x

Piddock, L.J.V., Alimi, Y., Anderson, J., De Felice, D., Moore, C.E., Røttingen, J.-A., Skinner, H., Beyer, P., 2024. Advancing global antibiotic research, development and access. Nat Med 30, 2432–2443. https://doi.org/10.1038/s41591-024-03218-w

Porwollik, S., Santiviago, C.A., Cheng, P., Long, F., Desai, P., Fredlund, J., Srikumar, S., Silva, C.A., Chu, W., Chen, X., Canals, R., Reynolds, M.M., Bogomolnaya, L., Shields, C., Cui, P., Guo, J., Zheng, Y., Endicott-Yazdani, T., Yang, H.-J., Maple, A., Ragoza, Y., Blondel, C.J., Valenzuela, C., Andrews-Polymenis, H., McClelland, M., 2014. Defined Single-Gene and Multi-Gene Deletion Mutant Collections in Salmonella enterica sv Typhimurium. PLOS ONE 9, e99820. https://doi.org/10.1371/journal.pone.0099820

Ramani, N., Hedeshian, M., Freundlich, M., 1994. micF antisense RNA has a major role in osmoregulation of OmpF in Escherichia coli. J Bacteriol 176, 5005–10. https://doi.org/10.1128/jb.176.16.5005-5010.1994

Rampersaud, A., Inouye, M., 1991. Procaine, a local anesthetic, signals through the EnvZ receptor to change the DNA binding affinity of the transcriptional activator protein OmpR. J Bacteriol 173, 6882–6888. https://doi.org/10.1128/jb.173.21.6882-6888.1991

Ricaurte, D., Huang, Y., Sheth, R.U., Gelsinger, D.R., Kaufman, A., Wang, H.H., 2024. High-throughput transcriptomics of 409 bacteria–drug pairs reveals drivers of gut microbiota perturbation. Nat Microbiol, 3 9, 561–575. https://doi.org/10.1038/s41564-023-01581-x

Ricci, V., Kaur, J., Stone, J., Piddock, L.J.V., 2023. Antibiotics do not induce expression of acrAB directly but via a RamA-dependent pathway. Antimicrob Agents Chemother 67, e0062023. https://doi.org/10.1128/aac.00620-23

Ritz, C., Baty, F., Streibig, J.C., Gerhard, D., 2015. Dose-Response Analysis Using R. PLoS One 10, e0146021. https://doi.org/10.1371/journal.pone.0146021

Rosenberg, E.Y., Bertenthal, D., Nilles, M.L., Bertrand, K.P., Nikaido, H., 2003. Bile salts and fatty acids induce the expression of Escherichia coli AcrAB multidrug efflux pump through their interaction with Rob regulatory protein. Mol Microbiol 48, 1609–1619. https://doi.org/10.1046/j.1365-2958.2003.03531.x

Rosner, J.L., Chai, T.J., Foulds, J., 1991. Regulation of ompF porin expression by salicylate in Escherichia coli. Journal of Bacteriology 173, 5631–5638. https://doi.org/10.1128/jb.173.18.5631-5638.1991

Rosner, J.L., Dangi, B., Gronenborn, A.M., Martin, R.G., 2002. Posttranscriptional activation of the transcriptional activator Rob by dipyridyl in Escherichia coli. J Bacteriol 184, 1407–16. https://doi.org/10.1128/JB.184.5.1407-1416.2002

Ruiz, C., Levy, S.B., 2014. Regulation of acrAB expression by cellular metabolites in Escherichia coli. Journal of Antimicrobial Chemotherapy 69, 390–399. https://doi.org/10.1093/jac/dkt352

Ruiz, C., Levy, S.B., 2010. Many Chromosomal Genes Modulate MarA-Mediated Multidrug Resistance in *Escherichia coli*. Antimicrob Agents Chemother 54, 2125–2134. https://doi.org/10.1128/AAC.01420-09

Sambrook, J., Fritsch, E.F., Maniatis, T., Russell, D.W., Green, M.R., 1989. Molecular cloning: a laboratory manual. Cold Spring Harbor Laboratory Press, Cold Spring Harbor, NY.

Savitski, M.M., Reinhard, F.B.M., Franken, H., Werner, T., Savitski, M.F., Eberhard, D., Molina, D.M., Jafari, R., Dovega, R.B., Klaeger, S., Kuster, B., Nordlund, P., Bantscheff, M., Drewes, G., 2014. Tracking cancer drugs in living cells by thermal profiling of the proteome. Science 346, 1255784. https://doi.org/10.1126/science.1255784

Schindelin, J., Arganda-Carreras, I., Frise, E., Kaynig, V., Longair, M., Pietzsch, T., Preibisch, S., Rueden, C., Saalfeld, S., Schmid, B., Tinevez, J.-Y., White, D.J., Hartenstein, V., Eliceiri, K., Tomancak, P., Cardona, A., 2012. Fiji: an open-source platform for biological-image analysis. Nat Methods 9, 676–682. https://doi.org/10.1038/nmeth.2019

Schneider, C.A., Rasband, W.S., Eliceiri, K.W., 2012. NIH Image to ImageJ: 25 years of image analysis. Nat Methods 9, 671–675. https://doi.org/10.1038/nmeth.2089

Schneiders, T., Levy, S.B., 2006. MarA-mediated Transcriptional Repression of the rob Promoter. Journal of Biological Chemistry 281, 10049–10055. https://doi.org/10.1074/jbc.M512097200

Seo, S.W., Kim, D., Szubin, R., Palsson, B.O., 2015. Genome-wide Reconstruction of OxyR and SoxRS Transcriptional Regulatory Networks under Oxidative Stress in Escherichia coli K-12 MG1655. Cell Reports 12, 1289–1299. https://doi.org/10.1016/j.celrep.2015.07.043

Shi, J., Wang, F., Li, F., Wang, L., Xiong, Y., Wen, A., Jin, Y., Jin, S., Gao, F., Feng, Z., Li, J., Zhang, Y., Shang, Z., Wang, S., Feng, Y., Lin, W., 2022. Structural basis of transcription activation by Rob, a pleiotropic AraC/XylS family regulator. Nucleic Acids Research 50, 5974–5987. https://doi.org/10.1093/nar/gkac433

Shimada, T., Takada, H., Yamamoto, K., Ishihama, A., 2015. Expanded roles of two-component response regulator OmpR in Escherichia coli: genomic SELEX search for novel regulation targets. Genes to Cells 20, 915–931. https://doi.org/10.1111/gtc.12282

Shimada, T., Yamamoto, K., Ishihama, A., 2011. Novel members of the Cra regulon involved in carbon metabolism in Escherichia coli. J Bacteriol 193, 649–659. https://doi.org/10.1128/JB.01214-10

Skarstad, K., Thöny, B., Hwang, D.S., Kornberg, A., 1993. A novel binding protein of the origin of the Escherichia coli chromosome. Journal of

Biological Chemistry 268, 5365–5370. https://doi.org/10.1016/S0021-9258(18)53330-5

Su, C.-C., Rutherford, D.J., Yu, E.W., 2007. Characterization of the multidrug efflux regulator AcrR from *Escherichia coli*. Biochemical and Biophysical Research Communications 361, 85–90. https://doi.org/10.1016/j.bbrc.2007.06.175

Sulavik, M.C., Houseweart, C., Cramer, C., Jiwani, N., Murgolo, N., Greene, J., DiDomenico, B., Shaw, K.J., Miller, G.H., Hare, R., Shimer, G., 2001. Antibiotic Susceptibility Profiles of *Escherichia coli* Strains Lacking Multidrug Efflux Pump Genes. Antimicrob Agents Chemother 45, 1126–1136. https://doi.org/10.1128/AAC.45.4.1126-1136.2001

Suzuki, S., Horinouchi, T., Furusawa, C., 2014. Prediction of antibiotic resistance by gene expression profiles. Nat Commun 5, 5792. https://doi.org/10.1038/ncomms6792

Teelucksingh, T., Thompson, L.K., Zhu, S., Kuehfuss, N.M., Goetz, J.A., Gilbert, S.E., MacNair, C.R., Geddes-McAlister, J., Brown, E.D., Cox, G., 2022a. A genetic platform to investigate the functions of bacterial drug efflux pumps. Nat Chem Biol 18, 1399–1409. https://doi.org/10.1038/s41589-022-01119-y

Teelucksingh, T., Thompson, L.K., Zhu, S., Kuehfuss, N.M., Goetz, J.A., Gilbert, S.E., MacNair, C.R., Geddes-McAlister, J., Brown, E.D., Cox, G., 2022b. A genetic platform to investigate the functions of bacterial drug efflux pumps. Nat Chem Biol 18, 1399–1409. https://doi.org/10.1038/s41589-022-01119-y

Tibshirani, R., 1996. Regression Shrinkage and Selection Via the Lasso. Journal of the Royal Statistical Society Series B: Statistical Methodology 58, 267–288. https://doi.org/10.1111/j.2517-6161.1996.tb02080.x

Tsaneva, I.R., Weiss, B., 1990. soxR, a locus governing a superoxide response regulon in Escherichia coli K-12. J Bacteriol 172, 4197–4205. https://doi.org/10.1128/jb.172.8.4197-4205.1990

Typas, A., Nichols, R.J., Siegele, D.A., Shales, M., Collins, S.R., Lim, B., Braberg, H., Yamamoto, N., Takeuchi, R., Wanner, B.L., Mori, H., Weissman, J.S., Krogan, N.J., Gross, C.A., 2008. High-throughput, quantitative analyses of genetic interactions in E. coli. Nat Methods 5, 781–787. https://doi.org/10.1038/nmeth.1240

Uehara, T., Parzych, K.R., Dinh, T., Bernhardt, T.G., 2010. Daughter cell separation is controlled by cytokinetic ring-activated cell wall hydrolysis. EMBO J 29, 1412–1422. https://doi.org/10.1038/emboj.2010.36

Vergalli, J., Bodrenko, I.V., Masi, M., Moynie, L., Acosta-Gutierrez, S., Naismith, J.H., Davin-Regli, A., Ceccarelli, M., van den Berg, B., Winterhalter, M., Pages, J.M., 2020. Porins and small-molecule translocation across the outer membrane of Gram-negative bacteria. Nat Rev Microbiol 18, 164–176. https://doi.org/10.1038/s41579-019-0294-2

Vinué, L., McMurry, L.M., Levy, S.B., 2013. The 216-bp marB gene of the marRAB operon in Escherichia coli encodes a periplasmic protein which reduces the transcription rate of marA. FEMS Microbiology Letters 345, 49–55. https://doi.org/10.1111/1574-6968.12182

Von Wintersdorff, C.J.H., Penders, J., Van Niekerk, J.M., Mills, N.D., Majumder, S., Van Alphen, L.B., Savelkoul, P.H.M., Wolffs, P.F.G., 2016. Dissemination of Antimicrobial Resistance in Microbial Ecosystems

through Horizontal Gene Transfer. Front. Microbiol. 7. https://doi.org/10.3389/fmicb.2016.00173

Weatherspoon-Griffin, N., Yang, D., Kong, W., Hua, Z., Shi, Y., 2014. The CpxR/CpxA Two-component Regulatory System Up-regulates the Multidrug Resistance Cascade to Facilitate Escherichia coli Resistance to a Model Antimicrobial Peptide *. Journal of Biological Chemistry 289, 32571–32582. https://doi.org/10.1074/jbc.M114.565762

Wu, J., Weiss, B., 1991. Two divergently transcribed genes, soxR and soxS, control a superoxide response regulon of Escherichia coli. J Bacteriol 173, 2864–2871. https://doi.org/10.1128/jb.173.9.2864-2871.1991

Yeh, P.J., Hegreness, M.J., Aiden, A.P., Kishony, R., 2009. Drug interactions and the evolution of antibiotic resistance. Nat Rev Microbiol 7, 460–466. https://doi.org/10.1038/nrmicro2133

Yoshida, T., Qin, L., Egger, L.A., Inouye, M., 2006. Transcription Regulation of *ompF* and *ompC* by a Single Transcription Factor, OmpR*. Journal of Biological Chemistry 281, 17114–17123. https://doi.org/10.1074/jbc.M602112200

Zhang, A., Rosner, J.L., Martin, R.G., 2008. Transcriptional activation by MarA, SoxS and Rob of two tolC promoters using one binding site: a complex promoter configuration for tolC in Escherichia coli. Molecular Microbiology 69, 1450–1455. https://doi.org/10.1111/j.1365-2958.2008.06371.x